

# SUCCESSIVE MODAL APPROXIMATION IN BEAMS THROUGH SPATIAL DATA

by  
Yogesh A. Raikhelkar



DEPARTMENT OF MECHANICAL ENGINEERING  
**INDIAN INSTITUTE OF TECHNOLOGY KANPUR**

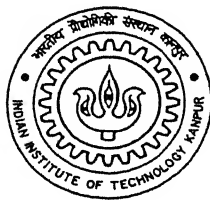
APRIL, 1999

# Successive Modal Approximation In Beams Through Spatial Data

*A thesis submitted  
in partial fulfilment of the requirements  
for the degree of*

MASTER OF TECHNOLOGY

by  
Yogesh A. Raikhelkar



*to the*

Department of Mechanical Engineering  
Indian Institute of Technology, Kanpur  
April 1999

0 1 JUN 1999/me

**CENTRAL LIBRARY**  
I. I. T., KANPUR

**Acc. No. A 128082**

TM  
ME/1999/m  
R12-8



A128082

*Dedicated to*  
***Aai and Baba***

# CERTIFICATE



It is certified that the work contained in the thesis entitled 'Successive Modal Approximation in Beams through Spatial Data', by Yogesh A. Raikhelkar, has been carried out under my supervision and this work has not been submitted elsewhere for a degree.

Nalinaksh Vyas.  
Nalinaksh S. Vyas 28/4/99

Associate Professor

Department of Mechanical Engineering

Indian Institute of Technology

Kanpur 208016

## ACKNOWLEDGEMENT

It gives me a great pleasure to express my sincere thanks with deep sense of gratitude to Dr. Nalinaksh Vyas, for his valuable guidance and providing me an environment of complete freedom for my thesis work. This work would not have been possible had it not been his constant encouragement. It was Dr. Vyas who introduced me to the field of vibrations. I must thank him for giving an opportunity to work on such an interesting topic in vibrations.

I am highly thankful to Ms. Lalitha for her cooperation throughout the work. She had always been a great hand of help. Thanks are also due to Mr. A. Chaterjee and Mr. A. A. Khan for their valuable suggestions and close association. The Vibration lab. people always made the atmosphere very lively and made me feel homely. I would like to give special thanks to Mr. M. M. Singh for his kind assistance and making services available, whenever required. I must say thanks to Amod and Sharad for their constant cheering throughout my work.

I would like to give special thanks to Mr. Adish Vaze, whose thesis was the foundation for the work, I have been doing towards my Master's program.

I would not forget the days spent with Neeraj, who has always been a great friend throughout my stay at IITK. I am also thankful to Santosh, Suma, Anil, Ganesh, Desai, Subodh, two Robots and all the Ghatmandali for making my stay at IIT very enjoyable and unforgettable.

I take this opportunity to express my deep love and respect to all the members of my family.

Lastly, I am thankful to one and all who were in one way or the other, associated with me towards the completion of my work.

*Yogesh Raikhelkar*

# ABSTRACT

Spatial Modal Testing is a parameter estimation approach, which provides spatial information regarding the dynamics of a structure, at a large number of points. The classical approach of obtaining frequency response function (FRF) estimates offers relatively little spatial information, for the emphasis is on observing the machine/component dynamics at a large number of frequencies at a limited number of specified locations on the machine/component. The FRF approach provides good accuracy on estimates of natural frequencies and damping ratios. The correctness of the estimates of mode shapes is, however, not comparable. Advances in sensor technologies facilitate measurements at a relatively large number of structure locations, and spatial modal analysis procedures seek to remove the deficiencies in the existing mode shape estimation procedures. The present study is an extension of some existing works on spatial modal analysis, dealing with single and two mode approximations. An algorithm, for estimation of the fundamental and desired number of successive modes, from spatial response data at multiple excitation frequencies, has been developed in the present study. Approximations of beam deflections, under specified harmonic excitation, are approximated through Forsythe polynomials, which can be compared with actual experimental measurements of the deflected beam. A Least Square technique is used to minimise the error between measured and Forsythe approximation data. Orthogonality properties of the Forsythe polynomials and normal mode functions are further employed to estimate individual mode shapes. Natural frequencies are obtained through standard relationships. An algorithm has been developed, for carrying out the procedure, successively, at various excitation frequencies, estimating two adjacent modes each time and simultaneously, refining existing previous modal information. The algorithm is demonstrated through computer simulations of the response of beams, with some standard boundary configurations. The analysis has been carried out in terms of non-dimensional parameters. The accuracy of the results is illustrated through comparisons of the estimated mode shapes with the 'exact' ones, available from classical beam theory.

# CONTENTS

LIST OF SYMBOLS	i
LIST OF FIGURES	ii
LIST OF TABLES	v
1. INTRODUCTION	1
2. SPATIAL DATA ANALYSIS	5
2.1 Forsythe polynomials	5
2.2 Estimation of adjacent mode shapes	6
2.3 Natural frequency estimates	10
2.4 Remarks	10
3. SUCCESSIVE MODAL APPROXIMATION	11
3.1 Algorithm for successive modal approximation	11
3.2 Non-dimensional parameters	17
3.3 Numerical illustrations	19
3.4 Remarks	62
4. CONCLUSIONS	69
REFERENCES	71



# LIST OF SYMBOLS

$y(x)$	Displacement
$\rho$	Mass density
$E$	Modulus of elasticity
$A$	Area of cross section
$I$	Area moment of inertia
$F$	Magnitude of applied force
$x_\mu$	Measurement station
$\omega$	Excitation frequency
$\omega_j$	$j^{th}$ natural frequency
$\psi_j(x_\mu)$	$j^{th}$ mode shape at station $x_\mu$
$\zeta_j$	$j^{th}$ damping ratio
$Y_r(x_\mu)$	Real component of approximated response
$Y_i(x_\mu)$	Imaginary component of approximated
$v_r(x_\mu)$	Real component of experimental response, at station $x_\mu$
$v_i(x_\mu)$	Imaginary component of experimental response, at station $x_\mu$
$p_k(x_\mu)$	$k^{th}$ Forsythe polynomial at station $x_\mu$
$\varepsilon_r(x_\mu)$	Least square error (real)
$\varepsilon_i(x_\mu)$	Least square error (imaginary)
$S_{jk}$	Constants in Forsythe polynomials
$\chi_j$	$j^{th}$ spatial frequency
$\kappa$	Non dimensional parameter ( $EI/\rho g A l^3$ )
$r_j$	$j^{th}$ natural frequency
$H(x)$	Non-dimensional response
$H_r(x_\mu)$	Real component of non-dimensional approximated response
$H_i(x_\mu)$	Imaginary component of non-dimensional approximated response
$q_r(x_\mu)$	Real component of non-dimensional measured response
$q_i(x_\mu)$	Imaginary component of non-dimensional measured response
$\overline{\varepsilon_r}(x_\mu)$	Non-dimensional least square error (real)
$\overline{\varepsilon_i}(x_\mu)$	Non-dimensional least square error (imaginary)

# LIST OF FIGURES

Figure	Description	Page
3.1(a)	Exact mode shapes of simply supported beam	13
3.1(b)	Exact mode shapes of fixed-fixed beam	13
3.1(c)	Exact mode shapes of cantilever beam	16
3.2(a)	In-phase response of simply supported beam (Location of excitation force, $x/l = 0.5$ ; Excitation frequency = 3.71 rad/s)	21
3.2(b)	Out of phase response of simply supported beam (Location of excitation force, $x/l = 0.5$ ; Excitation frequency = 3.71 rad/s)	21
3.3(a)	First approximation of mode 1: simply supported beam	22
3.3(b)	First approximation of mode 3: simply supported beam	22
3.4(a)	First approximation of Spatial frequency: mode 1: simply supported beam	23
3.4(b)	First approximation of Spatial frequency: mode 3: simply supported beam	23
3.5(a)	Error in first approximation of mode 1: simply supported beam	24
3.5(b)	Error in first approximation of mode 3: simply supported beam	24
3.6(a)	In-phase response of simply supported beam (Location of excitation force, $x/l = 0.5$ ; Excitation frequency = 38.856 rad/s)	26
3.6(b)	Out of phase response of simply supported beam (Location of excitation force, $x/l = 0.5$ ; Excitation frequency = 38.856 rad/s)	26
3.7(a)	In-phase response of simply supported beam after subtracting 1 <sup>st</sup> mode's contribution (Location of excitation force, $x/l = 0.5$ ; Excitation frequency = 38.856 rad s)	27
3.7(b)	Out of phase response of simply supported beam after subtracting 1 <sup>st</sup> mode's contribution (Location of excitation force, $x/l = 0.5$ ; Excitation frequency = 38.856 rad s)	27
3.8(a)	First approximation of mode 3: simply supported beam	28
3.8(b)	First approximation of mode 5: simply supported beam	28
3.9(a)	First approximation of Spatial frequency: mode 3: simply supported beam	29
3.9(b)	First approximation of Spatial frequency: mode 5: simply supported beam	29
3.10(a)	Error in first approximation of mode 3: simply supported beam	30
3.10(b)	Error in first approximation of mode 5: simply supported beam	30
3.11(a)	In-phase response of simply supported beam (Location of excitation force, $x/l = 0.33$ ; Excitation frequency = 17.781 rad/s)	31

3.11(b)	Out of phase response of simply supported beam (Location of excitation force, $x/l = 0.33$ ; Excitation frequency = Excitation frequency = 17.781 rad/s)	31
3.12(a)	In-phase response of simply supported beam after subtracting 1 <sup>st</sup> mode's contribution (Location of excitation force, $x/l = 0.33$ ; Excitation frequency = 17.781 rad/s)	32
3.12(b)	Out of phase response of simply supported beam after subtracting 1 <sup>st</sup> mode's contribution (Location of excitation force, $x/l = 0.33$ ; Excitation frequency = 17.781 rad/s)	32
3.13(a)	First approximation of mode 2: simply supported beam	33
3.13(b)	First approximation of mode 4: simply supported beam	33
3.14(a)	First approximation of Spatial frequency: mode 2 simply supported beam	34
3.14(b)	First approximation of Spatial frequency: mode 4 simply supported beam	34
3.15(a)	Error in first approximation of Spatial frequency: mode 2 simply supported beam	35
3.15(b)	Error in first approximation of Spatial frequency: mode 4 simply supported beam	35
3.16(a)	Refinement in mode shapes: mode 1: simply supported beam	37
3.16(b)	Refinement in mode shapes: mode 2: simply supported beam	37
3.16(c)	Refinement in mode shapes: mode 3: simply supported beam	38
3.16(d)	Refinement in mode shapes: mode 4: simply supported beam	38
3.16(e)	Refinement in mode shapes: mode 5: simply supported beam	39
3.17(a)	Refinement in Spatial frequency: mode1: simply supported beam	40
3.17(b)	Refinement in Spatial frequency: mode2: simply supported beam	40
3.17(c)	Refinement in Spatial frequency: mode3: simply supported beam	41
3.17(d)	Refinement in Spatial frequency: mode4: simply supported beam	41
3.17(e)	Refinement in Spatial frequency: mode5: simply supported beam	42
3.18(a)	First approximation of mode 1: fixed-fixed beam	43
3.18(b)	First approximation of mode 3: fixed-fixed beam	43
3.19(a)	First approximation of Spatial frequency: mode 1: fixed fixed beam	44
3.19(b)	First approximation of Spatial frequency: mode 3: fixed fixed beam	44
3.20(a)	First approximation of mode 3: fixed-fixed beam	46
3.20(b)	First approximation of mode 5: fixed-fixed beam	46
3.21(a)	First approximation of Spatial frequency: mode 3: fixed-fixed beam	47
3.21(b)	First approximation of Spatial frequency: mode 5: fixed-fixed beam	47
3.22(a)	First approximation of mode 2: fixed-fixed beam	48

3.22(b)	First approximation of mode 4: fixed-fixed beam	48
3.23(a)	First approximation of Spatial frequency: mode 2: fixed fixed beam	49
3.23(b)	First approximation of Spatial frequency: mode 4: fixed fixed beam	49
3.24(a)	Refinement in mode shapes: mode 1: fixed-fixed beam	50
3.24(b)	Refinement in mode shapes: mode 2: fixed-fixed beam	50
3.24(c)	Refinement in mode shapes: mode 3: fixed-fixed beam	51
3.24(d)	Refinement in mode shapes: mode 4: fixed-fixed beam	51
3.24(e)	Refinement in mode shapes: mode 5: fixed-fixed beam	52
3.25(a)	Refinement in Spatial frequency: mode1: fixed-fixed beam	53
3.25(b)	Refinement in Spatial frequency: mode2: fixed-fixed beam	53
3.25(c)	Refinement in Spatial frequency: mode3: fixed-fixed beam	54
3.25(d)	Refinement in Spatial frequency: mode4: fixed-fixed beam	54
3.25(e)	Refinement in Spatial frequency: mode5: fixed-fixed beam	55
3.26(a)	In-phase response of cantilever beam (Location of excitation force, $x/l = 1.0$ ; Excitaion frequency = 1.32 rad/s)	57
3.26(b)	Out of phase response of cantilever beam (Location of excitation force, $x/l = 1.0$ ; Excitaion frequency = 1.32 rad/s)	57
3.27(a)	First approximation of mode 1: cantilever beam	58
3.27(b)	First approximation of mode 2: cantilever beam	58
3.28(a)	First approximation of Spatial frequency: mode 1 : cantilever beam	59
3.28(b)	First approximation of Spatial frequency: mode 2 : cantilever beam	59
3.29(a)	First approximation of mode 2: cantilever beam	60
3.29(b)	First approximation of mode 2: cantilever beam	60
3.30(a)	First approximations of Spatial frequency: mode 2 : cantilever beam	61
3.30(b)	First approximations of Spatial frequency: mode 2 : cantilever beam	61
3.31(a)	Refinement in mode shapes: mode 1: cantilever beam	63
3.31(b)	Refinement in mode shapes: mode 2: cantilever beam	63
3.31(c)	Refinement in mode shapes: mode 3: cantilever beam	64
3.31(d)	Refinement in mode shapes: mode 4: cantilever beam	64
3.31(e)	Refinement in mode shapes: mode 5: cantilever beam	65
3.32(a)	Refinement in Spatial frequency: mode 1: cantilever beam	66
3.32(b)	Refinement in Spatial frequency: mode 2: cantilever beam	66
3.32(c)	Refinement in Spatial frequency: mode 3: cantilever beam	67
3.32(d)	Refinement in Spatial frequency: mode 4: cantilever beam	67
3.32(e)	Refinement in Spatial frequency: mode 5: cantilever beam	68

## LIST OF TABLES

Table	Description	Page
3.1	Estimated and exact natural frequencies of simply supported Beam	36
3.2	Estimated and exact natural frequencies of fixed-fixed beam	45
3.3	Estimated and exact natural frequencies of cantilever beam	62

# CHAPTER 1

## INTRODUCTION

Obtaining mathematical descriptions of the dynamic behaviour of machine components, is a major activity in vibration analysis. Modal Testing encompasses such experimental studies, for mathematical modeling. The form of the mathematical description or model varies considerably from one application to the other. It can be an estimate of natural frequency and damping factor, in one case, and estimating full mass-spring-dashpot model for another. One of the earliest developments in the area was by Kennedy and Pancu (1947) who evolved descriptions like ‘Resonance Testing’ and ‘Mechanical Impedance’, for applications involving natural frequency and damping determination of aircraft structures. Bishop and Gladwell (1963) provided methods for more precise measurements and applications. Major advances in transducers, electronics and digital analyzers, by 1970, helped to firmly establish modal testing as a powerful tool of experimental analysis. Reference can be made to papers by Ewins and Griffin (1981), Allemang (1984) and Mitchell (1984), for bibliographies of studies pertaining to basic modal testing methods. The text, by Ewins (1986) is widely referred to as a treatise encompassing most of the aspects of classical modal testing.

Estimation of natural frequencies and description of mode shapes are the most common modal testing applications. These permit their model identification and allow correlation with a theoretical model. In a classical approach this is done through obtaining frequency response function (FRF) estimates from time dependent forces and responses spatially distributed about the structure. The denominator, of the frequency response function, comprises of the spatially invariant natural frequency and damping parameters, while the numerator contains the spatial information on the mode shape of the structure.

The above classical procedure offers, relatively, little spatial information. For example, a typical test may have ten measurement locations on a structure, which is

provided harmonic excitation at a specified location. The excitation frequency is swept over the frequency range of interest and a Frequency Response Function (FRF) plot is obtained. These plots are then utilised for estimation of system parameters, like natural frequency, damping ratio, mode shape etc. While good accuracy is obtained on estimates of natural frequencies and damping ratios, the correctness of the estimates of mode shapes is not comparable. Subsequent generation of mass and stiffness matrix models is also not accurate. The primary reason, for these inaccuracies, is that response measurements are not made at sufficient number of locations on the structure. Advances in sensor technology and the advent of instruments like the Laser-Doppler Vibrometers, have facilitated measurements at a relatively large number of structure locations, in contrast to conventional sensors like accelerometers or proximity probes. Moreover, the measurement points can be located with a much greater degree of accuracy, through a Laser beam measurement technique. The alternative to this approach is to obtain spatial information at many more points at a fixed frequency. This has recently become realizable through developments in Laser Doppler data acquisition techniques. The scanning laser is able to acquire velocity information at a number of spatial locations on the structure with sufficient density, accuracy and speed to offer the possibility of extraction of modal parameters from spatially intensive arrays as opposed to the classical frequency intensive format. The need for exploring the spatial data intensive procedure arises from the problems faced in validating analytical structural models. These models, typically finite element models, are characterized by a large number of spatial degrees of freedom.

Reference can be made to the works of Archibald and Wicks (1991), Archibald (1992), and by West et al (1993), for attempts towards spatial modal analysis. Standard autoregressive models as in Pisarenko Harmonic Decomposition (Pisarenko, 1973) and Oversize Total Least Squares, have been used to approximate a normal mode function of the beam and are shown to yield unbiased results in the presence of measurement noise. West et al (1993) have also, alternatively employed the recursive form of Forsythe polynomials to approximate a normal mode function. The orthogonality property of Forsythe polynomials, yields easier least square formulation

and removes the ill conditioning problem while extracting the Forsythe coefficients from measured data.

The above attempts were, however, restricted to approximation of a single normal mode function of a beam by a polynomial function. The steady state vibration amplitude was obtained at various points along the length of a beam, for an excitation frequency, very close to one of its natural frequencies. The excitation frequency being very close to a natural frequency, it was assumed that contribution from adjacent modes is negligible and the deformed beam shape resembles the corresponding normal function of the beam. This is, however, not be always possible for, firstly it requires an *a-priori* knowledge of the natural frequencies of the beam and secondly, it may not always be possible to place the excitation force accurately enough on the structure, so as to constrain the response to a particular mode.

Vaze (1998) developed a general procedure, for a beam excited at a specified frequency and location, to estimate the modal participation of adjacent modes, from steady state spatial data. He employed recursive form of Forsythe polynomials for his analysis. Characteristic properties of beam modes lying on either side of the excitation frequency were determined. The analysis was thus, restricted to estimation of two natural modes of the beam.

The present study attempts to extend the work, cited above, for estimation of more than two natural modes. An algorithm, for estimation of the fundamental and desired number of successive modes, from spatial response data at multiple excitation frequencies, has been developed. The mode shapes of the beam have been approximated through Forsythe polynomials and an approximation of the beam deflection under a given excitation is generated. This approximation can be compared with actual experimental measurements of the deflected beam. A Least Square technique is used to minimise the error between measured and Forsythe approximation data, through adjustments of the coefficients of Forsythe polynomials. Orthogonality properties of the normal mode functions are further employed to decompose the Forsythe polynomial representation into the individual mode shapes of the beam contributing to the response. Natural frequencies can be obtained through



standard relationships. An algorithm has been developed, for carrying out the procedure successively, at various excitation frequencies, estimating two adjacent modes each time and simultaneously, refining existing previous modal information.

The algorithm is demonstrated through computer simulations of the response of beams with some standard boundary configurations. Analysis has been carried out in terms of nondimensional parameters. Accuracy of the results is illustrated through comparisons of the estimated mode shapes with the 'exact' ones, available from classical beam theory.

Chapter 2 describes the spatial modal analysis procedure. The algorithm for estimation of successive mode shapes along with the numerical studies is given in Chapter 3. Chapter 4 gives the conclusions of the present study and outlines the scope for future work.

## CHAPTER 2

### ANALYSIS OF SPATIAL DATA

The procedure, developed for analysis of steady state, forced vibration response data for estimation of modal participation, is discussed in this chapter. The beam is excited at a desired frequency and contribution, of the two natural modes of the beam, lying on either side of the excitation frequency, to beam response is estimated. The focus is on obtaining accurate descriptions of the mode shapes. Estimates of natural frequencies result as a by-product of the procedure.

The beam response is obtained at a number of spatial points along its length, in terms of the in-phase and out-of-phase vibration amplitudes. Recursive form of Forsythe polynomials is employed to approximate the deflected beam shape. Least square technique is employed to minimise the error between the approximated and measured responses, to obtain the coefficients of Forsythe polynomials. Orthogonality properties of normal mode functions are further employed to decompose the Forsythe polynomial representation into individual mode shapes of the beam contributing to the response. Standard relations give the natural frequencies from estimated spatial frequencies.

#### 2.1 Forsythe Polynomials

Orthogonal polynomials are most suited to approximate the dynamic deflection of beams, in view of the orthogonality property of their natural modes. Forsythe polynomials have been used by West et al(1993) to approximate the fundamental beam mode. They found that such a formulation of beam response is easier and removes ill conditioning. In view of these properties, Forsythe polynomials have been employed in the present study also, for extraction of mode shapes from spatial data.

Forsythe polynomials are defined as (Forsythe, 1957)

$$p_0(x) = 1$$

$$p_1(x) = xp_0(x) - \alpha_1 p_0(x) \quad (2.1)$$

$$p_{i+1}(x) = xp_i(x) - \alpha_{i+1} p_i(x) - \beta_i p_{i-1}(x)$$

with

$$\alpha_{i+1} = \sum_{\mu=1}^N x_{\mu} [p_i(x_{\mu})]^2 / \sum_{\mu=1}^N [p_i(x_{\mu})]^2 \quad (2.2)$$

$$\beta_i = \sum_{\mu=1}^N x_{\mu} p_i(x_{\mu}) p_{i-1}(x_{\mu}) / \sum_{\mu=1}^N [p_i(x_{\mu})]^2 \quad (2.3)$$

## 2.2 Estimation of adjacent mode shapes

For an Euler beam excited at a point  $x = a$  along its length, by a force  $F_0 e^{i\omega t}$ , the steady state response can be written, in standard form, as

$$y(x) = \sum_{j=1}^{\infty} [F \psi_j(a) \psi_j(x) (\omega_j^2 - \omega^2) / \{(\omega_j^2 - \omega^2)^2 + 4\xi_j^2 \omega^2\} - i2F \psi_j(x) \psi_j(a) \xi_j \omega_j \omega / \{(\omega_j^2 - \omega^2)^2 + 4\xi_j^2 \omega^2\}] e^{i\omega t} \quad (2.4)$$

In the above

$$F = \text{force / beam mass} = F_0 / \rho A l$$

$$\omega_j = j\text{th natural frequency}$$

$$\psi_j = j\text{th mode shape}$$

$$\xi_j = j\text{th equivalent modal damping ratio}$$

Employing the Forsythe polynomials, the  $j$ th mode shape of the beam is expressed as,

$$\psi_j(x) = \sum_{k=0}^h S_{jk} p_k(x) \quad (2.5)$$

where

$$S_{jk} \quad j = 1, 2, 3 \dots ; \quad k = 1, 2, 3 \dots h$$

are the constants to be estimated from the measured data.

Defining

$$A_j = F\psi_j(a)(\omega_j^2 - \omega^2) / \{(\omega_j^2 - \omega^2)^2 + 4\xi_j^2\omega_j^2\} \quad (2.6)$$

$$B_j = 2F\psi_j(a)\omega_j\omega\xi_j / \{(\omega_j^2 - \omega^2)^2 + 4\xi_j^2\omega_j^2\} \quad (2.7)$$

The displacement response of the beam, equation (2.4), can be rewritten as

$$y(x) = \sum_{j=1}^{\infty} [A_j\psi_j(x) - iB_j\psi_j(x)]e^{i\omega x} \quad (2.8)$$

Substitution of equation (2.8) in (2.5) gives

$$y(x) = \sum_{j=1}^{\infty} \left[ (A_j - iB_j) \sum_{k=1}^h \{S_{jk}p_k(x)\} \right] e^{i\omega x} \quad (2.9)$$

Considering that only two natural modes (with natural frequencies  $\omega_m$  and  $\omega_{m+1}$ ) of the beam, lying on either side of the excitation frequency  $\omega$  (i.e.  $\omega_m < \omega < \omega_{m+1}$ ), predominantly contribute to the response (ignoring the contribution of the natural modes lying farther away from the excitation frequency), the beam response of equation (2.9), reduces to the approximation

$$y(x) = [(A_m - iB_m) \sum_{k=1}^h \{S_{mk}p_k(x)\} + (A_{m+1} - iB_{m+1}) \sum_{k=1}^h \{S_{m+1,k}p_k(x)\}]e^{i\omega x} \quad (2.10)$$

The magnitudes of the real and imaginary components of the response then, are,

$$\begin{aligned} Y_r(x) &= A_m \sum_{k=1}^h S_{mk}p_k(x) + A_{m+1} \sum_{k=1}^h S_{m+1,k}p_k(x) \\ Y_i(x) &= B_m \sum_{k=1}^h S_{mk}p_k(x) + B_{m+1} \sum_{k=1}^h S_{m+1,k}p_k(x) \end{aligned} \quad (2.11)$$

Let  $\nu_r(x_\mu)$  and  $\nu_i(x_\mu)$  be the real and imaginary components of the response amplitude actually measured, experimentally, at stations  $x_\mu$ , ( $\mu = 1, N$ ) along the

length of the beam. The corresponding Forsythe form of approximation formulated through equation (2.10), can be written as

$$\begin{aligned}
 Y_r(x_\mu) &= A_m \sum_{k=1}^h S_{mk} p_k(x_\mu) + A_{m+1} \sum_{k=1}^h S_{m+1,k} p_k(x_\mu) \\
 Y_i(x_\mu) &= B_m \sum_{k=1}^h S_{mk} p_k(x_\mu) + B_{m+1} \sum_{k=1}^h S_{m+1,k} p_k(x_\mu)
 \end{aligned} \tag{2.12}$$

The least square error between the measured amplitudes and their Forsythe approximations of equation (2.12) are

$$\begin{aligned}
 \varepsilon_r &= \sum_{\mu=1}^N [Y_r(x_\mu) - v_r(x_\mu)]^2 \\
 \varepsilon_i &= \sum_{\mu=1}^N [Y_i(x_\mu) - v_i(x_\mu)]^2
 \end{aligned} \tag{2.13}$$

Noting the orthogonality property of the Forsythe polynomials

$$\sum_{\mu=1}^N p_i(x_\mu) p_j(x_\mu) = 0 \quad i \neq j \tag{2.14}$$

and minimizing the errors with respect to the constants  $S_{mk}$  and  $S_{m+1,k}$  ( $k = 1, 2, \dots, h$ )

the following set of equations are obtained

$$\begin{aligned}
 A_m S_{mk} + A_{m+1} S_{m+1,k} &= c_k \\
 B_m S_{mk} + B_{m+1} S_{m+1,k} &= d_k \quad k = 1, 2, \dots, h
 \end{aligned} \tag{2.15}$$

with

$$\begin{aligned}
 c_k &= \sum_{\mu=1}^N v_r(x_\mu) p_k(x_\mu) / \sum_{\mu=1}^N [p_k(x_\mu)]^2 \\
 d_k &= \sum_{\mu=1}^N v_i(x_\mu) p_k(x_\mu) / \sum_{\mu=1}^N [p_k(x_\mu)]^2
 \end{aligned} \tag{2.16}$$

The expressions for constants  $S_{mk}$  and  $S_{m+1,k}$  can be written, from equations (2.14) and (2.15) as,

$$\begin{aligned} S_{mk} &= (c_k B_{m+1} / A_{m+1} - d_k) / [(B_{m+1} / A_{m+1} - B_m / A_m) A_m] \\ S_{m+1,k} &= (c_k B_m / A_m - d_k) / [(B_{m+1} / A_{m+1} - B_m / A_m)(-A_{m+1})] \end{aligned} \quad (2.17)$$

The orthogonality properties of the mode shapes of a beam of constant properties over its span ( $x=0$  to  $x=l$ ) require that

$$\int_0^l \psi_i(x) \psi_j(x) dx = 0 \quad i \neq j \quad (2.18)$$

$$\int_0^l \psi''_i(x) \psi''_j(x) dx = 0 \quad i \neq j \quad (2.19)$$

In terms of the Forsythe approximation the above modal orthogonality implies,

$$\begin{aligned} \sum_{\mu=1}^N \sum_{k=0}^h S_{ik} p_k(x_\mu) \sum_{k=0}^h S_{jk} p_k(x_\mu) &= 0 \quad i \neq j \\ \sum_{\mu=1}^N \sum_{k=0}^h S_{ik} p''_k(x_\mu) \sum_{k=0}^h S_{jk} p''_k(x_\mu) &= 0 \quad i \neq j \end{aligned} \quad (2.20)$$

Substitution in the above, from equations (2.17) for modes  $m$  and  $m+1$  and noting the relations (2.18) and (2.19), one obtains

$$\sum_{\mu=1}^N \sum_{k=0}^h (c_k B_{m+1} / A_{m+1} - d_k)(c_k B_m / A_m - d_k) p_k^2(x_\mu) = 0 \quad (2.21)$$

$$\sum_{\mu=1}^N \sum_{k=0}^h (c_k B_{m+1} / A_{m+1} - d_k) p''_k(x_\mu) \sum_{k=0}^h (c_k B_m / A_m - d_k) p''_k(x_\mu) = 0 \quad (2.22)$$

Using the values of  $c_k, d_k$  (computed from experimental data, equation (2.16)) equations (2.21) and (2.22) can be readily solved for the ratios  $B_m / A_m$  and  $B_{m+1} / A_{m+1}$ . These ratios are further substituted in equations (2.17) to obtain the constants  $S_{mk}$  and  $S_{m+1,k}$  as multiples of  $A_m$  and  $A_{m+1}$  respectively.

Usage of  $S_{mk}$  and  $S_{m+1,k}$ , thus determined, in equation (2.17), give the approximations for the  $m$ th and  $(m+1)$ th mode shapes,  $\psi_m(x)$  and  $\psi_{m+1}(x)$ , respectively.

## 2.3 Natural Frequency Estimates

The mode shapes of a beam, irrespective of its boundary conditions, are governed by the differential equation,

$$\psi''''_m(x) = \chi_m^4 \psi_m(x) \quad (2.23)$$

where  $(\cdot)$  denotes differentiation with respect to  $x$ .

The spatial frequency  $\chi_m$  is related to the natural frequency  $\omega_m$  of the beam as,

$$\chi_m^4 = \omega_m^2 (\rho A / EI) \quad (2.24)$$

( $\rho$ ,  $A$ ,  $E$ ,  $I$  being the mass density, area of cross section, modulus of elasticity and area moment of inertia of beam).

The spatial frequency can be obtained from (2.23) as,

$$\chi_m^4 = S_{mk} p_k''''(x_\mu) / S_{mjk} p_k(x_\mu) \quad (2.25)$$

and the natural frequency  $\omega_m$  can be readily calculated from equation (2.24).

## 2.4 Remarks

Participation of two modes, lying on either side of the excitation frequency, in the overall response of the beam, can be approximately quantified through the procedure developed. Successive application of the algorithm at different excitation frequencies for estimation of desired number of mode shapes and their refinement is described in the next chapter.

## CHAPTER 3

### SUCCESSIVE MODAL APPROXIMATION

The procedure developed for estimation of adjacent modal participation, in the previous chapter, is employed to successively estimate the characteristics of the desired number of modes. The step-by-step procedure to carry out these approximations is described here, along with numerical illustrations for some of the common type of boundary configurations, namely, simply-supported, clamped-clamped and cantilever. The accuracy of the estimates and mode shape refinement is also discussed.

#### 3.1 Algorithm for successive modal approximation

Following the procedure described in the previous chapter, the characteristics of desired number of modes can be obtained by repeated application of the algorithm, through appropriate selection of

- (i) frequency of excitation force and
- (ii) location of the excitation force.

In a practical situation the boundary conditions of beams, may not behave ideally, i.e. the boundary configuration may not ideally be simply supported or fixed-fixed or cantilever etc. Since the focus of the present study is to obtain an accurate mode shape description, one of its major application can be in the area of obtaining correct definitions of the boundary conditions of a given beam configuration. Though, this task has not been attempted in the present study, it has been kept as a guideline in developing the step-by-step procedure for successive modal estimation.

Depending on boundary configurations a beam can be expected to have natural modes from any one of the following categories-

- (i) nodes at both ends (e.g. simply-supported, fixed-fixed, one end fixed- other end simply-supported etc.)



- (ii) node at one end and anti-node at the other end (e.g. cantilever i.e. fixed at one end and free at the other end)
  - (iii) anti-nodes at both the ends (e.g. free-free case)
- (Beams with intermediate supports are not discussed here)

3

The first mode in category (iii) corresponds to the zero natural frequency case, which signifies rigid body mode. The higher modes, however, belong to category (i), and therefore the vibration mode categories reduce to the first two listed above. Modal approximation algorithms are developed for Category (i) and Category (ii) separately.

Category (i) nodes at both ends (e.g. simply-supported, fixed-fixed, etc.)

Typical mode shapes of simply supported and fixed-fixed beam configurations are shown in Figures 3.1 (a) and (b), respectively. The mode shapes can be seen to be of two types -

- (a) symmetric with respect to the mid-point (odd modes,  $2i - 1$ ,  $i = 1, 2, \dots$ )
- (b) anti-symmetric with respect to the mid-point (even modes,  $2i$   $i = 1, 2, \dots$ )

### Step 1: Estimation of Symmetric Modes

The first step is to select the location of the excitation force at, approximately, the mid-point of the beam. Such a mid-point excitation is expected to primarily energize the symmetric modes (the nodal points of anti-symmetric modes being at the beam mid-point). The frequency of the excitation force needs to be chosen appropriately. An *a-priori* estimate of the fundamental frequency, if available, from basic test tests, like the rap-test, can help (the case, of no *a-priori* knowledge of the fundamental frequency, is discussed later). In case such an estimate,  $p_1$ , is available, the excitation frequency,  $\omega_1$ , can be chosen to be slightly above this frequency (say  $\omega_1 = 1.2p_1$ ) so that the response is primarily contributed from the first two odd modes (i.e. mode 1 and mode 3). Ignoring the contributions from higher symmetric modes (mode 5, mode 7 etc.), the approximations for the first and third mode shapes can be obtained, through the methodology discussed in the previous chapter. Simultaneously, approximations of the first and third natural frequencies are also obtained.

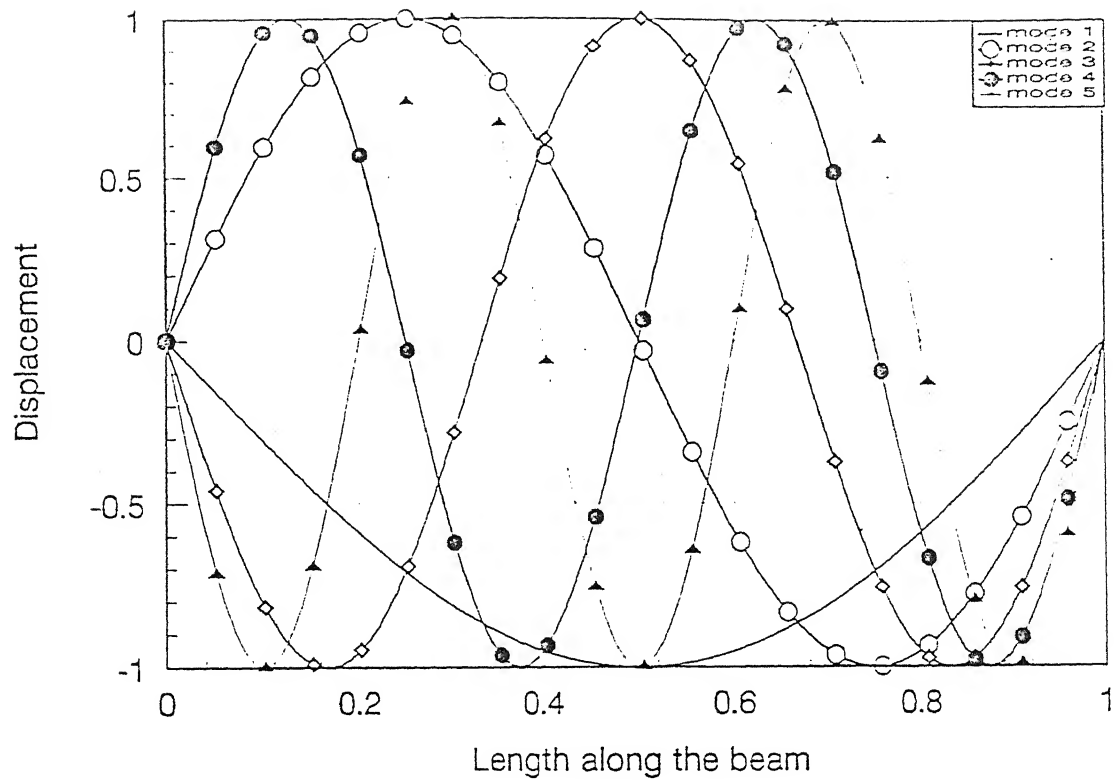


Fig. 3.1(a) Exact mode shapes of simply supported beam

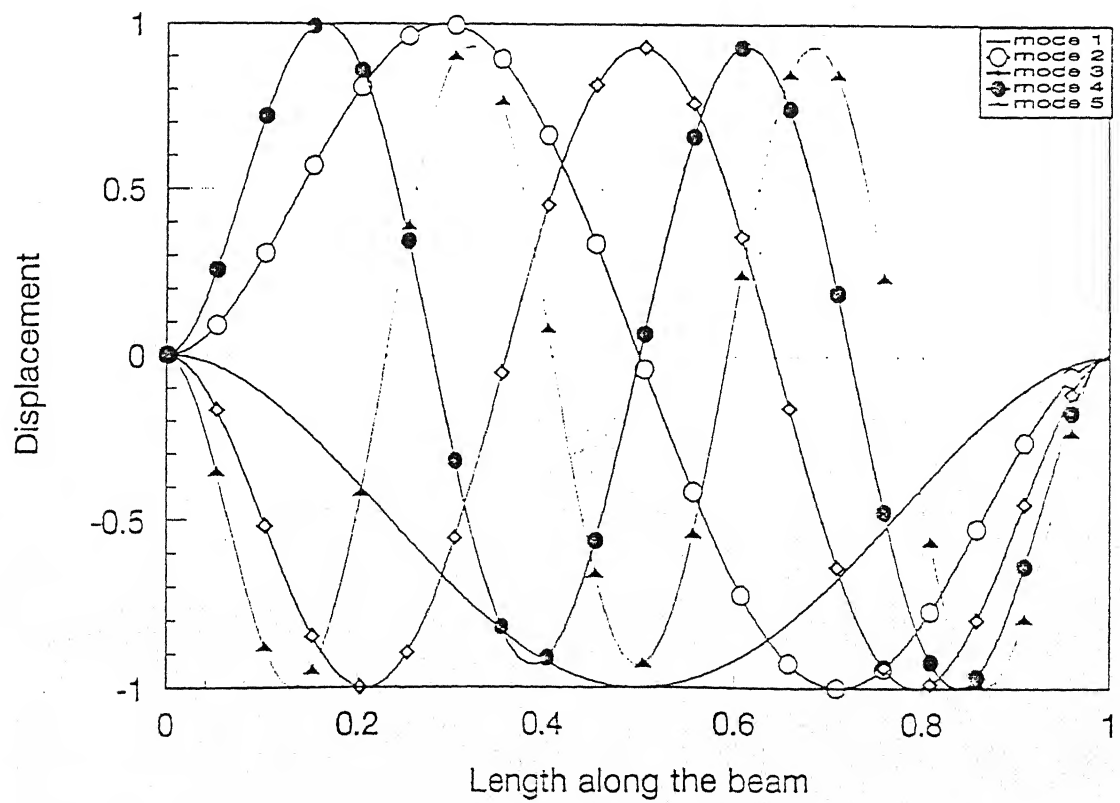


Fig. 3.1(b) Exact mode shapes of fixed-fixed beam

Armed with an approximation of the third natural frequency,  $p_3$ , the next step would be to excite the beam, at its mid-point, at a frequency,  $\omega_2$ , slightly above its third natural frequency (say  $\omega_2 = 1.2p_3$ ). The response now, has contributions from primarily from the third and fifth modes. However, it may also contain significant contribution from the first mode. Since, the first mode has already been approximated, its contribution can be subtracted from the response and the resultant can be fed as input to the algorithm for estimation of the third and fifth mode shapes and natural frequencies. The next excitation frequency,  $\omega_3$ , can be above the fifth natural frequency  $p_5$  and the process can be continued further for estimation of the desired number of symmetric modes. All these estimates can be termed as ‘first approximations’.

### Step 2: Estimation of Anti-Symmetric Modes

The ‘first approximations’ of the anti-symmetric modes can be obtained through a similar step-by-step procedure. From the knowledge of the nodal points of the symmetric modes, estimated as described above, the location of excitation force, can be chosen close to such a nodal point so as to suppress the contribution of the corresponding mode in the response. Choosing the nodal point of mode 3 (at a distance  $l/3$  or  $2l/3$ , from one of the ends), the beam can be given an excitation at a frequency,  $\omega_4$ , such that  $p_1 < \omega_4 < p_3$ . The modes that will get excited are 1, 2, 4, 5,... The contributions of mode 1 and 5, which have already been estimated above, can be subtracted from the total response and the resultant can be fed as input to the algorithm for obtaining the ‘first estimates’ of the anti-symmetric modes 2 and 4. The process can be continued further, through excitation at the nodal points of the symmetric mode 5 and so on, to get the ‘first estimates’ of the higher anti-symmetric modes.

### Step 3: Refinement

It should be noted that, the algorithm gives an estimate of two modes, at a time. The ‘first estimates’ carry errors, since the algorithm treats the beam response to be constituted of just the two modes that it estimates. Refinement can be carried out, by repeating Steps 1 and 2. Since the ‘first estimates’ of the modes are now available, the

contribution of all others, except for the two modes being refined can be subtracted from the total response of the beam, before feeding it as input to the algorithm. The iterations can continue in this manner, till the difference between two successive sets of estimates is less than desired accuracy.

Category (ii) node at one end - anti-node at the other end (e.g. cantilever)

Typical mode shapes of a cantilever beam are shown in Figures 3.1 (c). Unlike, the previous category, the modes of a cantilever beam cannot be classified as symmetric or anti-symmetric and it would be simpler to keep the location of excitation identically at the free-end, for all runs of the algorithm.

#### First Estimates:

As in the previous category, if an *a-priori* knowledge of the first natural frequency,  $p_1$ , exists the excitation frequency,  $\omega_1$ , can be chosen to be slightly above  $p_1$  (say,  $\omega_1 = 1.2 p_1$ ), so that the primary contributions to the beam response are from mode 1 and 2. 'First estimates' of these two modes can be obtained by feeding this response as input to the algorithm. Having estimated the natural frequencies of modes 1 and 2, the excitation frequency can be slightly above the second natural frequency (say,  $\omega_2 = 1.2 p_2$ ). The contribution of mode 1, through its 'first estimate', can be subtracted from the beam response, so that the resultant has contributions mainly, from modes 2 and 3. Feeding this resultant as input to the algorithm, modes 2 and 3 are determined. The procedure can be continued by, next, exciting the beam at a frequency slightly higher than the highest natural frequency determined, for obtaining the 'first estimates' of the higher modes.

#### Refinement:

The 'first estimates' can be refined, by repeating the above process. However, this time the contributions of all modes, except the two of interest, are to be subtracted from the beam responses, through their 'first estimates'. The resultant of the response, thus, is a better representation of the contributions of the two modes being estimated by the algorithm.

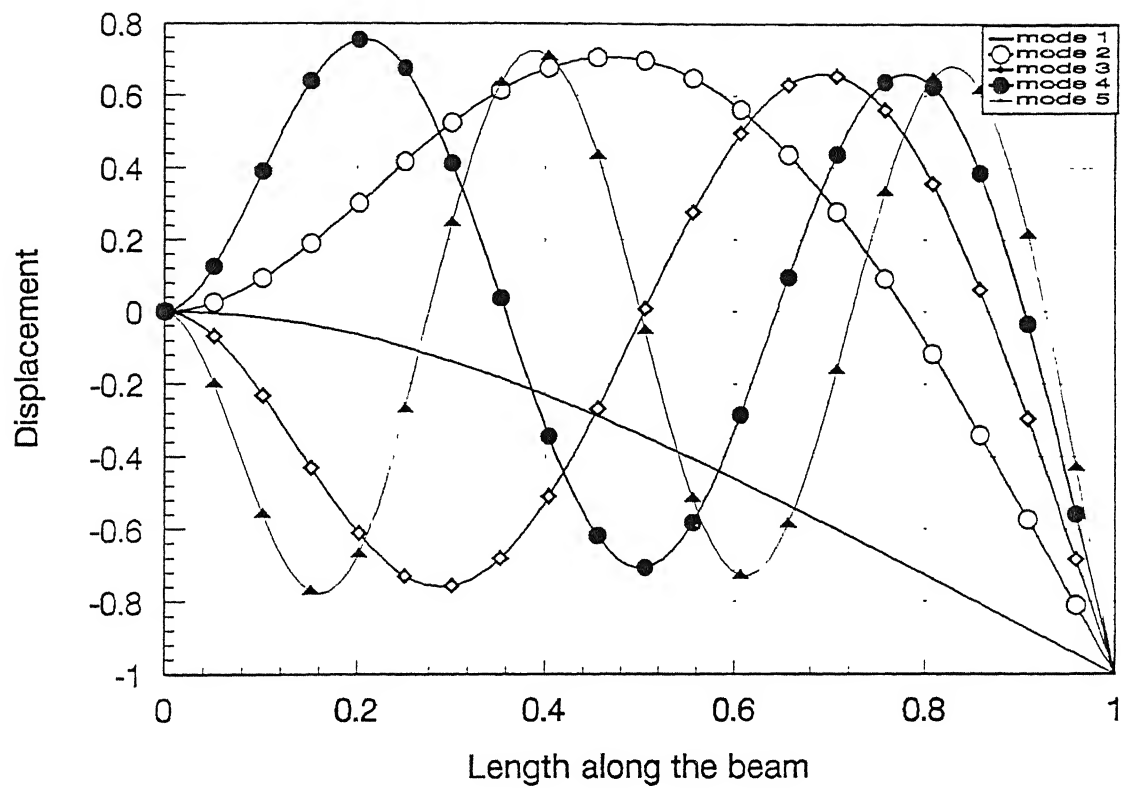


Fig. 3.1(c) Exact mode shapes of cantilever beam

In the procedures described above, the starting point was excitation of the beams at a frequency slightly above their fundamental frequency. In cases where an *a-priori* knowledge of this fundamental frequency may not exist, the frequency chosen to excite the beam lies between the  $i$ th and  $(i+1)$ th natural frequencies, the algorithm takes the entire response of the beam to be constituted of the  $i$ th and  $(i+1)$ th modes and gives estimates of these two mode shapes. The numerical values of  $i$  and  $(i+1)$  can be readily found out from the mode shapes, by counting the number of nodes and anti-nodes. The algorithm will also give estimates of the  $i$ th and  $(i+1)$ th natural frequencies. By judiciously choosing the next excitation frequency lower than the  $i$ th natural frequency and continuing the process, the fundamental frequency can be traced back.

It should be noted here, that the procedures outlined can not be employed as a black box. Step-by-step analysis of the results is essential along with the step-by-step application of the algorithm.

The procedures have been illustrated through computer simulation. The illustrations are carried out in terms of nondimensional parameters.

### 3.2 Non-Dimensional Parameters

The response of the beam, subjected to a desired excitation, is simulated through a computer program employing standard response formulae (Timoshenko, 1928). This simulated response is treated as the 'measured' response of the beam and fed as input to the modal estimation algorithm described in the previous chapter.

The response of a beam, subjected to a force  $F_0 e^{i\alpha x}$  at a point  $x = a$ , along its length, can be written in nondimensional terms as (refer, equation 2.4)

$$H(x) = \sum_{j=1}^{\infty} [\bar{A}_j \psi_j(x) - \bar{B}_j \psi_j(x)] e^{i\alpha x} \quad (3.1)$$

where

$$H(x) = y(x) / y_{st}$$

and

$$\begin{aligned}
y_{st} &= F / \rho A l \omega_1^2 \\
r_j &= \omega / \omega_j \\
\bar{A}_j &= \psi_j(a)(1 - r_j^2) / ((1 - r_j^2)^2 + 4\xi_j^2 r_j^2) \\
\bar{B}_j &= \psi_j(a)(2r_j) / ((1 - r_j^2)^2 + 4\xi_j^2 r_j^2)
\end{aligned} \tag{3.2}$$

The geometric and material properties of the beam are incorporated in a nondimensional parameter,  $\kappa$ , defined as

$$\kappa = [EI / \rho g A l^3]^{(1/2)} \tag{3.3}$$

( $g$ , the gravitational acceleration is taken as  $9.81 \text{ m/s}^2$ ).

The nondimensional parameter,  $\kappa$ , establishes the relationship between the  $j$ th spatial frequency  $\chi_j$  and the  $j$ th natural frequency  $\omega_j$ , through the following expression (refer equation 2.24)

$$\omega_m = \chi_m^2 \kappa (gl^3)^{1/2} \tag{3.4}$$

Referring to equations (2.4)-(2.9) and taking the response to be constituted primarily of the  $m$ th and  $(m+1)$ th beam modes, which lie on either side of the excitation frequency,  $\omega$ , the magnitudes of the real and imaginary components of the response the nondimensionalised Forsythe approximation of the response are

$$\begin{aligned}
H_r(x) &= \bar{A}_m \sum_{k=1}^h S_{mk} p_k(x) + \bar{A}_{m+1} \sum_{k=1}^h S_{m+1,k} p_k(x) \\
H_i(x) &= \bar{B}_m \sum_{k=1}^h S_{mk} p_k(x) + \bar{B}_{m+1} \sum_{k=1}^h S_{m+1,k} p_k(x)
\end{aligned} \tag{3.5}$$

Defining, the real and imaginary components of the measured response in nondimensional terms as

$$\begin{aligned}
q_r(x) &= v_r(x) \omega_1^2 / (F / \rho A l) \\
q_i(x) &= v_i(x) \omega_1^2 / (F / \rho A l)
\end{aligned} \tag{3.6}$$

the non-dimensionalised least square errors are

$$\begin{aligned}
\bar{\varepsilon}_r &= \sum_{\mu=1}^N [H_r(x) - q_r(x)]^2 \\
\bar{\varepsilon}_i &= \sum_{\mu=1}^N [H_i(x) - q_i(x)]^2
\end{aligned} \tag{3.7}$$

The non-dimensionalised errors are now minimized with respect to  $S_{mk}$  and  $S_{m+1,k}$  ( $k = 1, 2, \dots, h$ ) for estimation of the constants  $S_{mk}$  and  $S_{m+1,k}$  and subsequently the  $m$ th and  $(m+1)$ th modal parameters, as described in the previous chapter.

### 3.3 Numerical illustrations

The numerical studies for successive modal parameter estimation has been carried out for the following three beam configurations.

- (i) Simply-Supported
- (ii) Cantilever (Clamped-Free)
- (iii) Fixed-fixed (Clamped-Clamped).

The estimation, using the computer simulated response is carried out for a value of the nondimensional beam parameter,  $\kappa = 0.1$ . The procedure is illustrated for estimation of the first five beam modes. The damping ratios,  $\xi_1, \dots, \xi_5$ , are chosen as 0.02 for illustration. The nondimensional input force amplitude,  $F / \rho g A l$  is kept as 100 in all the cases.

#### Simply supported:

The illustration is carried, with an assumption that an *a-priori* knowledge of the fundamental frequency exists. (This frequency can be readily obtained, as mentioned



earlier, through simple rap-tests and analysis of the consequent transient response) The fundamental frequency, in this case (with  $\kappa = 0.1$ ) is 3.09 rads/s, (Rao-1986)

The step-by-step modal estimation procedure is implemented as follows.

- (a) The beam is harmonically excited at its mid-point at a frequency of 3.71 rads/s ( $= 1.2 \times 3.09$  rads/s). Figures 3.2 (a) and (b) show the in-phase and out-of-phase components of the computer simulated spatial response  $H(x)$ , using equation (3.2). The response is plotted as a function of the nondimensional distance,  $x/l$ , along the beam. The response of the beam is constituted of contributions from all the symmetric natural modes (modes 1, 3, 5,.....) of the beam. The estimation procedure is applied by picking up this spatial response at hundred number of points along the beam. Reference can be made to a previous study (Vaze, 1998) for a discussion on the influence of the number of these measurement points and the influence of possible random measurement errors. The algorithm was found to be robust in the presence of measurement noise. The estimates of modes lying adjacent to the excitation frequency (mode 1 and mode 3, in this case) are shown in Figs. 3.3 (a) and (b), along with the exact mode shapes of the beam. The estimate of the corresponding spatial frequencies,  $\chi$ , are shown in Figs. 3.4 (a) and (b) and the error in mode shapes is as shown in Fig. 3.5 (a) and (b). It should be noted here that estimates of the spatial frequencies,  $\chi$ , (Rao-1986) can be obtained through application of equation (2.25) at any point  $x_\mu$ , along the beam. Figs. 3.4 (a), (b) show the estimates of  $\chi$  at all measurement points. The exact spatial frequencies are also shown in the graphs as straight lines. The error in the estimates of  $\chi$  can be seen to be considerable. Also, the error is not identical across the beam length. It needs to be emphasized that the computation of the spatial frequency  $\chi$ , involves a fourth order numerical differentiation. A central-difference scheme is employed for this numerical differentiation, which carries inherent errors.

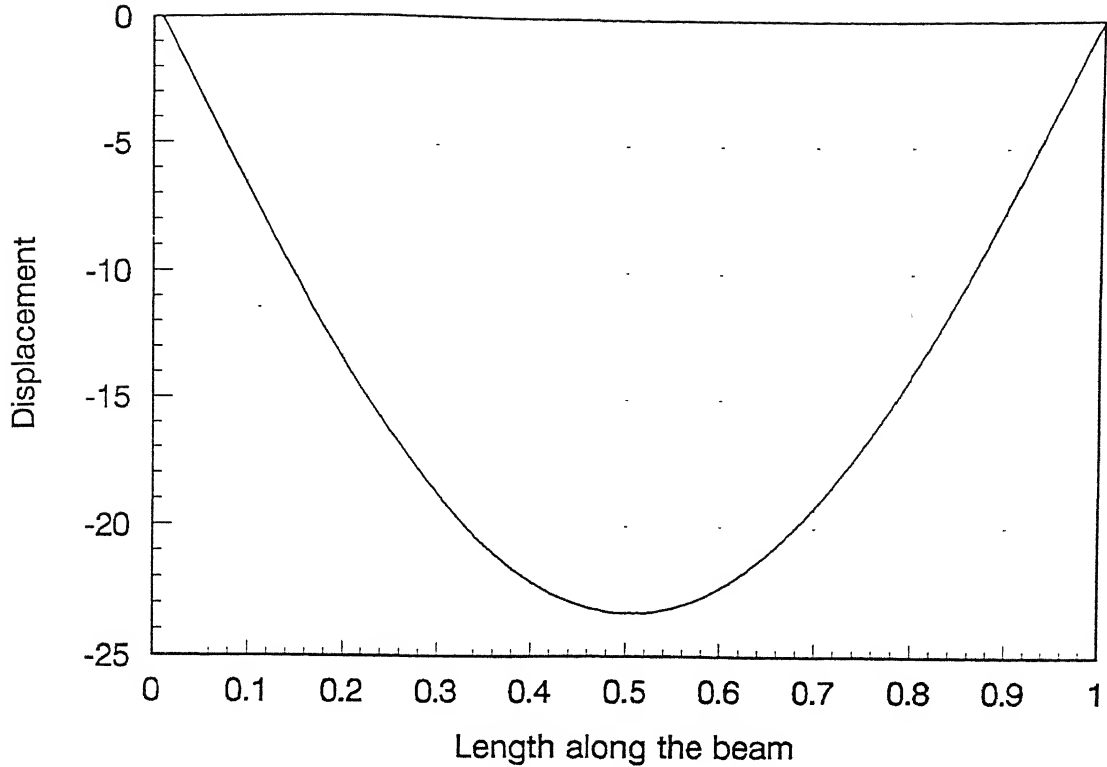


Fig 3.2(a) In-phase response of simply supported beam  
 (Location of excitation force,  $x/l = 0.5$   
 Excitation frequency = 3.71 rad/s)

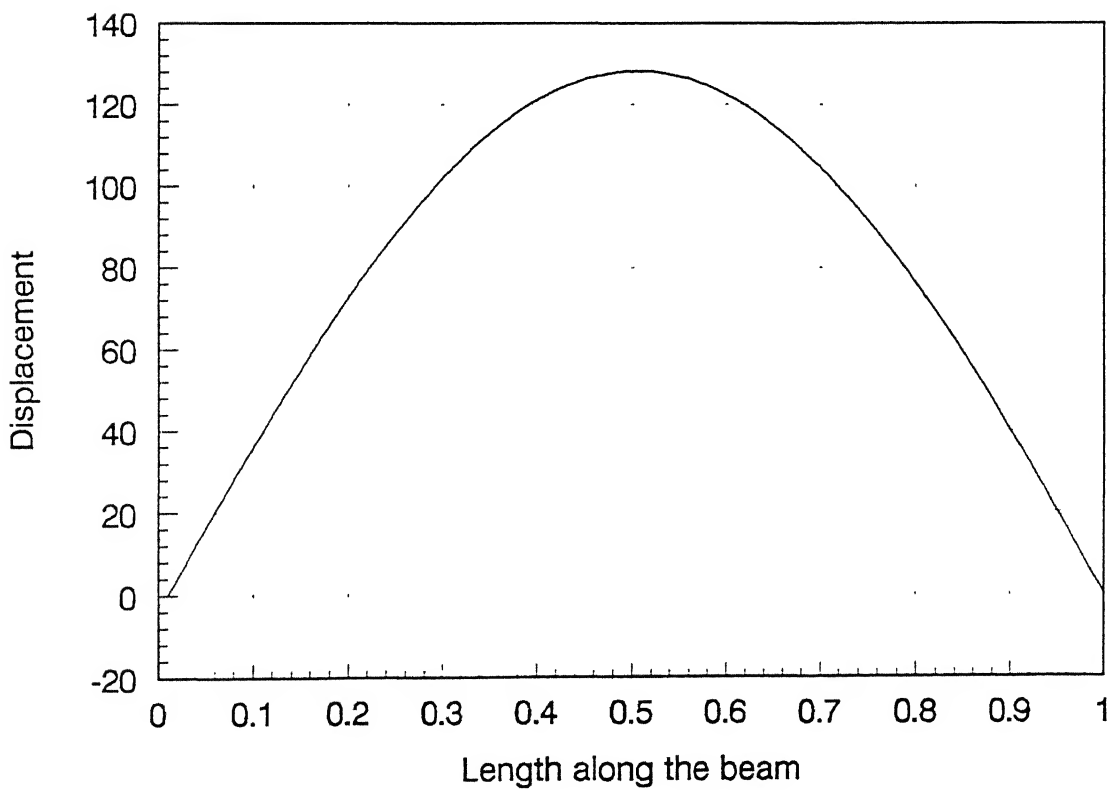


Fig. 3.2(b) Out of phase response of simply supported beam  
 (Location of excitation force,  $x/l = 0.5$   
 Excitation frequency = 3.71 rad/s)

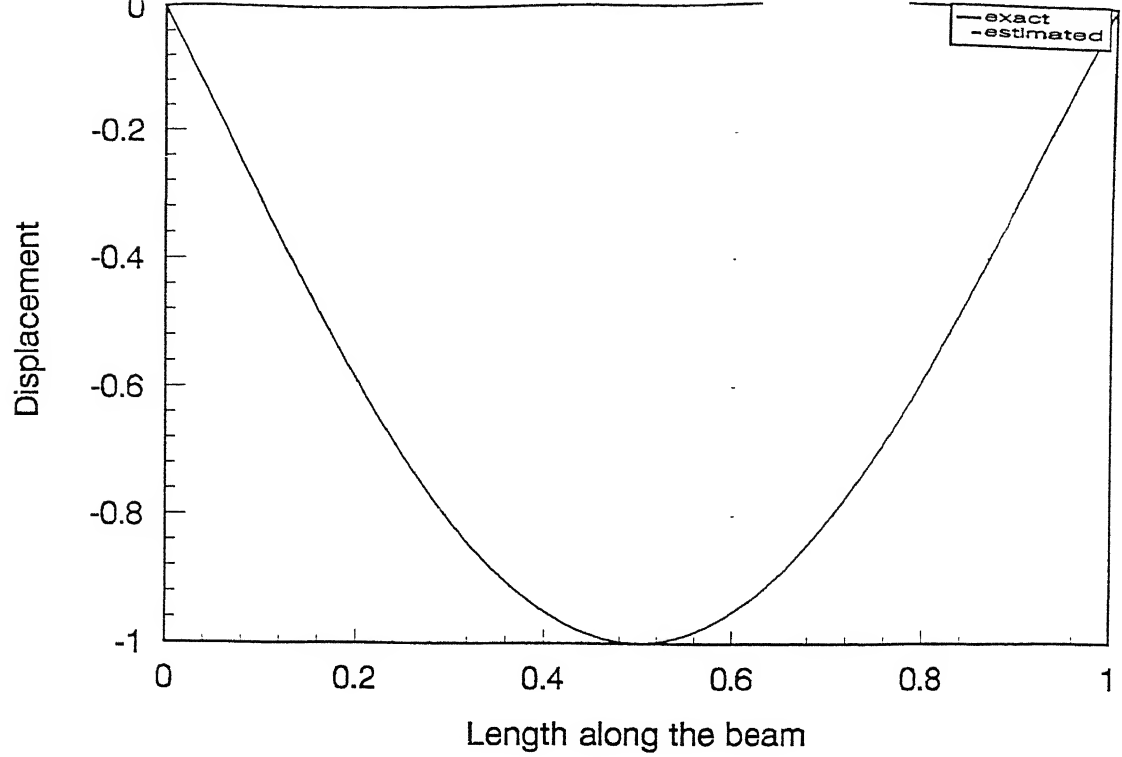


Fig. 3.3(a) First approximation of mode 1: simply supported beam

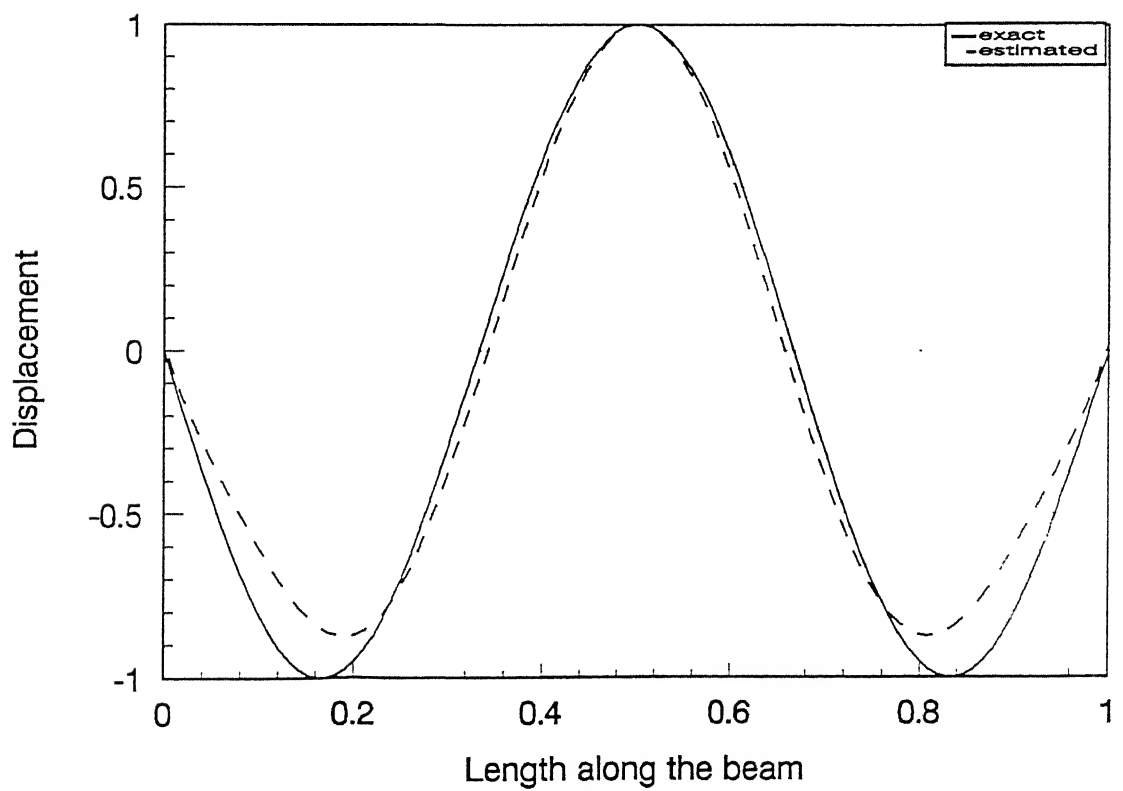


Fig. 3.3(b) First approximation of mode 3: simply supported beam

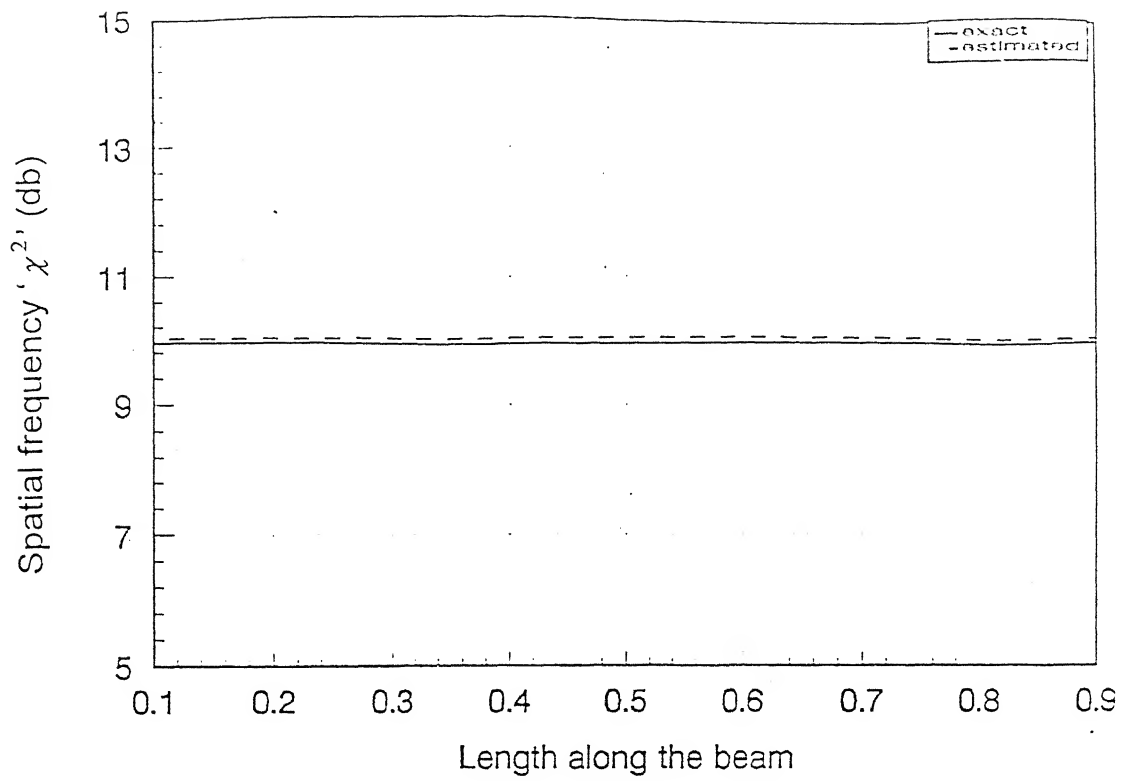


Fig. 3.4(a) First approximation of Spatial frequency: mode 1: simply supported beam.

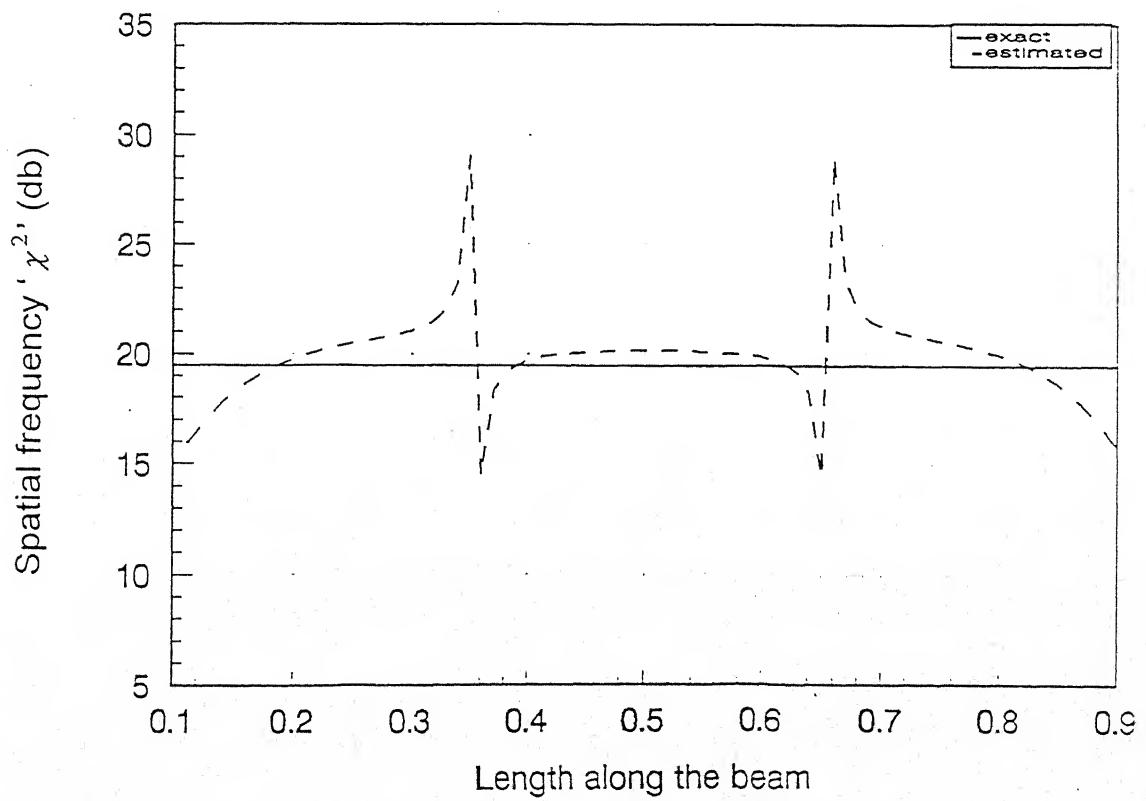


Fig. 3.4(b) First approximation of Spatial frequency: mode 3: simply supported beam

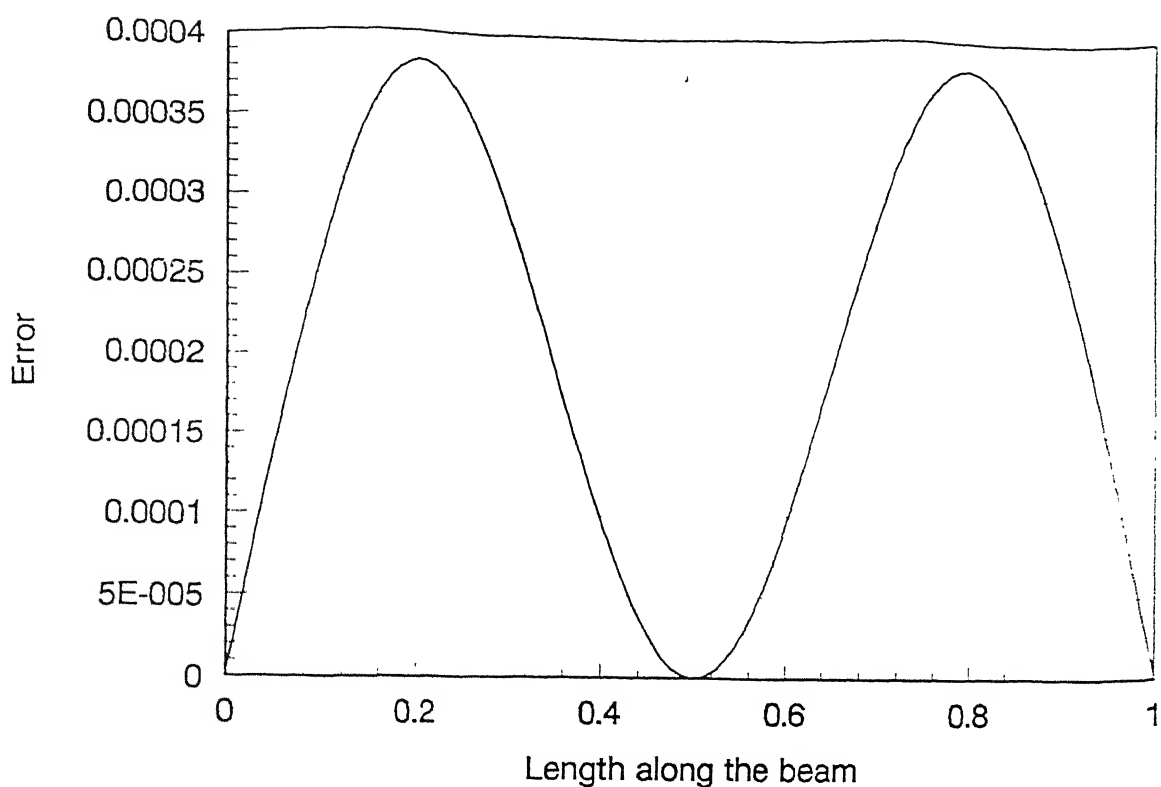


Fig. 3.5(a) Error in the first approximation of mode 1: simply supported beam

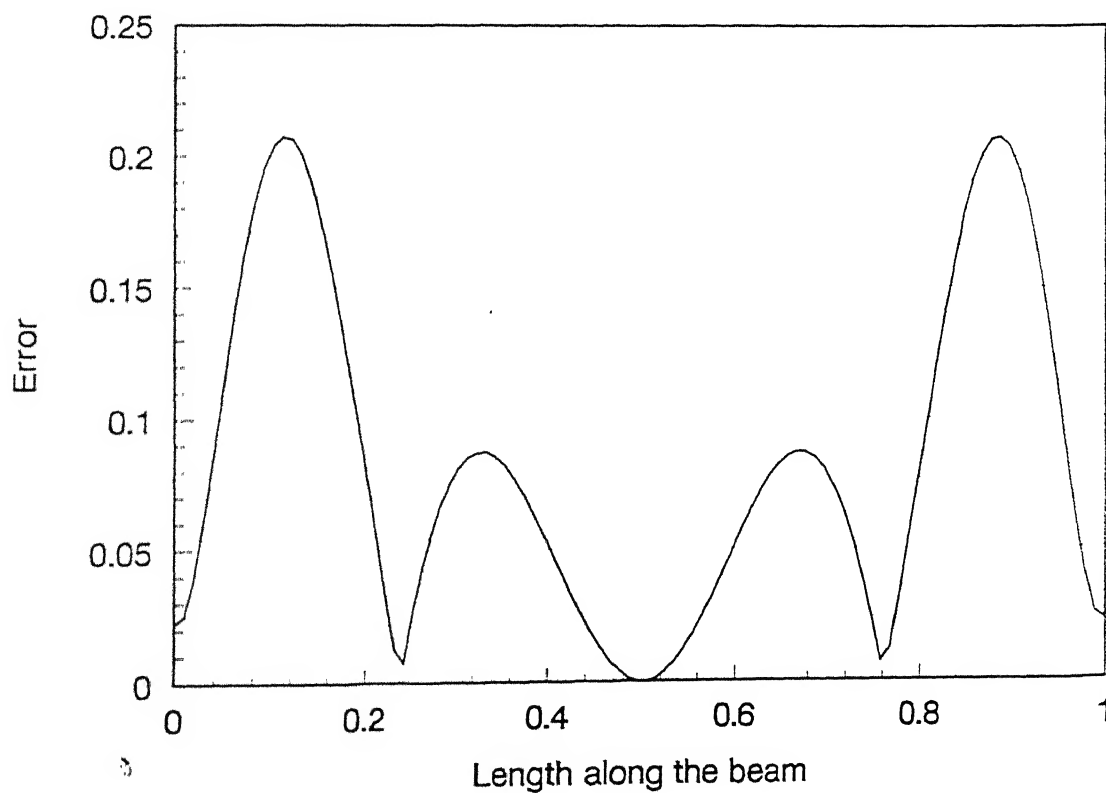


Fig. 3.5(b) Error in the first approximation of mode 3: simply supported beam

It was observed, during the present study, that the numerical differentiation scheme is not ideally suited for the spatial frequency and consequent natural frequency estimation. It can be said that natural frequency estimation should be carried out through conventional modal analysis routes (free or forced vibration tests), while the focus of spatial analysis of the present study should remain confined to obtaining accurate descriptions of mode shapes. However, for the present work, the means of the  $\chi$  curves are taken as the estimates of the spatial frequencies. The corresponding natural frequencies, consequently computed using equation (2.24) are 3.081 rads/s. for mode 1 and 32.480 rads/s. for mode 3.

- (b) The excitation is next applied at the mid-point, at a frequency of 38.856 rads/s. ( $=1.2 \times 32.380$  rads/s.). The beam response is shown in Figs. 3.6 (a), (b). The contribution of the first mode, estimated above, is subtracted from this response. The resultant, shown in Figs. 3.7 (a), (b), is fed as input to the algorithm and modes 3 and 5 are estimated. The estimated mode shapes, spatial frequencies and the error in mode shapes are given in Figs. 3.8 (a), (b), 3.9 (a), (b) and 3.10 (a), (b) respectively. The natural frequencies computed using equation (2.24) are 31.528 rads/s. for mode 3 and 37.409 rads/s. for mode 5.
- (c) The anti-symmetric modes are estimated now, by choosing the excitation force location at  $x/l = 1/3$ , which is a nodal point of mode 3. The simulated response is given in Figs. 3.11 (a), (b). The excitation frequency is the mean of the estimated first and third natural frequencies estimated above ( $17.781$  rads/s.  $= \{3.081 + 32.480\}/2$ ). The beam response is shown in Figs. 3.11 (a), (b). The contribution of the first mode, estimated in (a), is subtracted from this response. The resultant, shown in Figs. 3.12 (a), (b), is fed as input to the algorithm and modes 2 and 4 are estimated. The estimated mode shapes, spatial frequencies and the errors in mode shapes are given in Figs. 3.13 (a), (b), 3.14 (a), (b), and 3.15 (a), (b) respectively. The natural frequencies computed using equation (2.24) are 16.905 rads/s. for mode 2 and 75.386 rads/s. for mode 4.

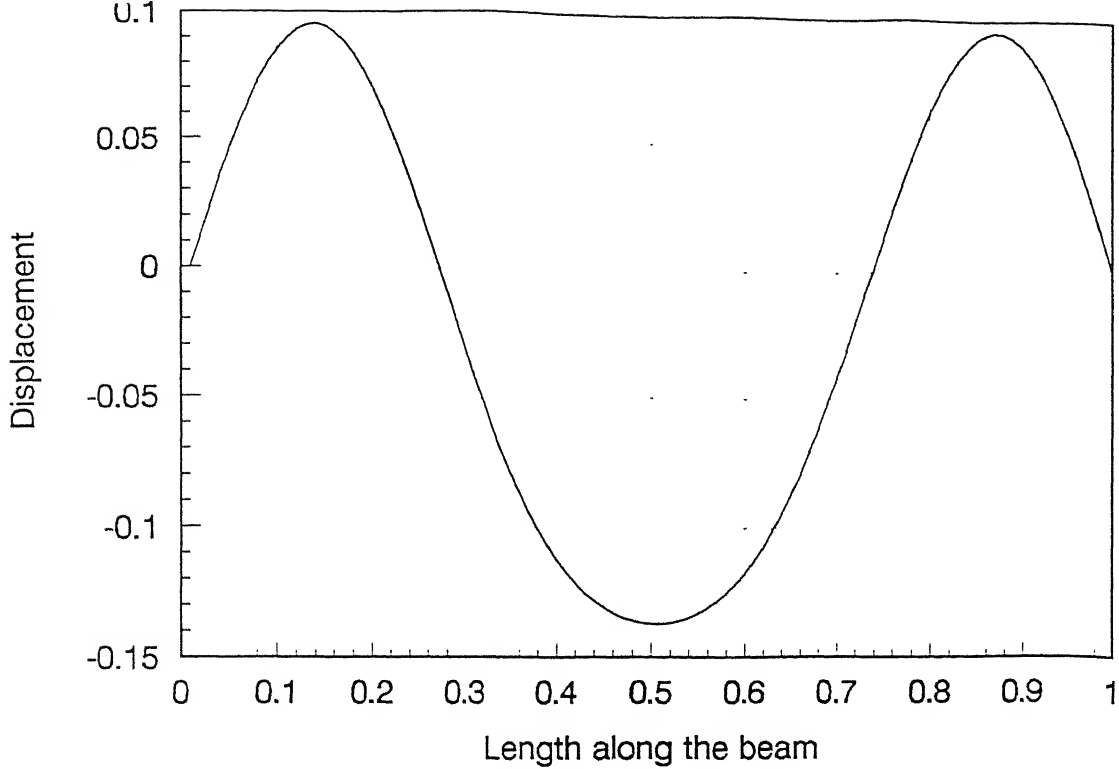


Fig. 3.6(a) In-phase response of the simply supported beam  
 (Location of excitation force,  $x/l = 0.5$   
 Excitation frequency = 38.856 rad/s)

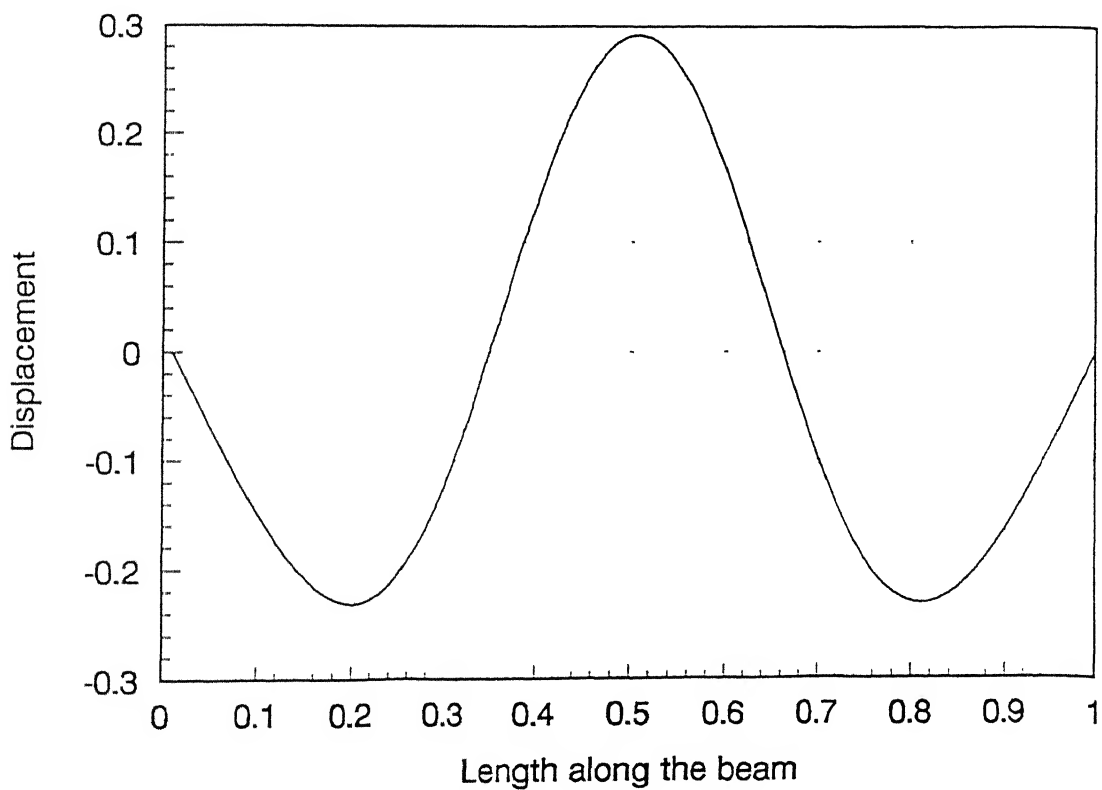


Fig. 3.6(b) Out of phase response of the simply supported beam  
 (Location of excitation force,  $x/l = 0.5$   
 Excitation frequency = 38.856 rad/s)

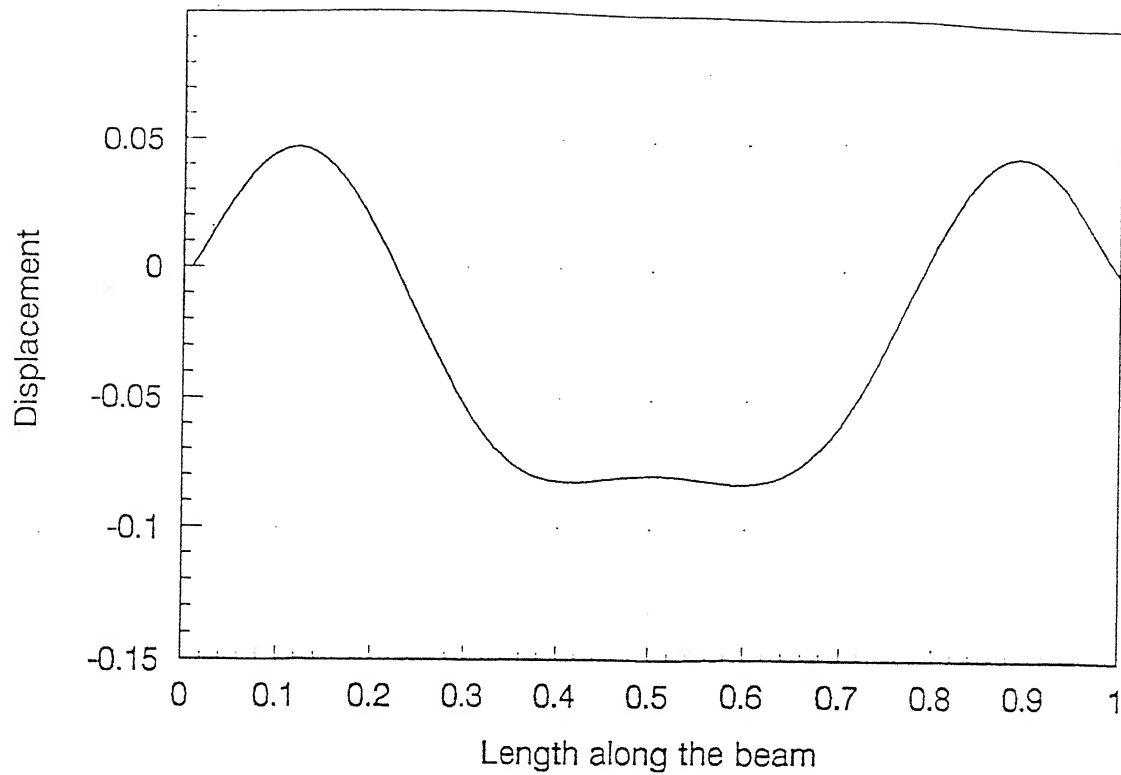


Fig. 3.7(b) Out of phase response of simply supported beam after subtracting the contribution of 1<sup>st</sup> mode  
 (Location of excitation force,  $x/l = 0.5$   
 Excitation frequency = 38.856 rad/s)

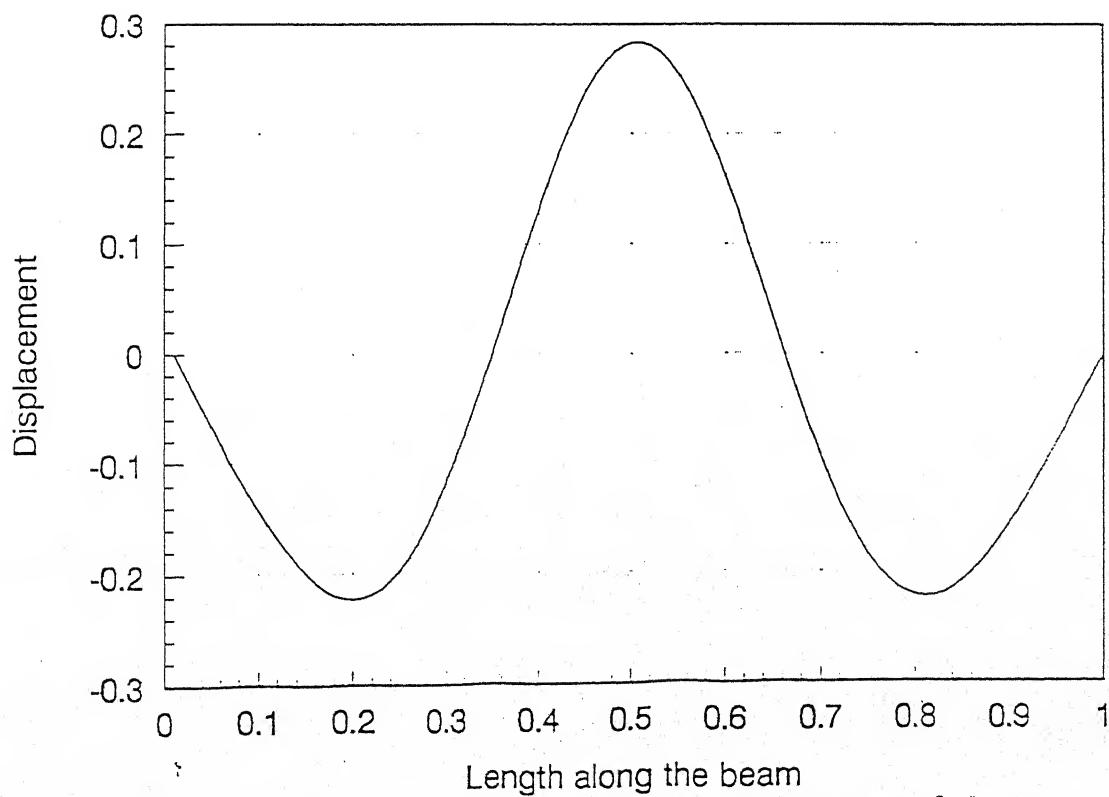


Fig. 3.7(a) In-phase response of simply supported beam after subtracting the contribution of 1<sup>st</sup> mode  
 (Location of excitation force,  $x/l = 0.5$   
 Excitation frequency = 38.856 rad/s)



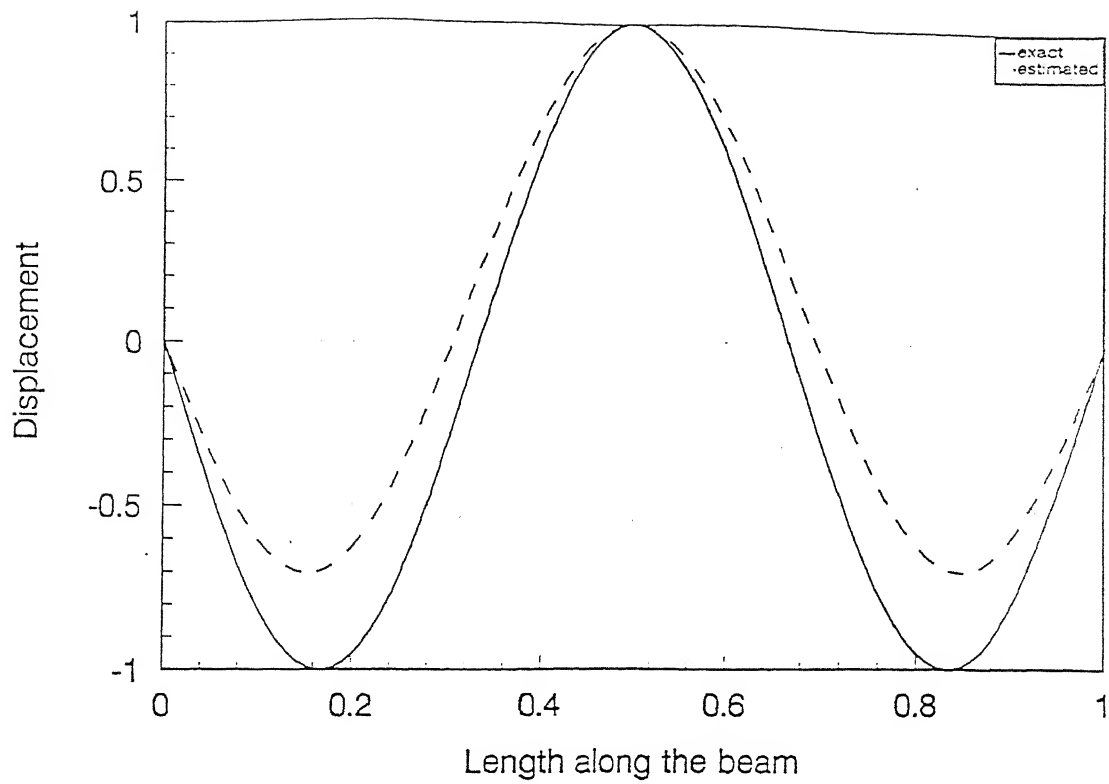


Fig. 3.8(a) First approximation of mode 3; simply supported beam

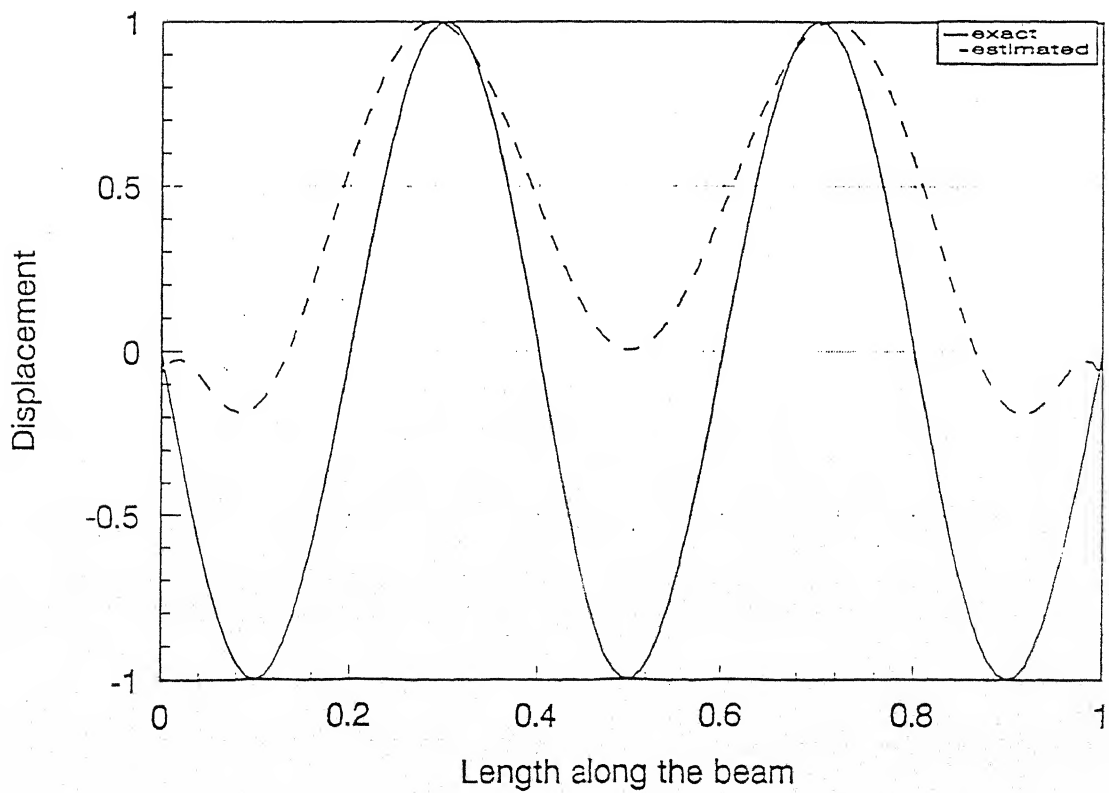


Fig. 3.8(b) First approximation of mode 5 : simply supported beam

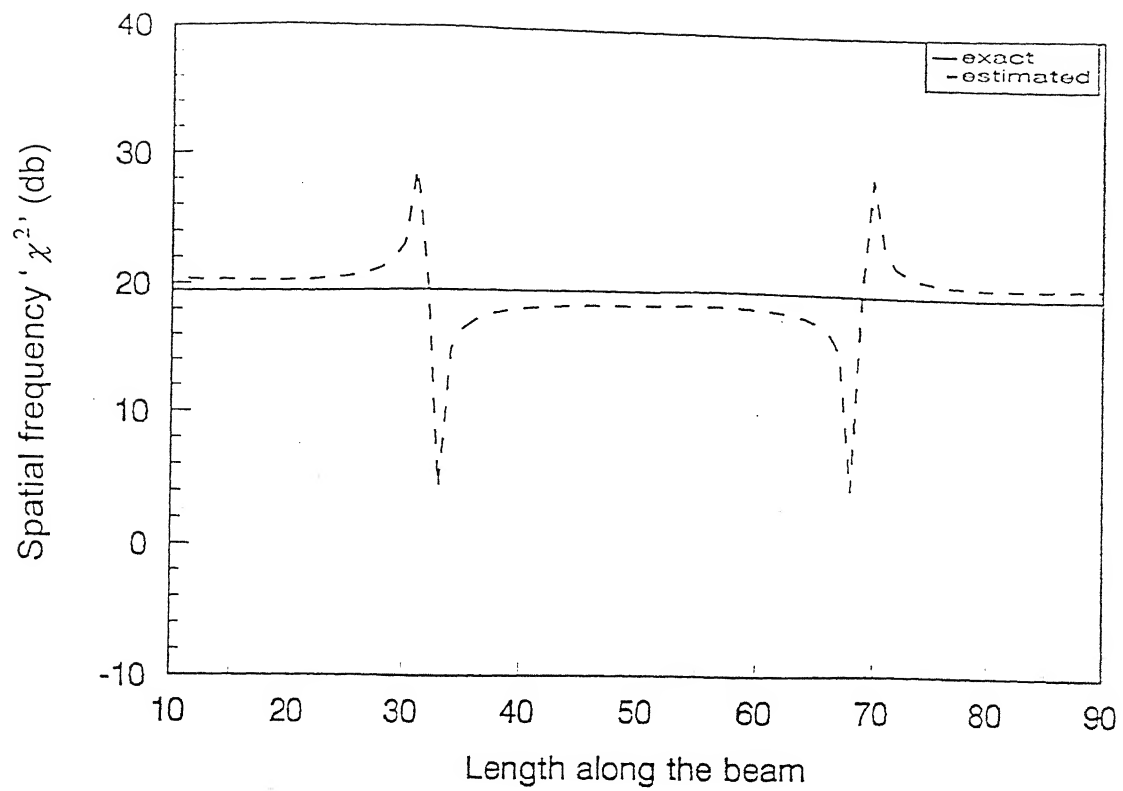


Fig. 3.9(a) First approximation of Spatial frequency: mode 3: simply supported beam

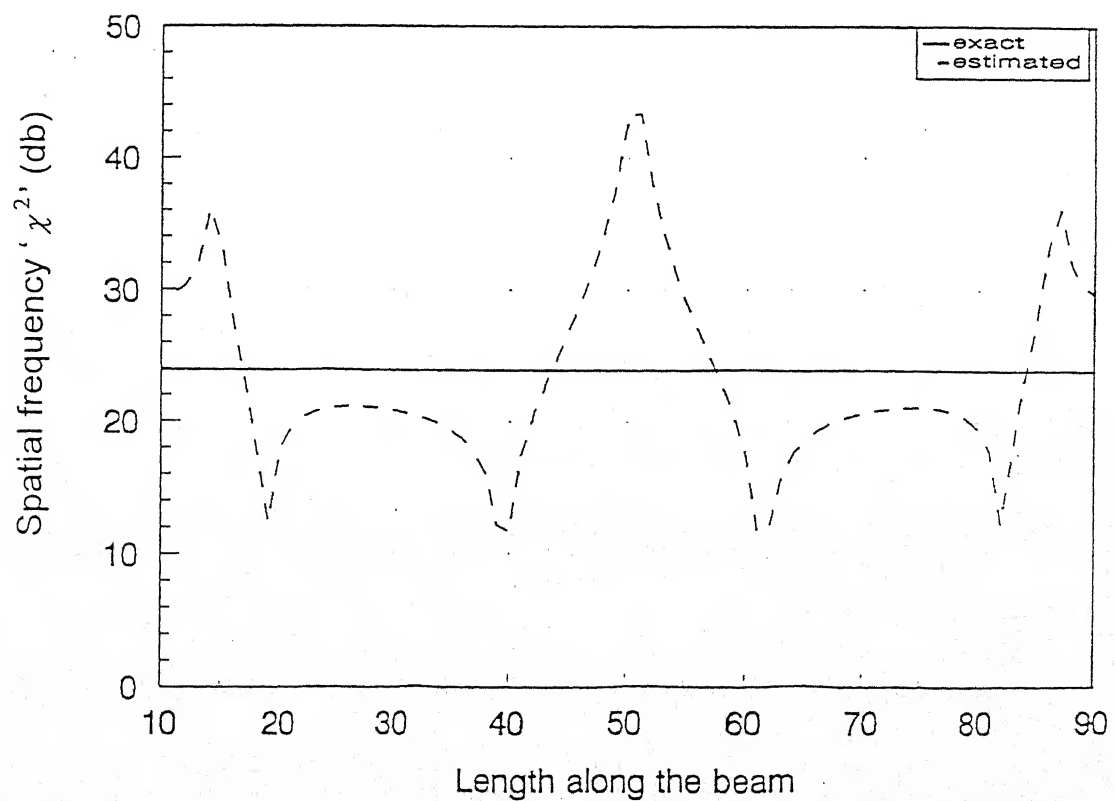


Fig. 3.9(b) First approximation of Spatial frequency: mode 5: simply supported beam

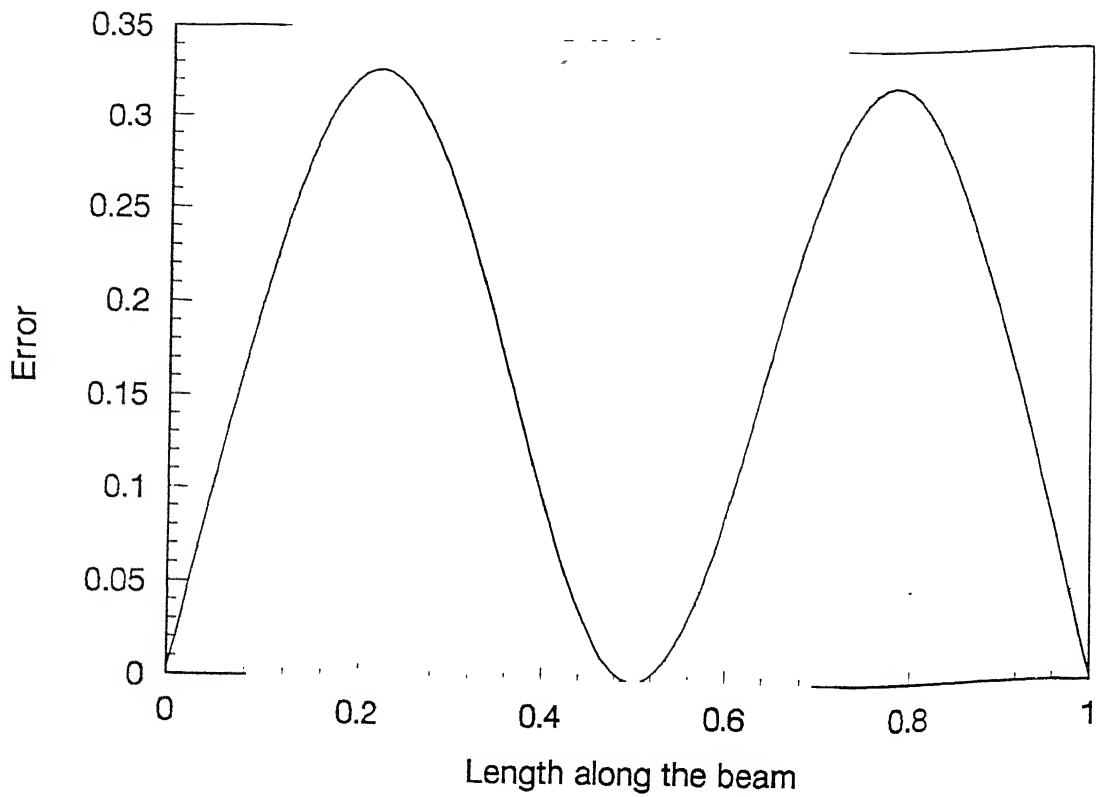


Fig. 3.10(a) Error in the first approximation of mode 3; simply supported beam

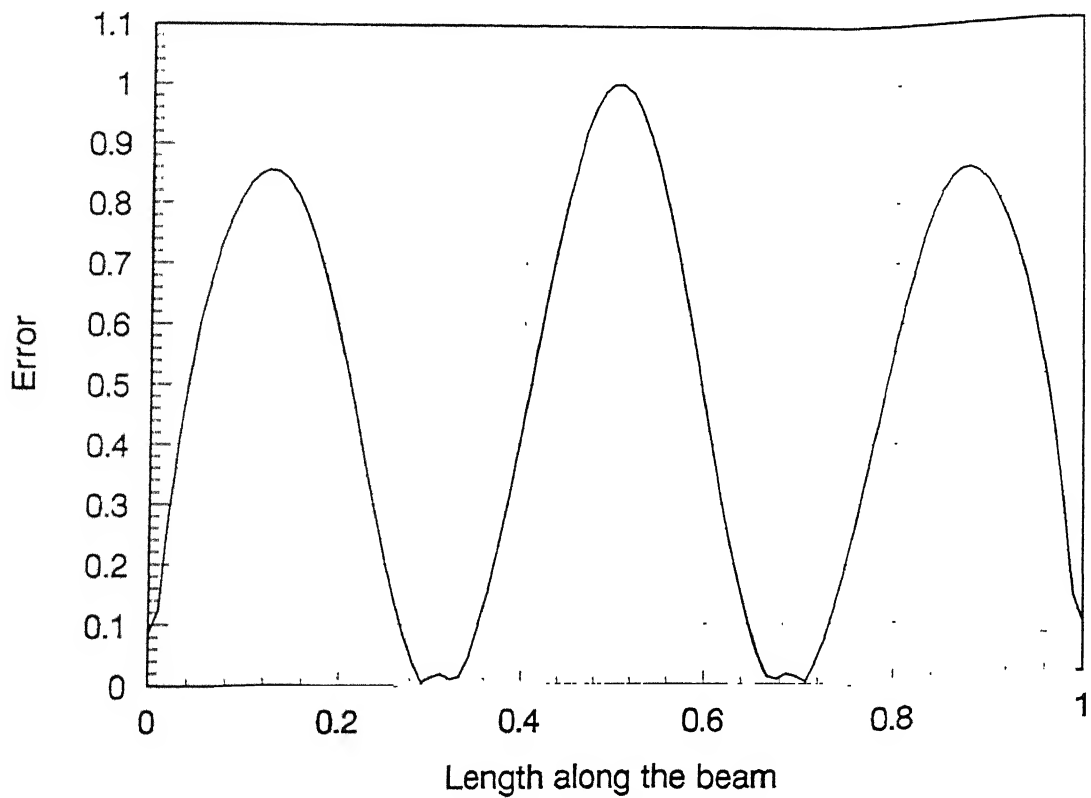


Fig. 3.10(b) Error in the first approximation of mode 5: simply supported beam

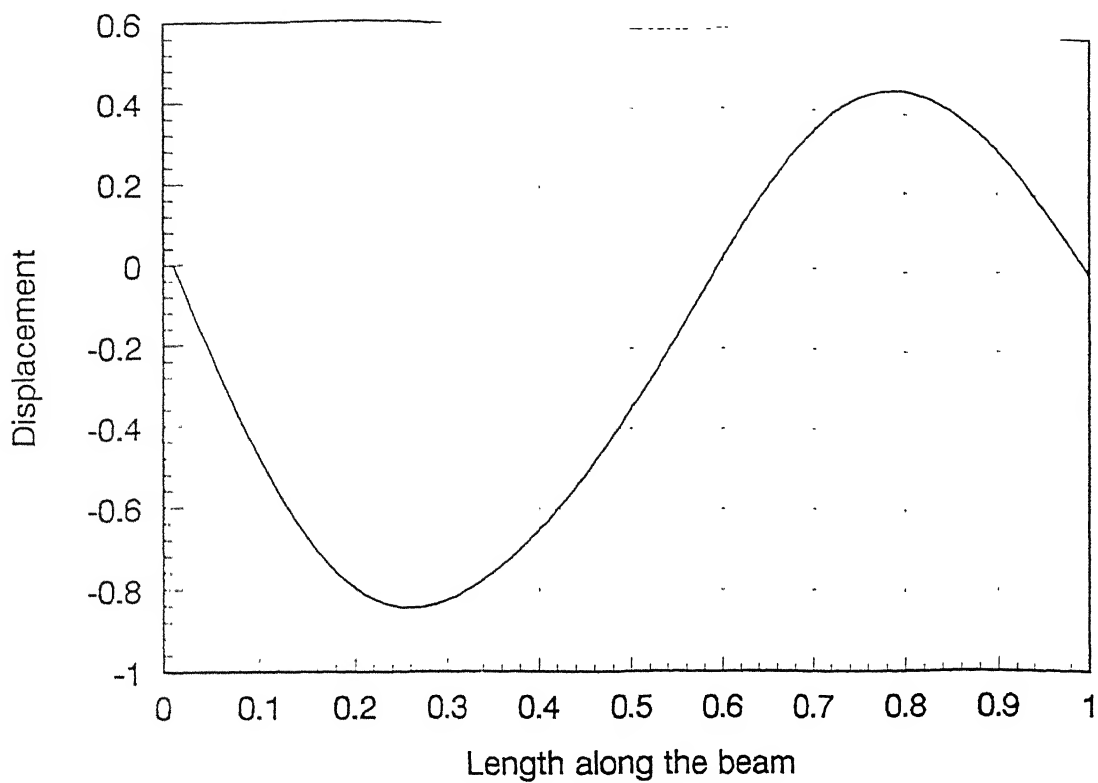


Fig. 3.11(a) In-phase response of the simply supported beam  
 (Location of excitation force,  $x/l = 0.33$   
 Excitation frequency = 17.781 rad/s)

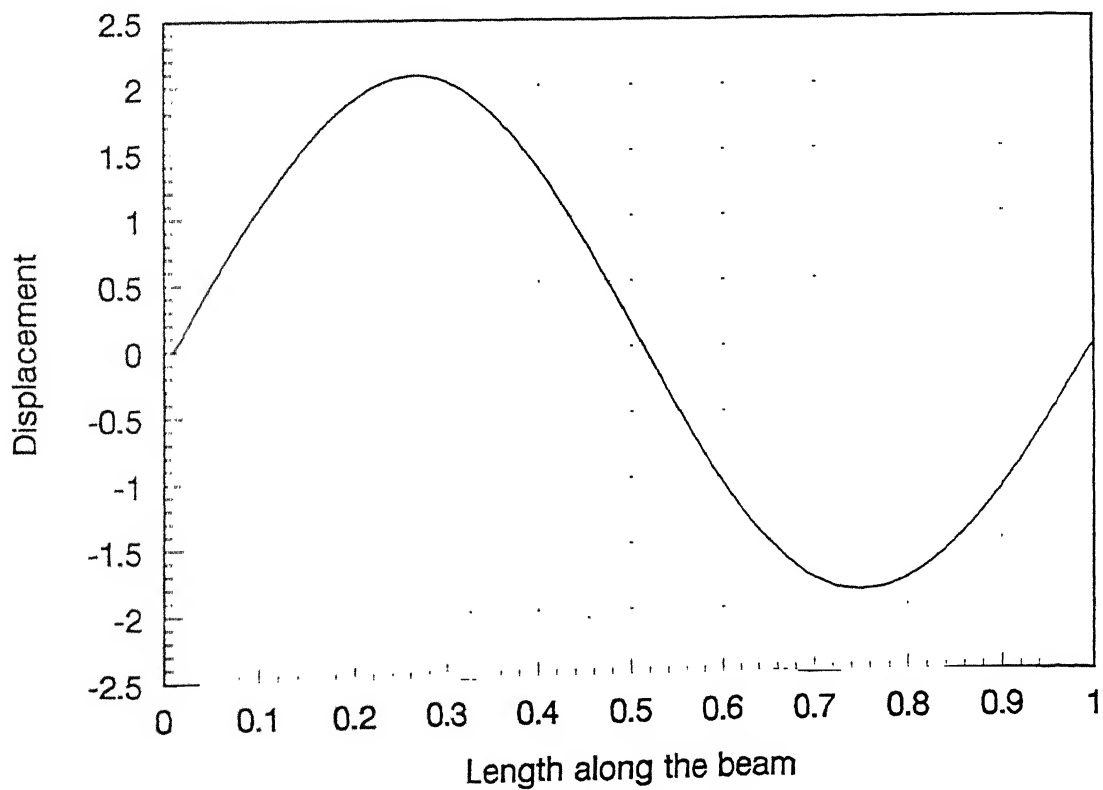


Fig. 3.11(b) Out of phase response of the simply supported beam  
 (Location of excitation force,  $x/l = 0.33$ )

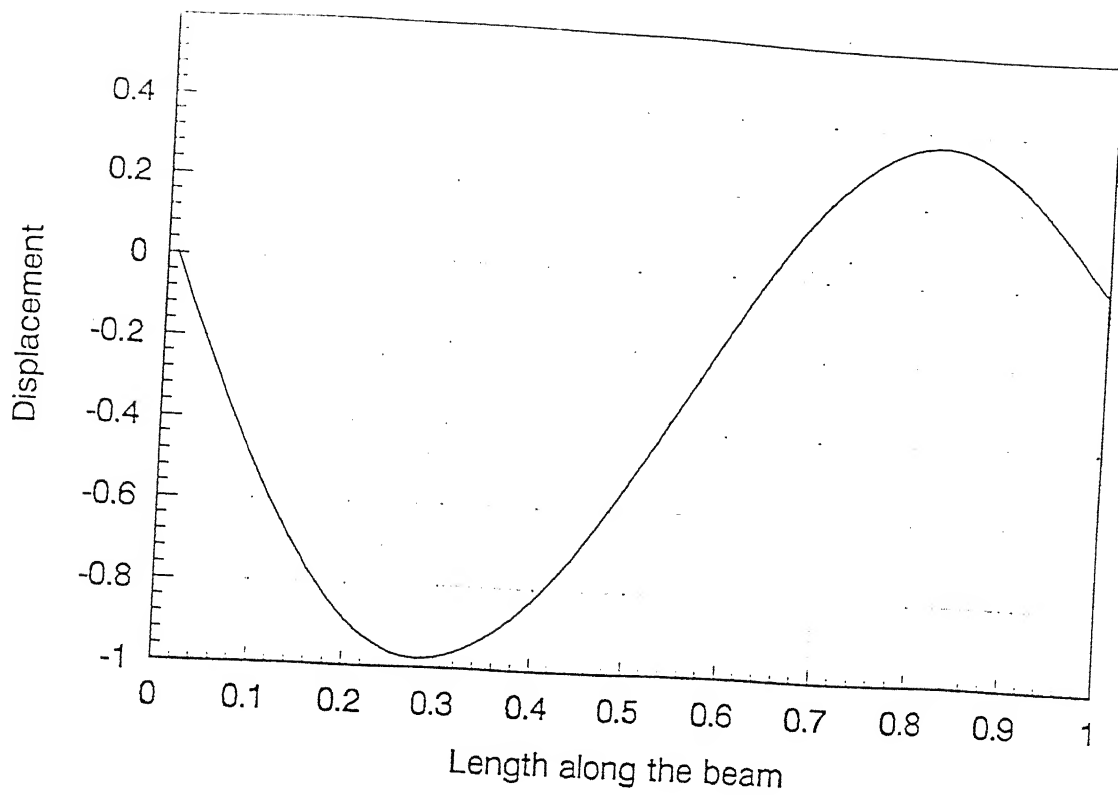


Fig. 3.12(a) In-phase response of simply supported beam after subtracting the contribution of 1<sup>st</sup> mode  
 (Location of excitation force,  $x/l = 0.33$   
 Excitation frequency = 17.781 rad/s)

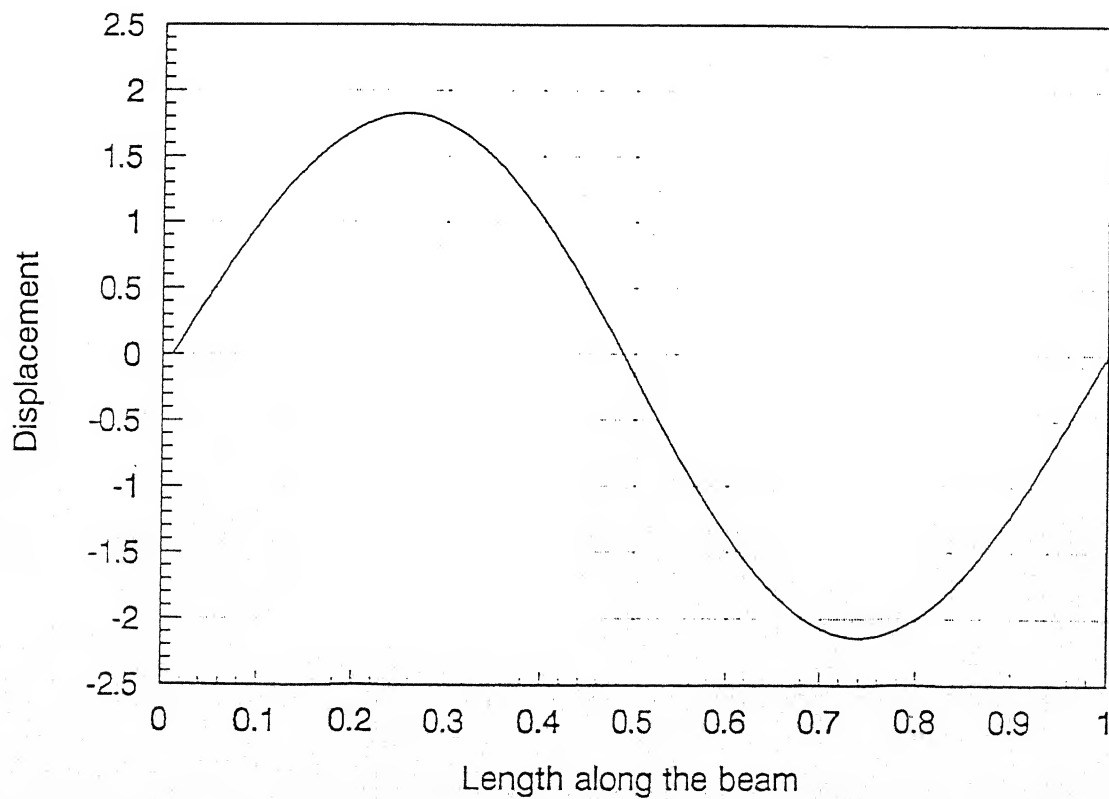


Fig. 3.12(a) Out of phase response of simply supported beam after subtracting the contribution of 1<sup>st</sup> mode  
 (Location of excitation force,  $x/l = 0.33$   
 Excitation frequency = 17.781 rad/s)

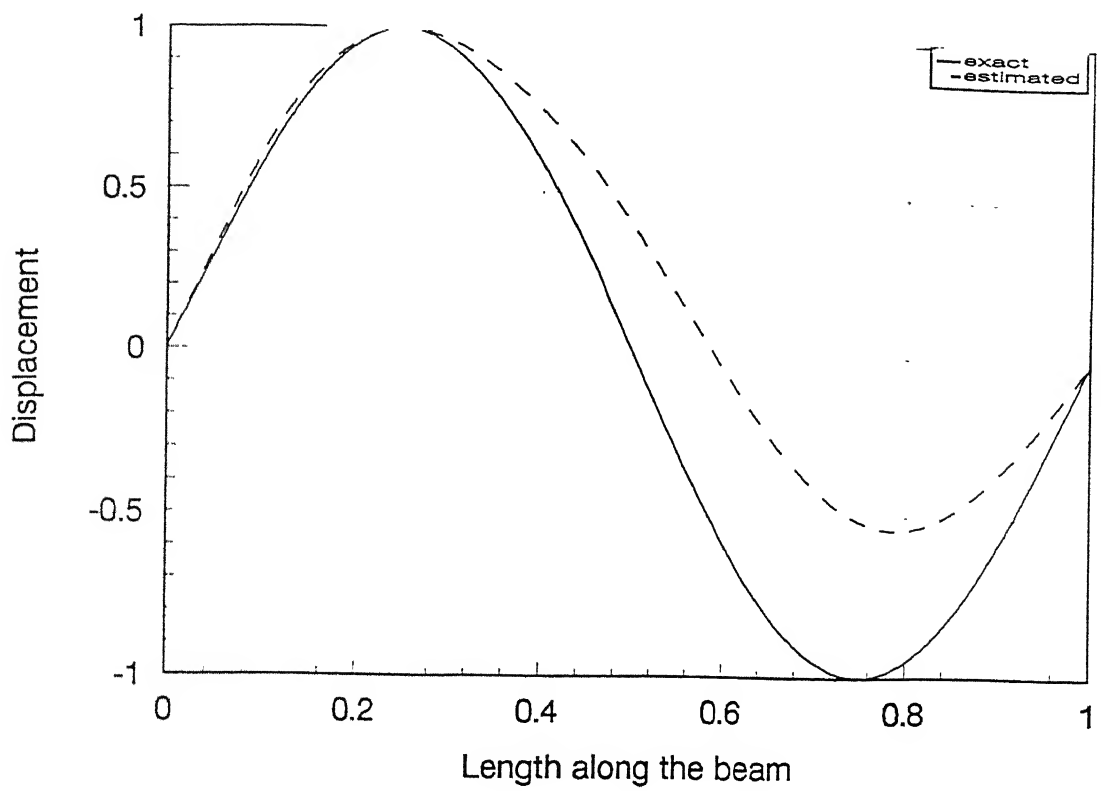


Fig. 3.13(a) First approximation of mode 2: simply supported beam

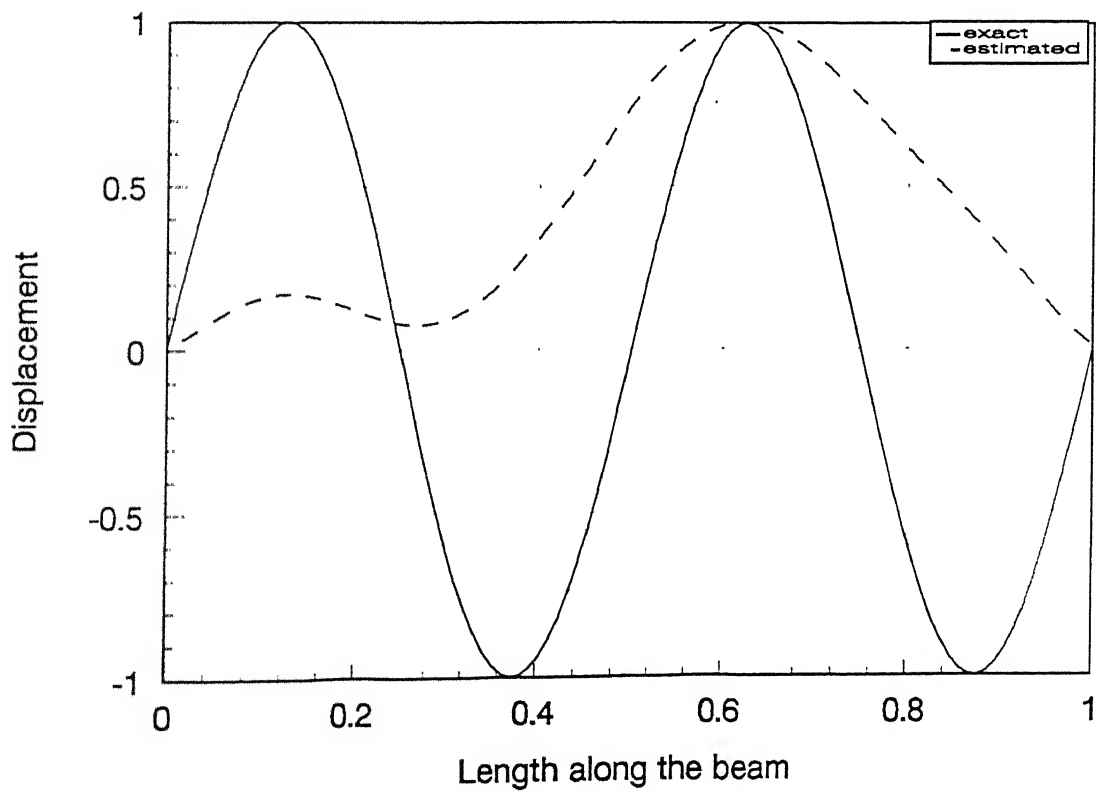


Fig. 3.13(b) First approximation of mode 4: simply supported beam

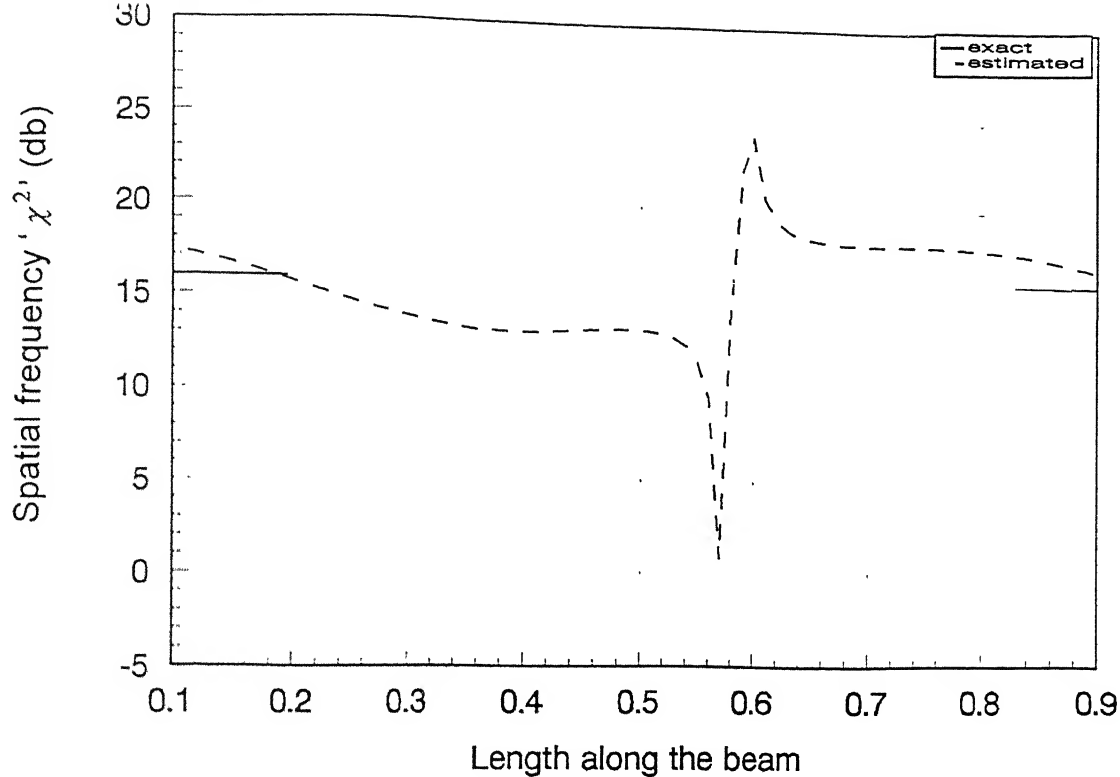


Fig. 3.14(a) First approximation of Spatial frequency: mode 2: simply supported beam

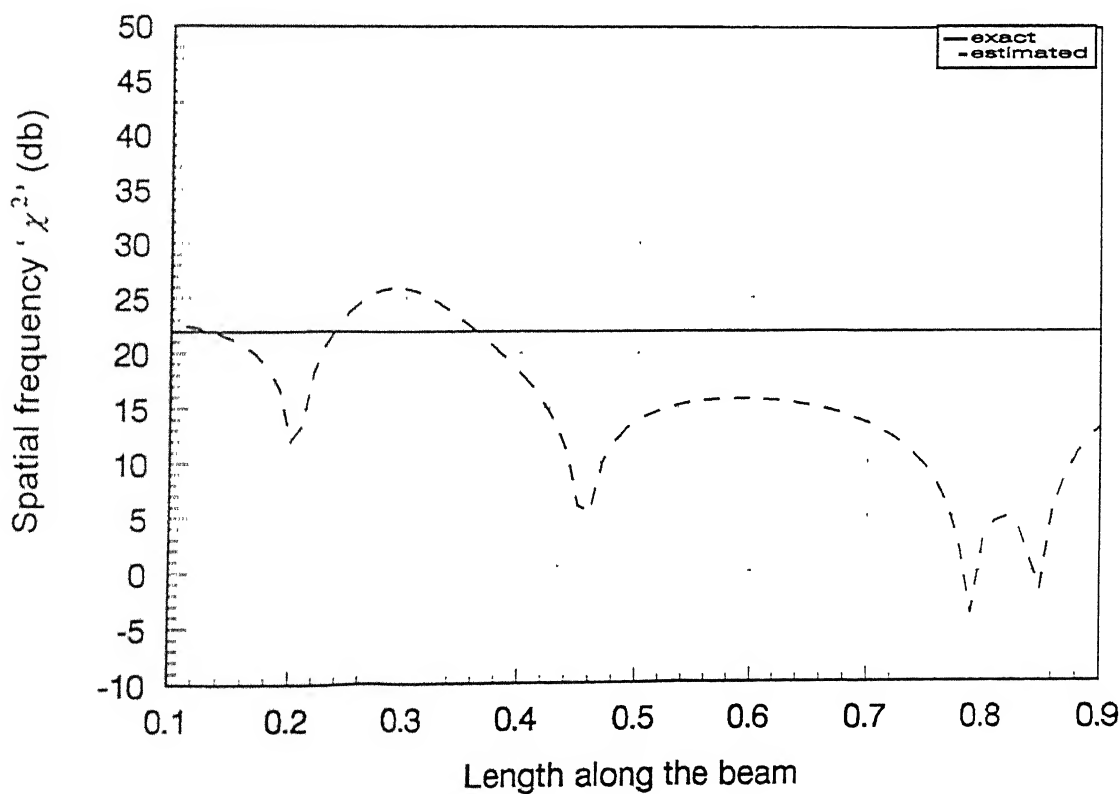


Fig. 3.14(b) First approximation of Spatial frequency: mode 4: simply supported beam

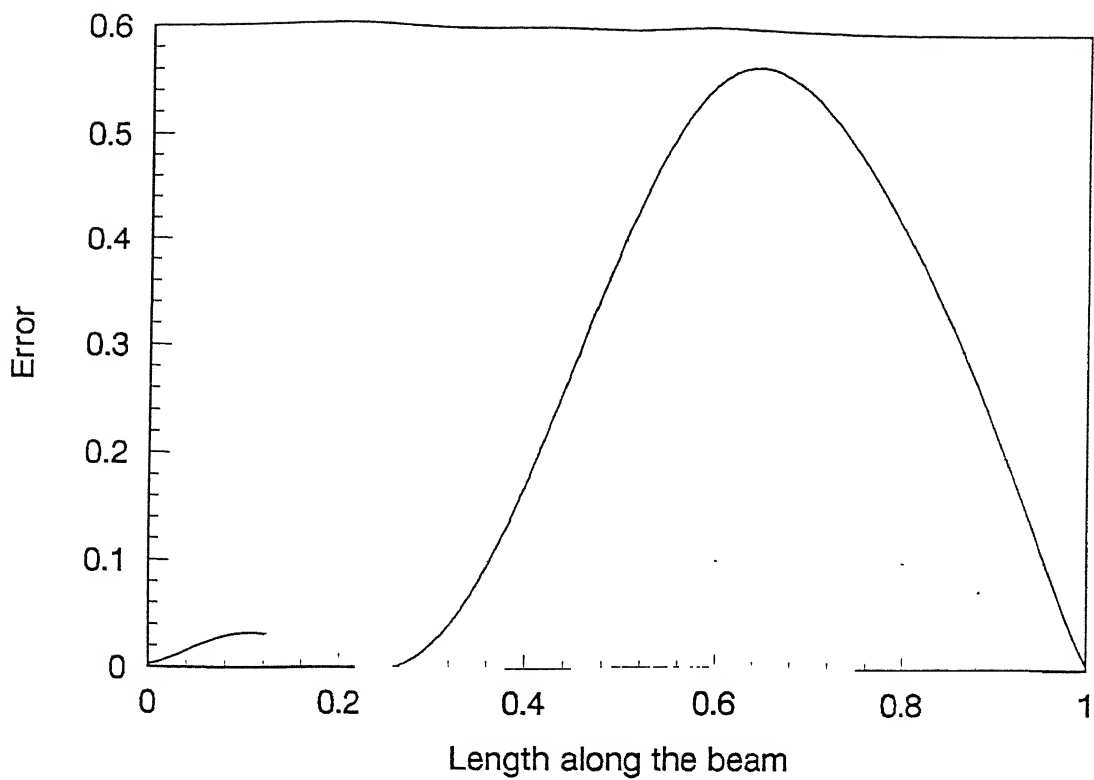


Fig. 3.15(a) Error in the first approximation of mode 2: simply supported beam

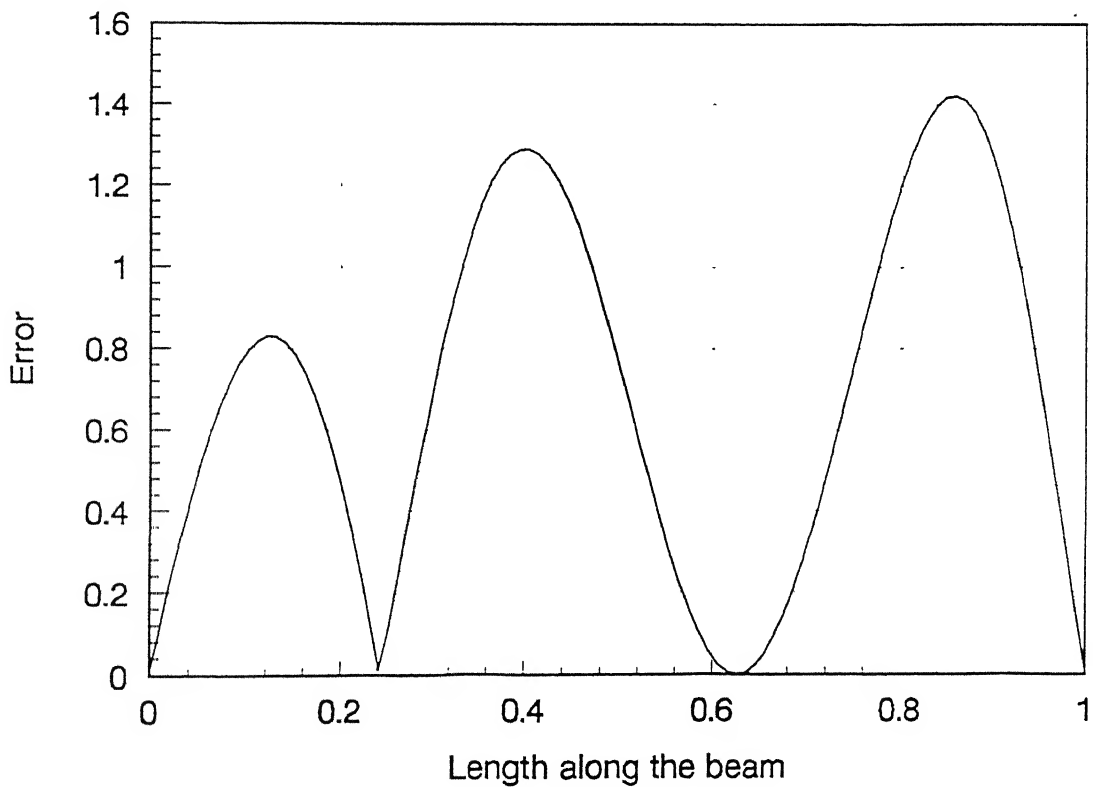


Fig. 3.15(b) Error in the first approximation of mode 4: simply supported beam



The above forms ‘the first estimates’ of the modal characteristics of the simply supported beam under consideration. Refined mode shapes and spatial frequencies are obtained by carrying out repeated iterations of the procedure, in a manner described previously. The refinement obtained in the first five mode shapes are shown in Figs. 3.16 (a)-(e), while the corresponding data on the spatial frequencies is depicted in Figs 3.17 (a)-(e). The natural frequencies  $\omega_m$ , obtained in each iteration, through the formula given in equation (2.24), are listed in Table 3.1, along with the corresponding exact values.

**Table 3.1 Estimated and Exact Natural Frequencies  
of Simply Supported Beam**

	Mode 1	Mode 2	Mode 3	Mode 4	Mode 5
Iteration 1	3.081	16.905	32.480	75.386	37.409
Iteration 2	3.085	12.638	30.597	54.848	72.648
Iteration 3	3.088	12.607	29.572	51.298	72.651
Exact	3.091	12.365	27.821	49.460	77.281

Fixed –Fixed (clamped-clamped):

The procedure in this case, follows a pattern similar to that in the previous case, since both configurations carry antinodes at the ends and belong to the same category defined earlier. The fundamental frequency, in this case, with non-dimensional parameter,  $\kappa = 0.1$  was found out to be 7.0rads/s.

- (a) The beam is harmonically excited at its mid-point ( $x/l=0.5$ ), at a frequency equal to 8.4 rads/s ( $= 1.2 \times 7.00\text{rads/s}$ ), so that the response is primarily constituted of the fundamental mode and the next symmetric mode (i.e. mode 3). Figures 3.18 (a) and (b) show the ‘first estimates’ of modes 1 and 3. The ‘first estimates’ of the corresponding spatial frequencies,  $\chi$ , are shown in Figs. 3.19(a), (b) along with the exact values. The natural frequencies computed from the mean of the  $\chi$  curves, are 7.151 rads/s. for mode 1 and .42.226 rads/s. for mode 3.

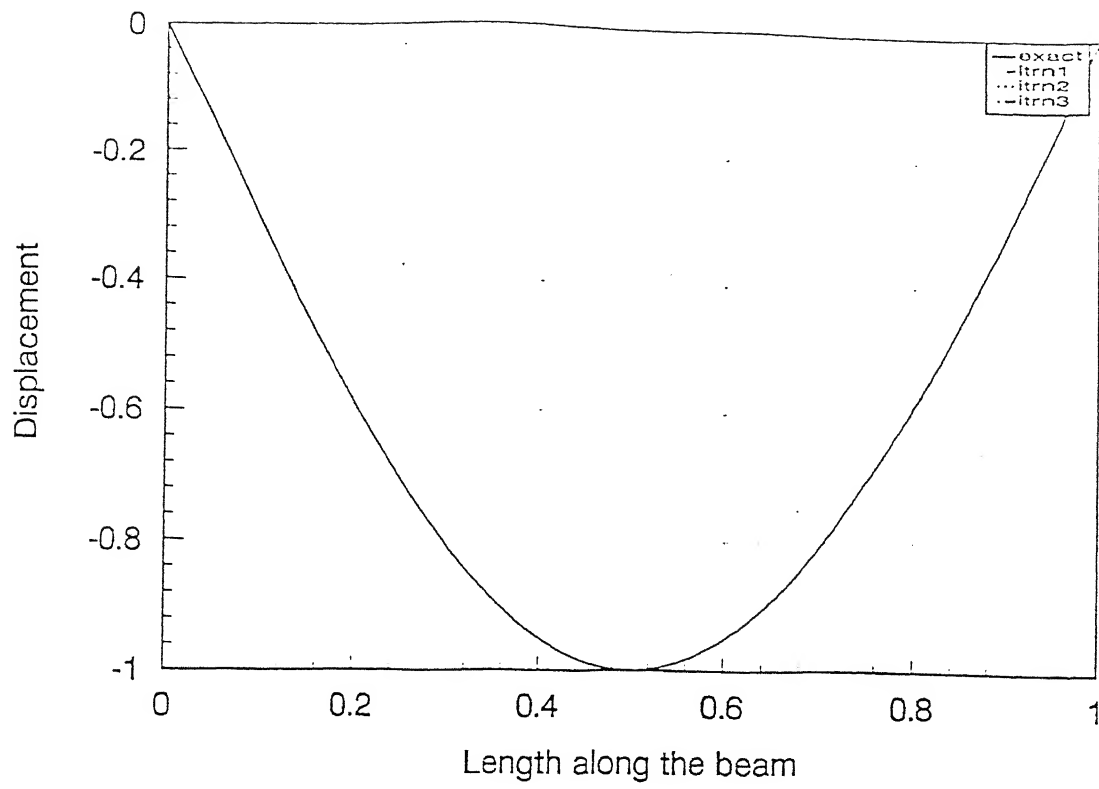


Fig. 3.16(a) Refinement in mode shapes: mode 1: simply supported beam

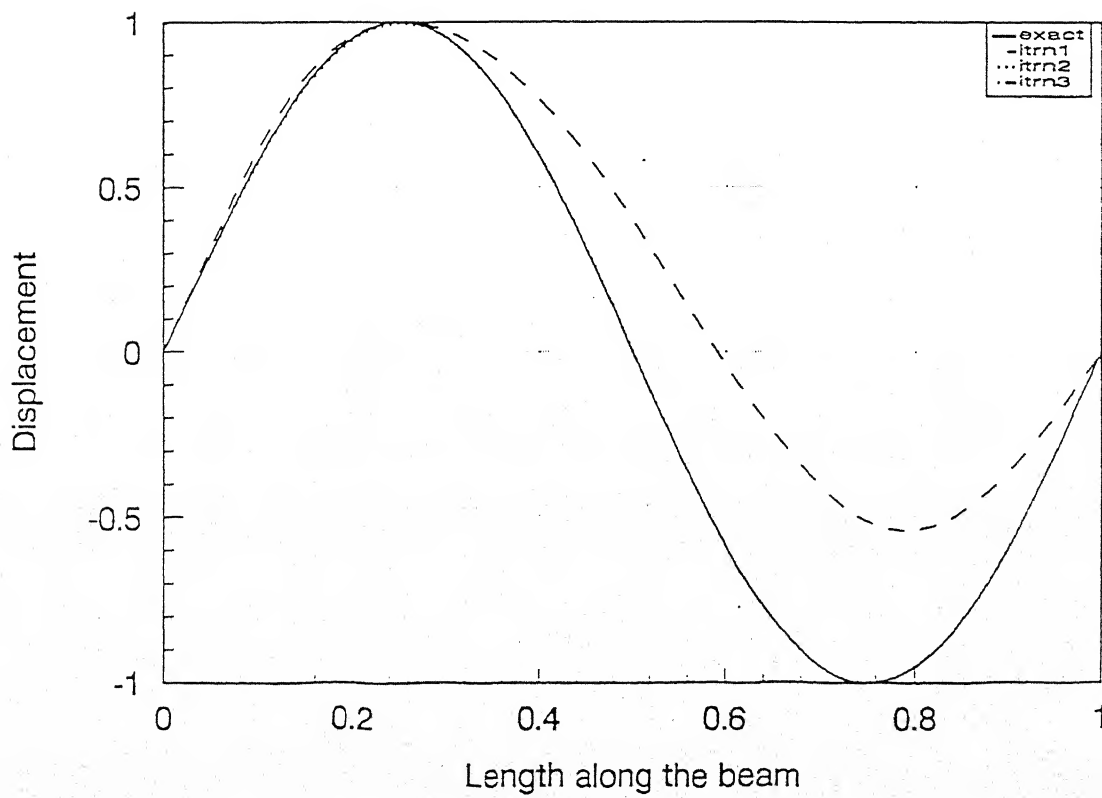


Fig. 3.16(b) Refinement in mode shapes: mode 2: simply supported beam

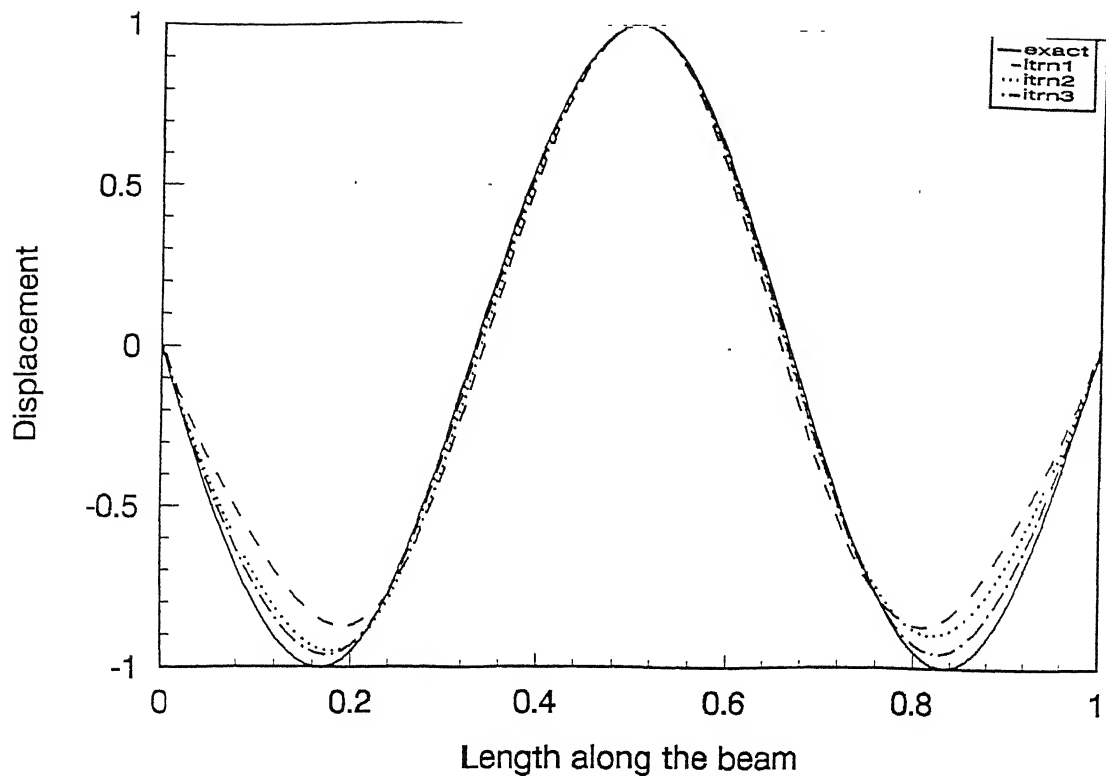


Fig. 3.16(c) Refinement in mode shapes: mode 3: simply supported beam

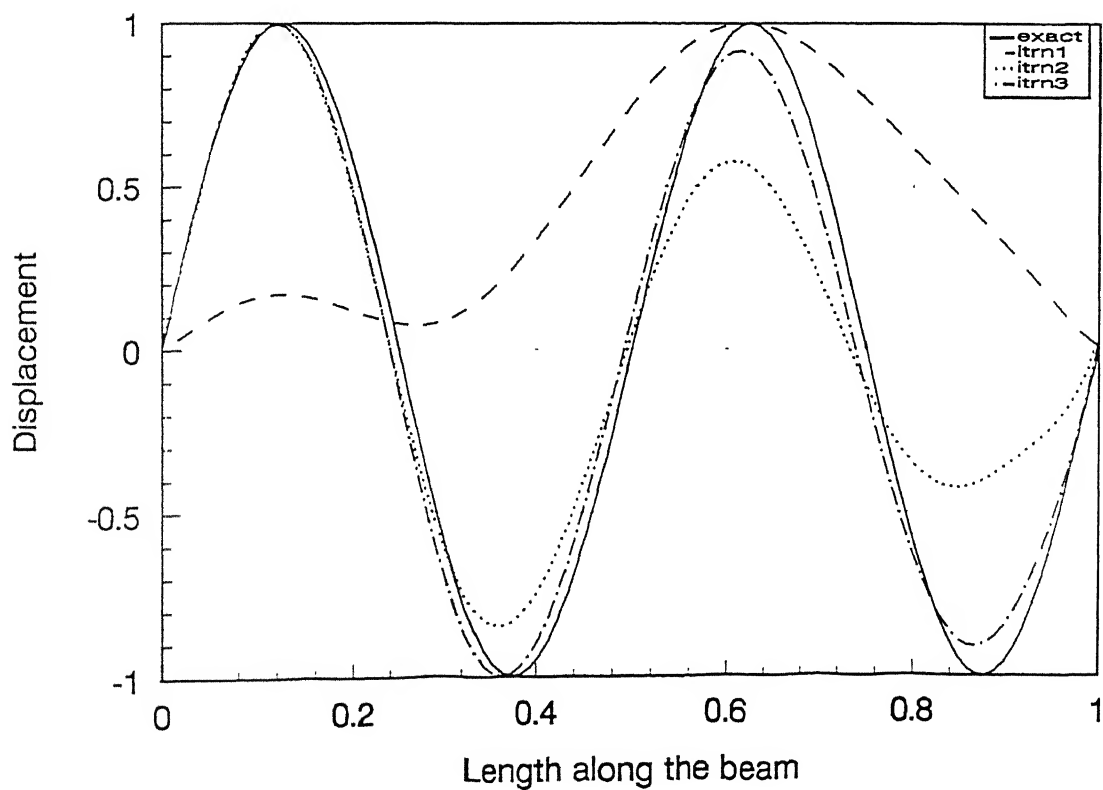


Fig. 3.16(d) Refinement in mode shapes: mode 4: simply supported beam

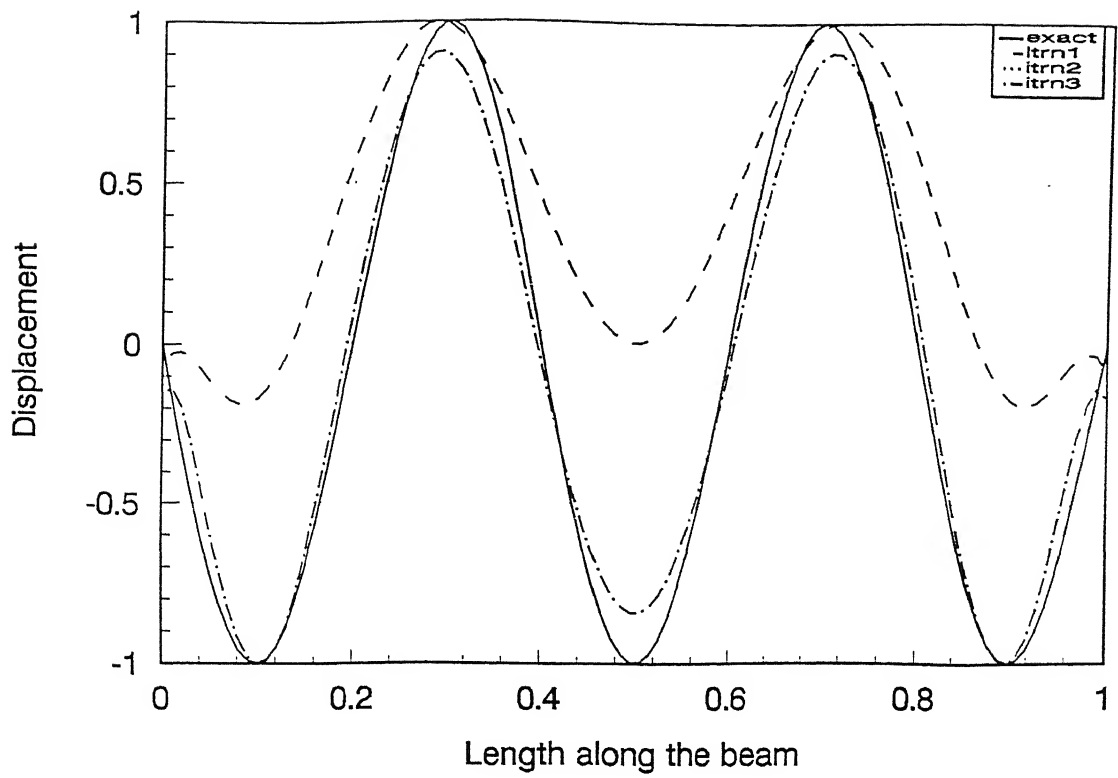


Fig. 3.16(e) Refinement in mode shapes: mode 5: simply supported beam

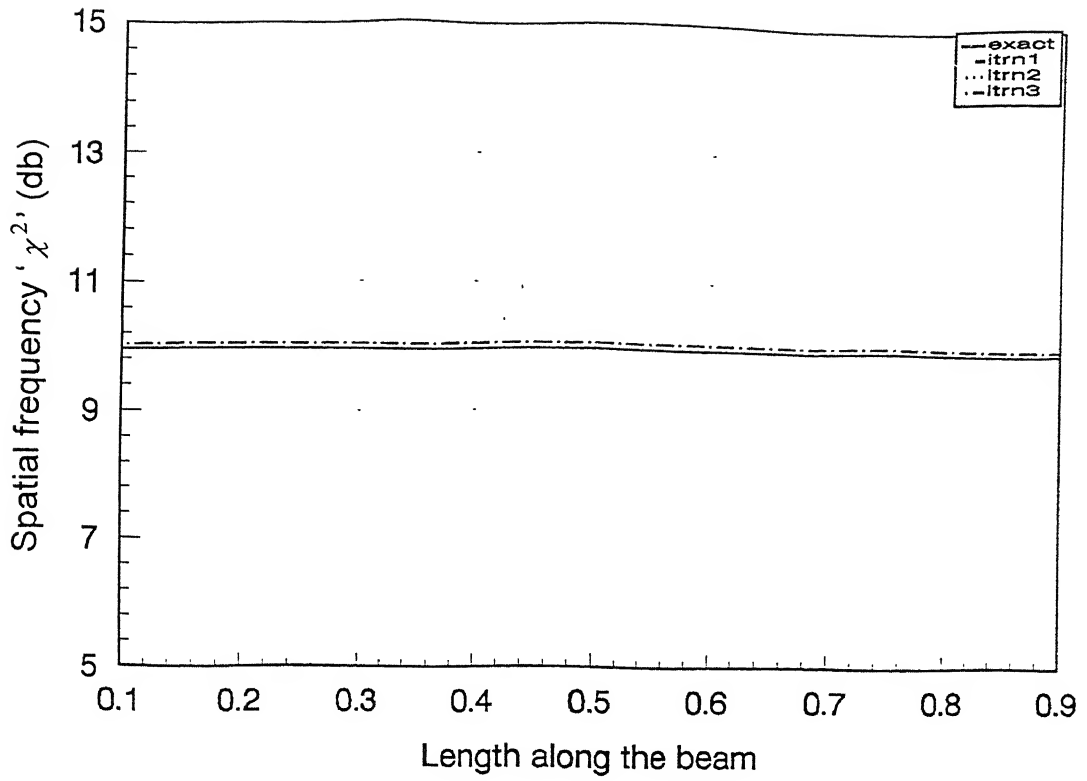


Fig. 3.17(a) Refinement in Spatial frequency: mode 1: simply supported beam

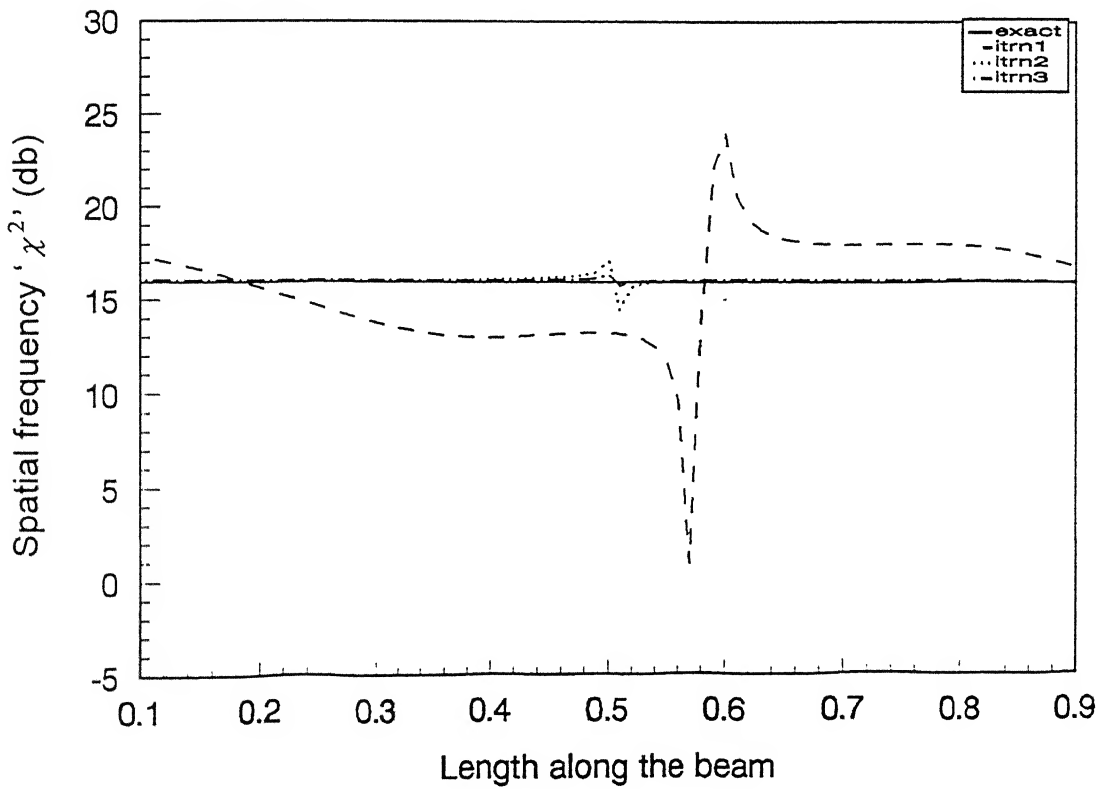


Fig. 3.17(b) Refinement in Spatial frequency: mode 2: simply supported beam

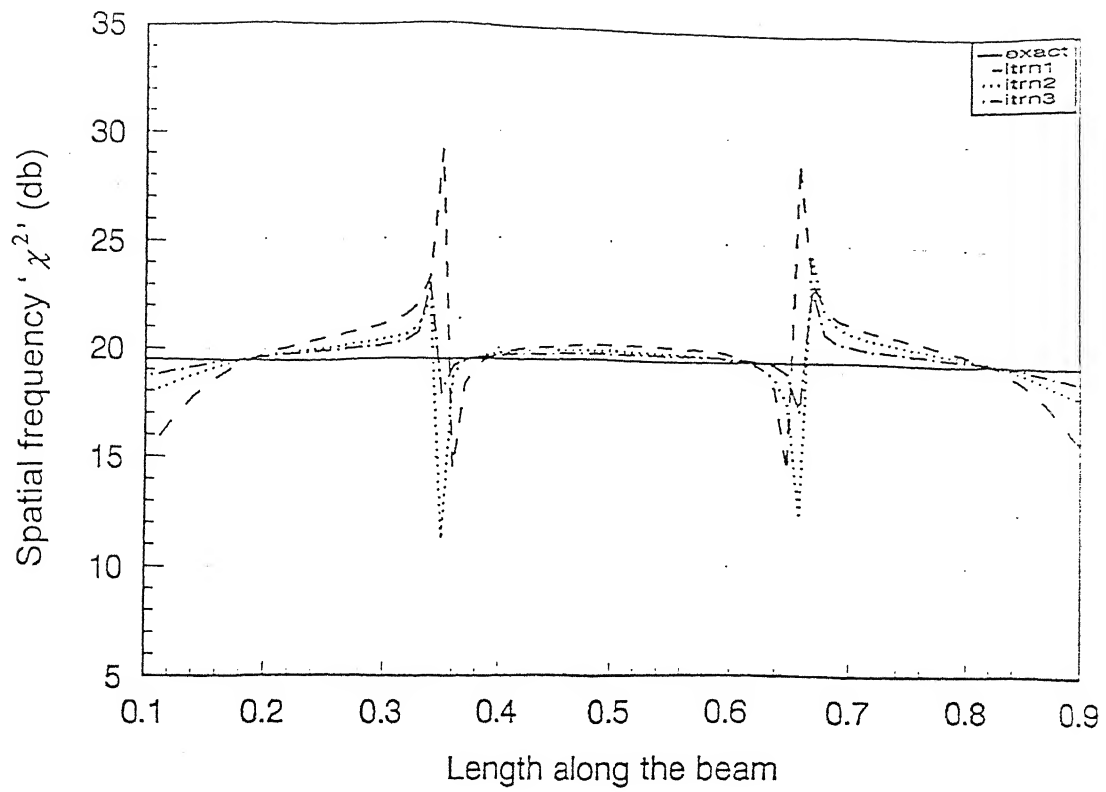


Fig. 3.17(c) Refinement in Spatial frequency: mode 3: simply supported beam

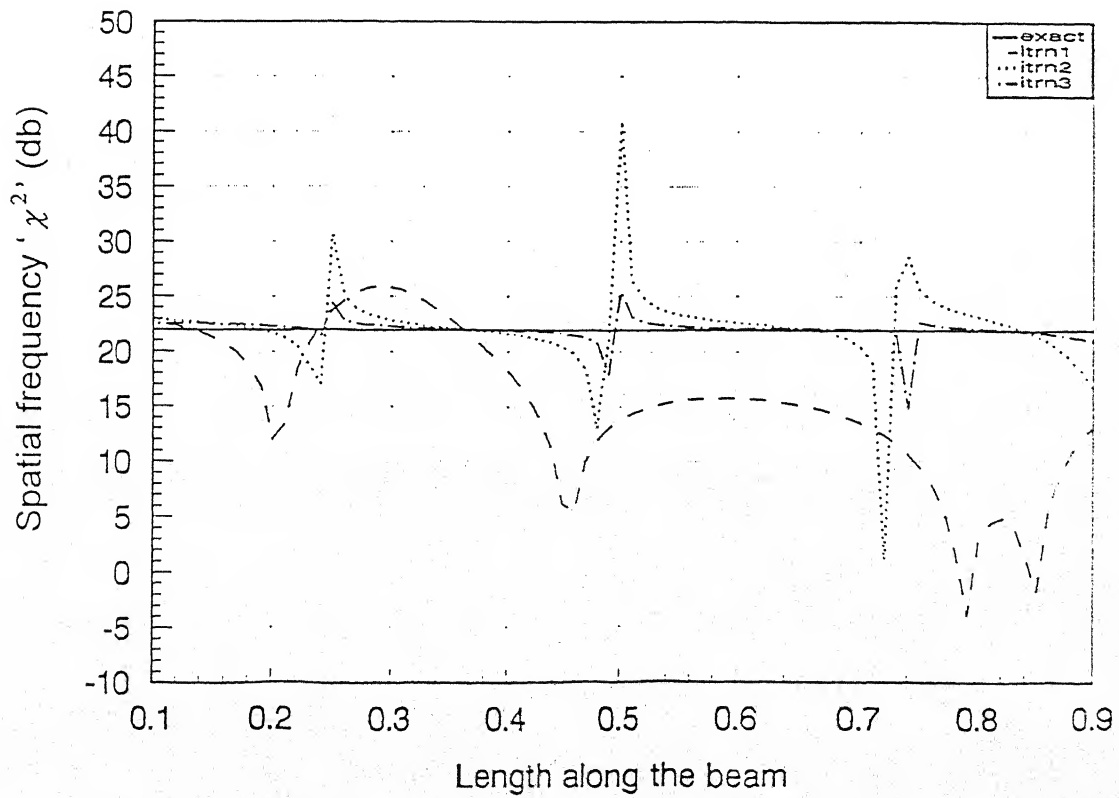


Fig. 3.17(d) Refinement in Spatial frequency: mode 4: simply supported beam

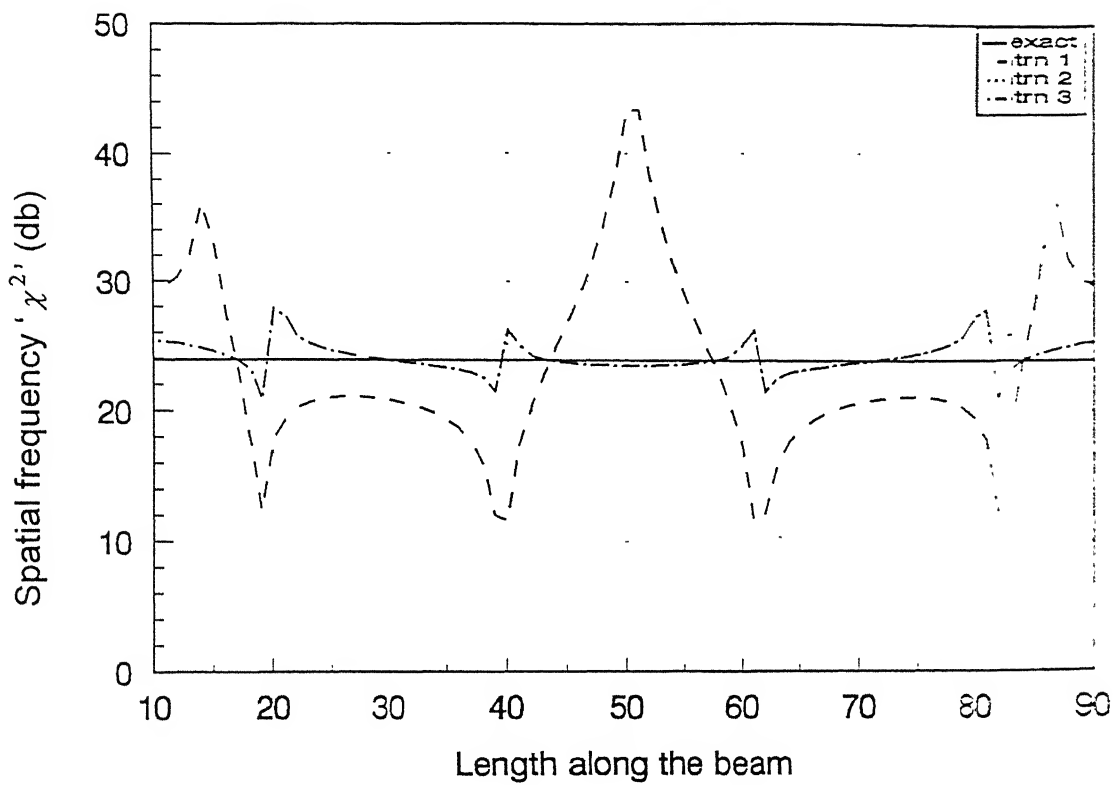


Fig. 3.17(e) Refinement in Spatial frequency: mode 5: simply supported beam

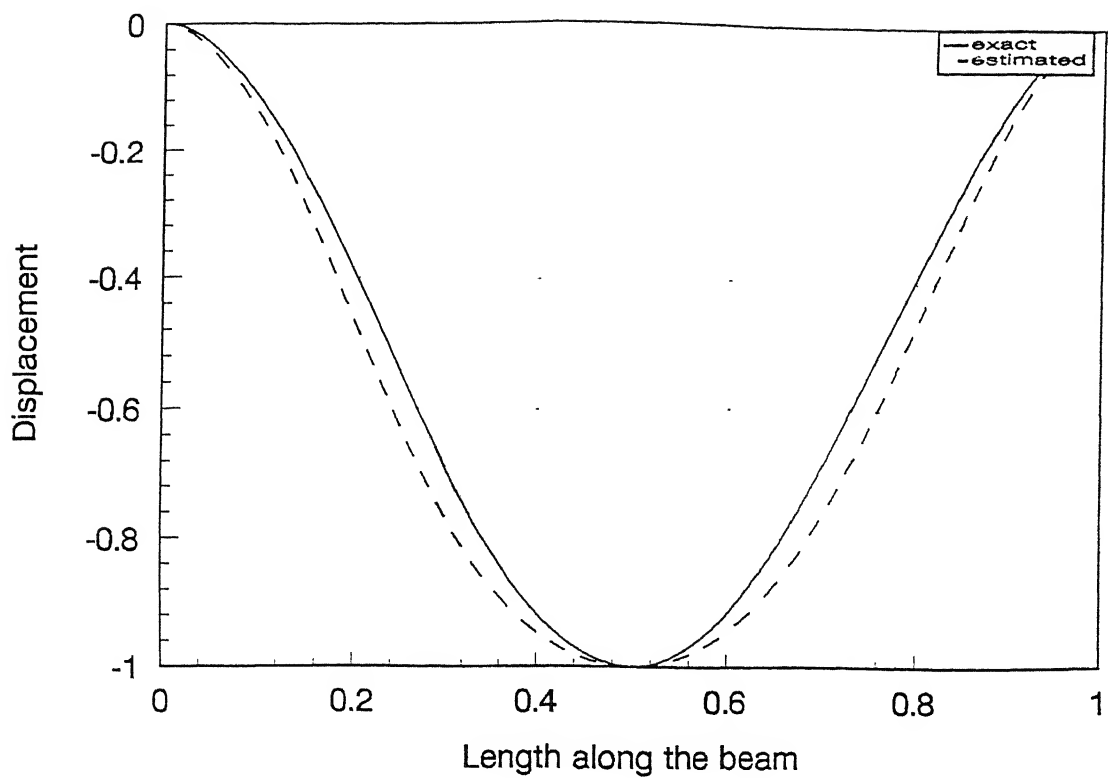


Fig. 3.18(a) First approximation of mode 1: fixed-fixed beam

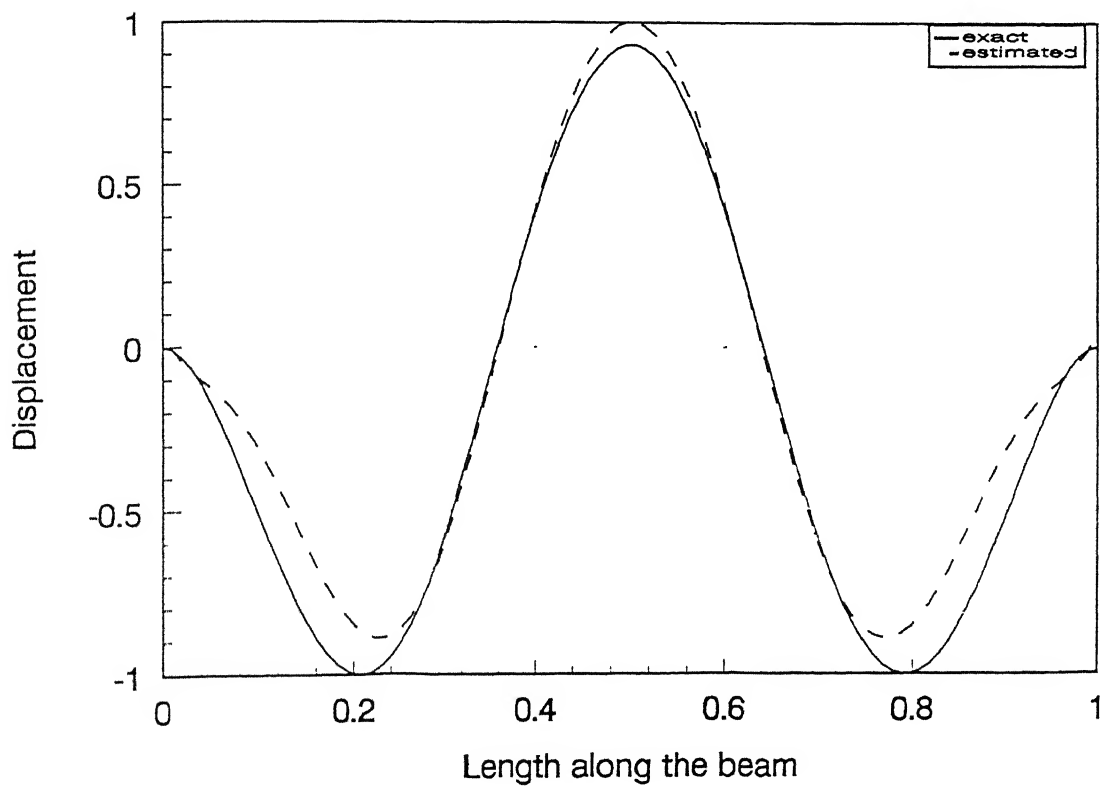


Fig. 3.18(b) First approximation of mode 3: fixed-fixed beam



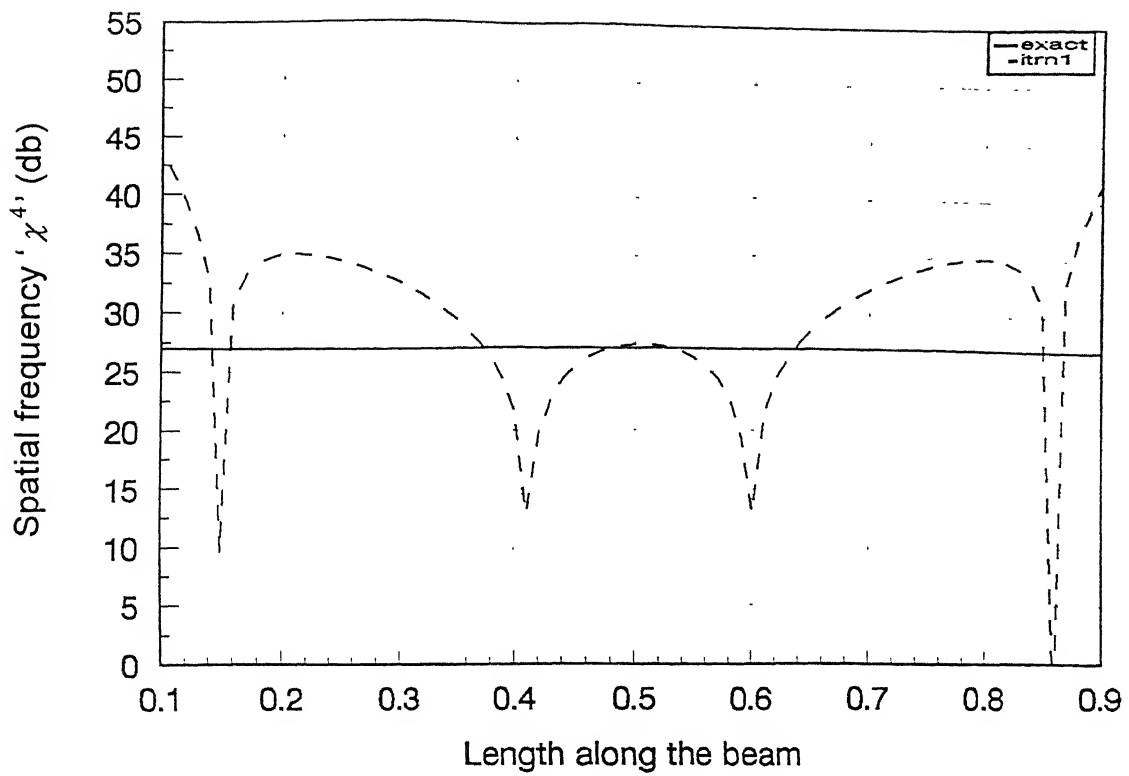


Fig. 3.19(a) First approximation of Spatial frequency: mode 1: fixed-fixed beam

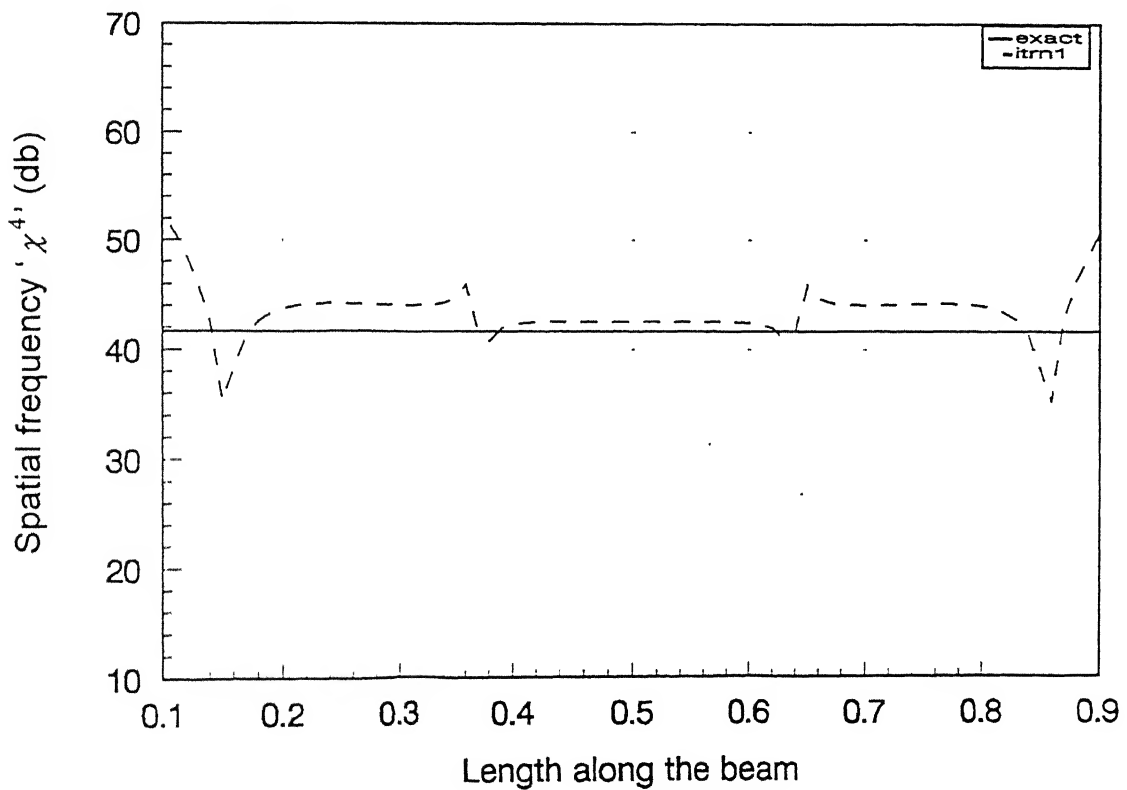


Fig. 3.19(b) First approximation of Spatial frequency: mode 3: fixed-fixed beam

- (b) For estimation of the next set of symmetric modes (3 and 5), mid-point excitation is given, to the beam, at a frequency of 50.671 rads/s. ( $=1.2 \times 42.226$ ). The contribution of the first mode, estimated in step (a), is subtracted from this response. The resultant is fed as input to the algorithm and modes 3 and 5 are estimated. The estimated mode shapes and spatial are given in Fig. 3.20 (a), (b), Fig.3.21 (a), (b) respectively. The natural frequencies computed from the mean of the spatial frequency curves are 33.110 rads/s. for mode 3 and 72.951 rads/s. for mode 5.
- (c) In order to estimate the anti-symmetric modes (2,4,.....), excitation is provided at the nodal point ( $x/l=0.35$ ) of the third mode estimated in step (b). The excitation frequency is 24.688 rads/s. ( $=\text{mean of 1}^{\text{st}} \text{ and } 3^{\text{rd}} \text{ estimated natural frequencies}$ ). The contribution of the first mode, estimated in (a), is subtracted from the response. The resultant is fed as input to the algorithm and modes 2 and 4 are estimated. The estimated mode shapes and spatial frequencies are given in Figs. 3.22 (a)-(b) and 3.23(a)-(b), respectively. The estimates for the natural frequencies computed using the mean of the spatial frequency curves are 16.693 rads/s. for mode 2 and 41.097 rads/s. for mode 5 respectively.

Refinements of the above 'first estimates' are carried out in a manner similar to that described in the simply supported case. This refinement in mode shapes and spatial frequencies is illustrated in Figs. 3.24 (a)-(e) and Figs 3.25 (a)-(e), respectively. The natural frequencies  $\omega_m$ , obtained through the formula given in equation (2.24) are listed in Table 3.2, for each iteration, along with the corresponding exact values.

**Table 3.2 Estimated and Exact Natural Frequencies  
of fixed-fixed beam**

	Mode 1	Mode 2	Mode 3	Mode 4	Mode 5
Iteration 1	7.150	16.693	42.226	41.097	72.951
Iteration 2	6.799	17.908	41.094	52.221	84.067
Iteration 3	6.799	17.978	40.643	52.671	84.094
Exact	7.000	19.316	37.868	62.597	93.510

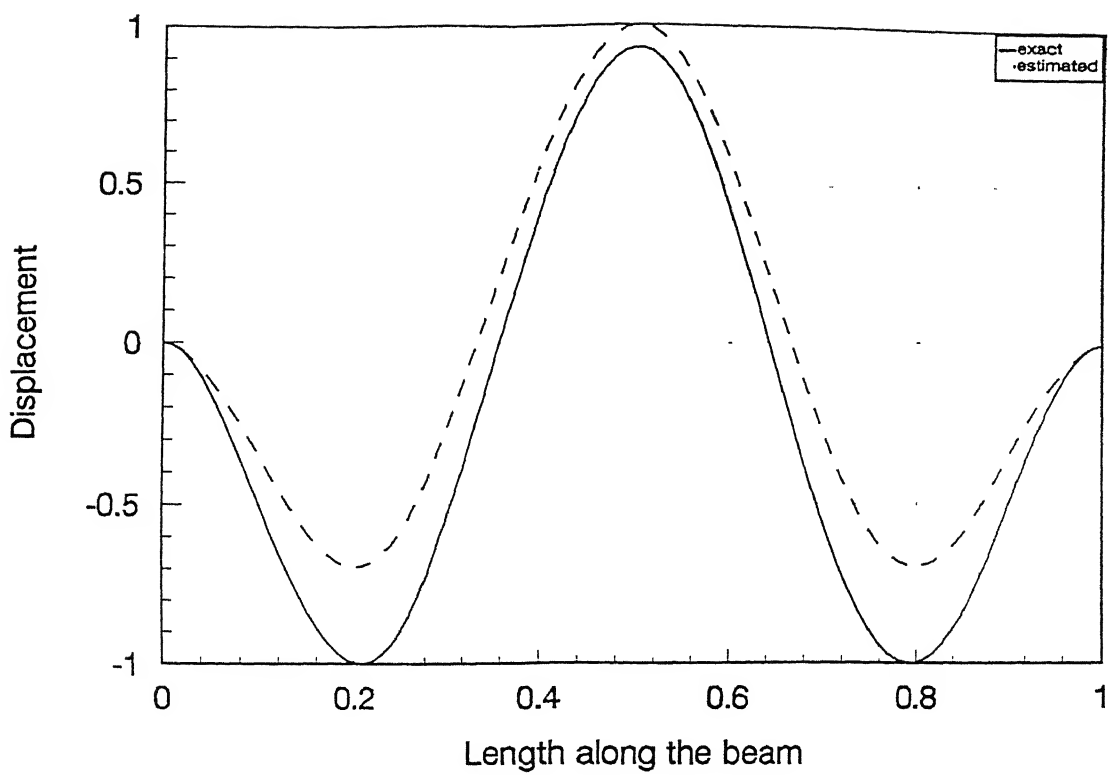


Fig. 3.20(a) First approximation of mode 3: fixed-fixed beam

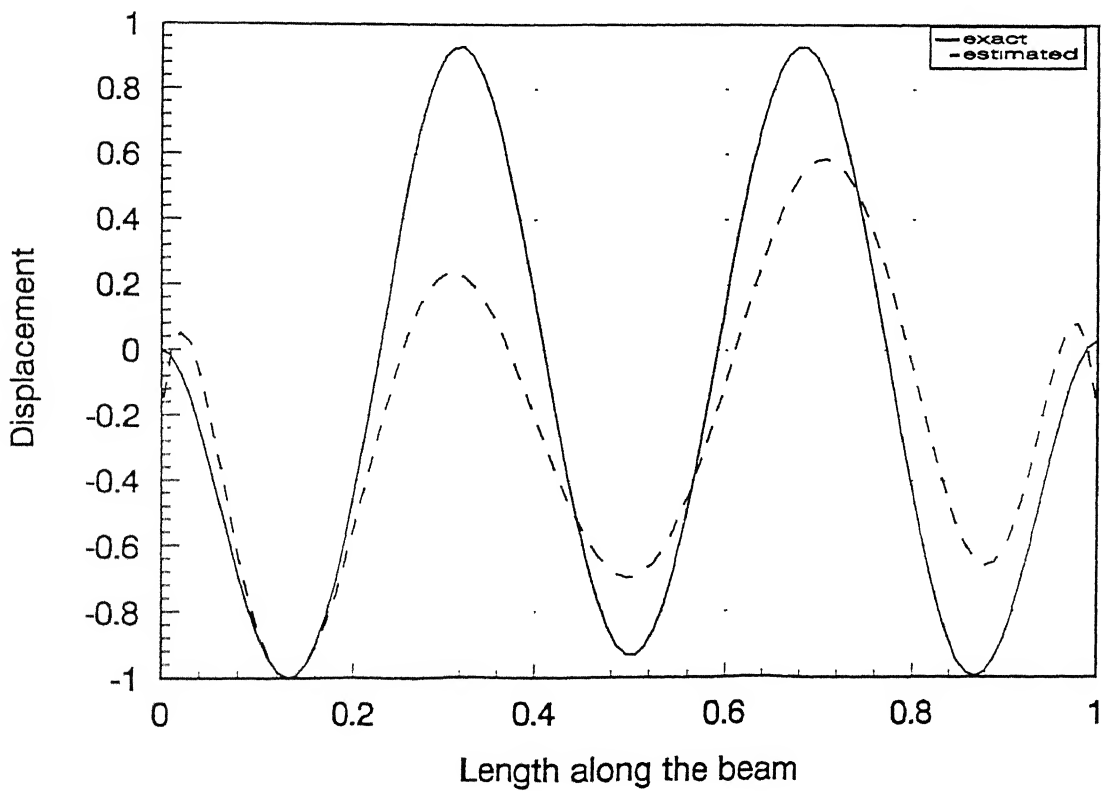


Fig. 3.20(b) First approximation of mode 5: fixed-fixed beam

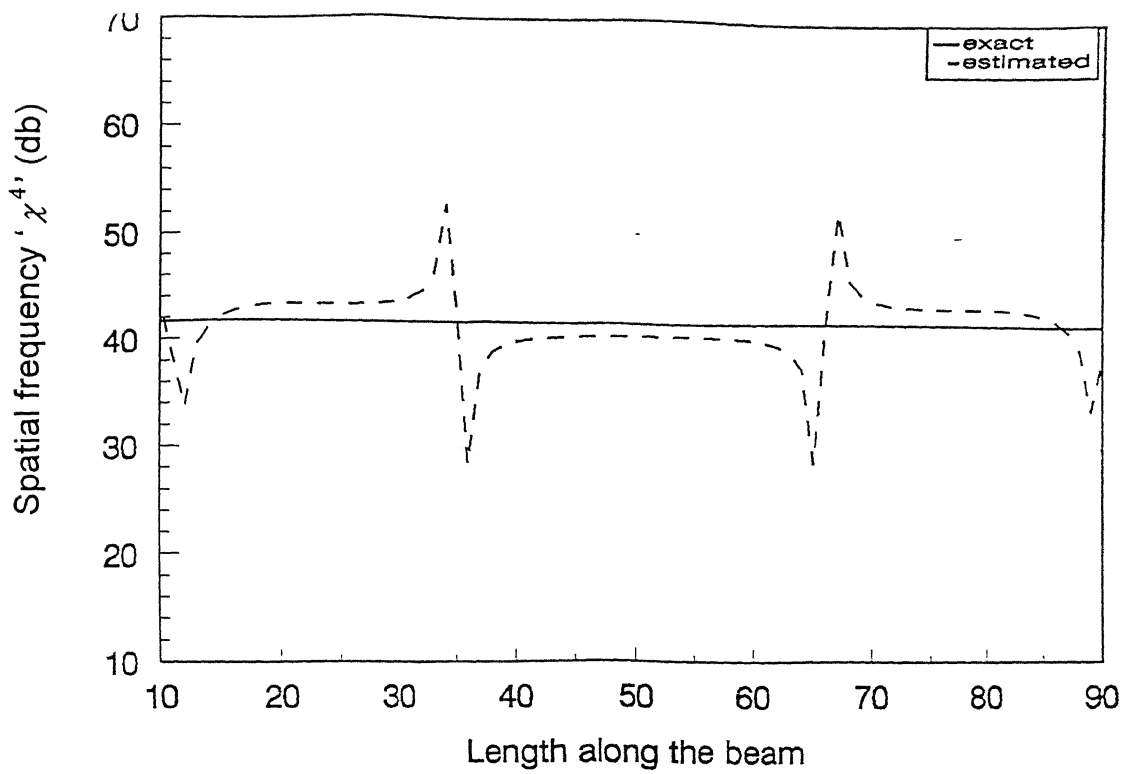


Fig. 3.21(a) First approximation of Spatial frequency: mode 3: fixed-fixed beam

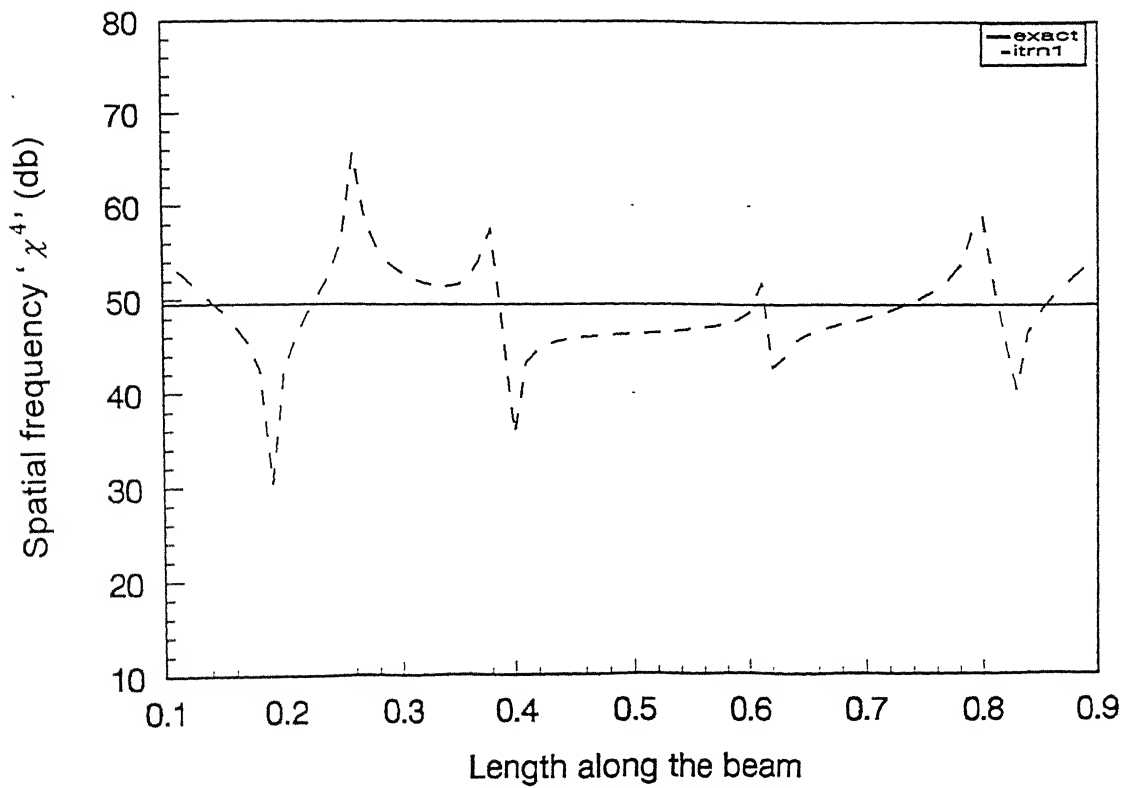


Fig. 3.21(b) First approximation of Spatial frequency: mode 5: fixed-fixed beam

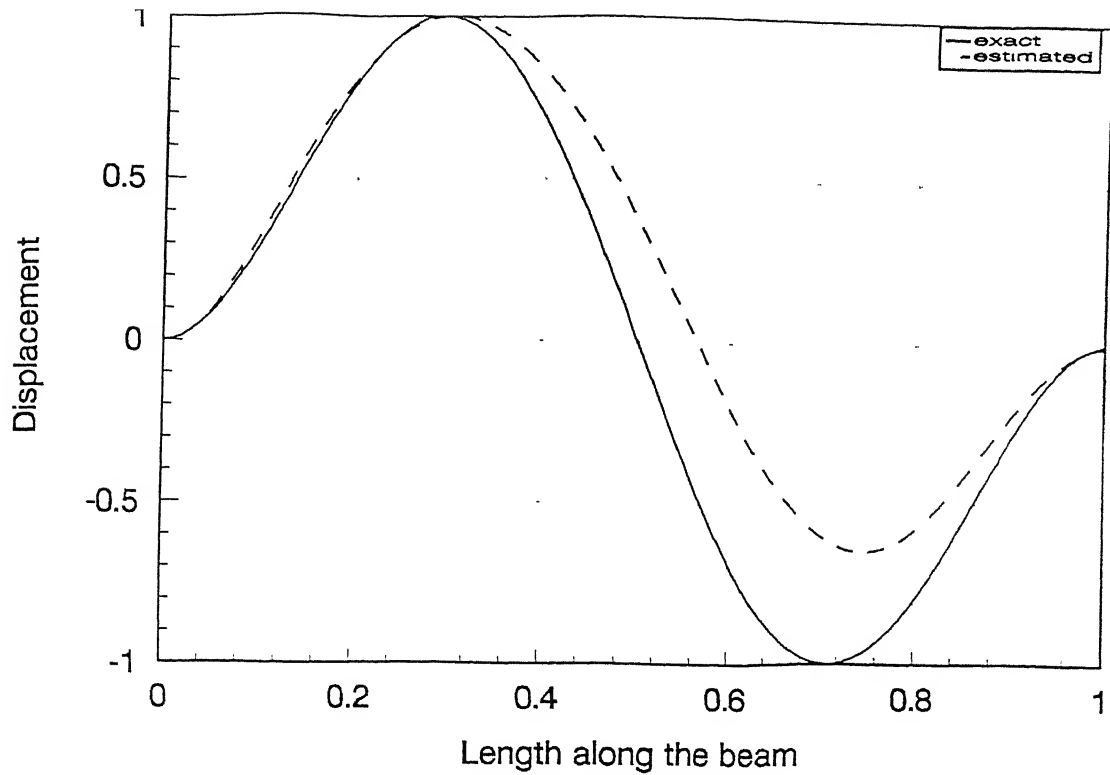


Fig. 3.22(a) First approximation of mode 2: fixed-fixed beam

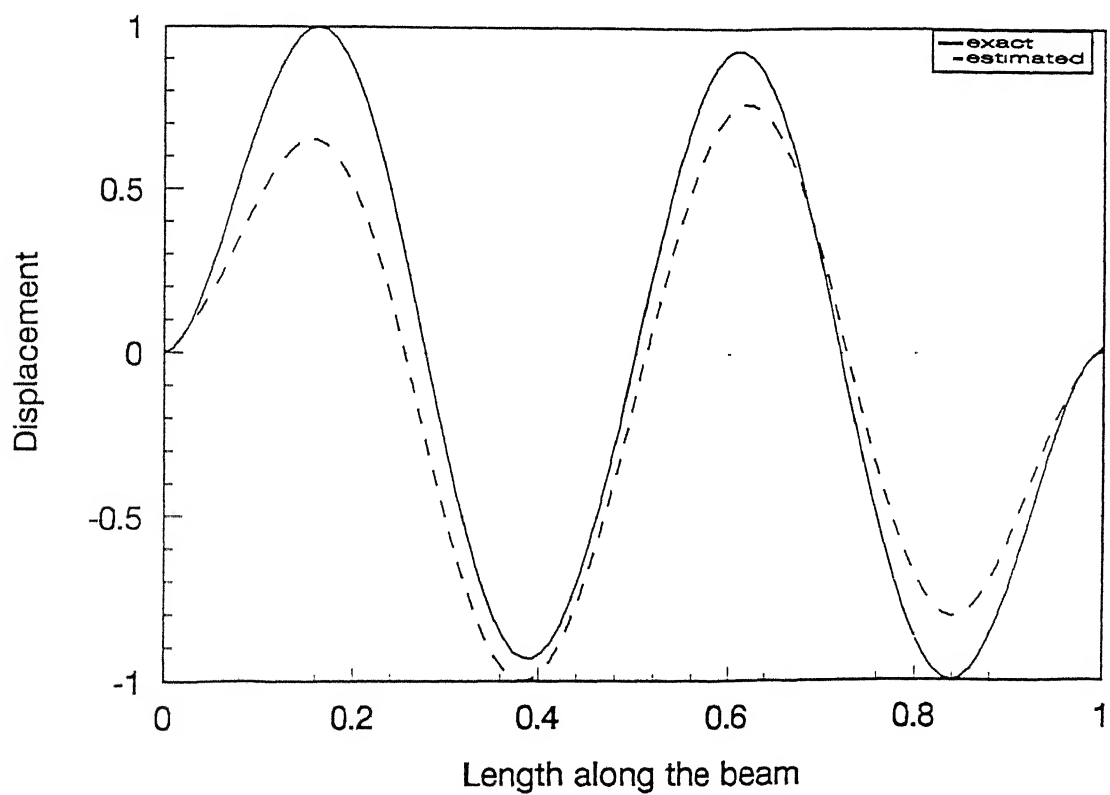


Fig. 3.22(b) First approximation of mode 4: fixed-fixed beam

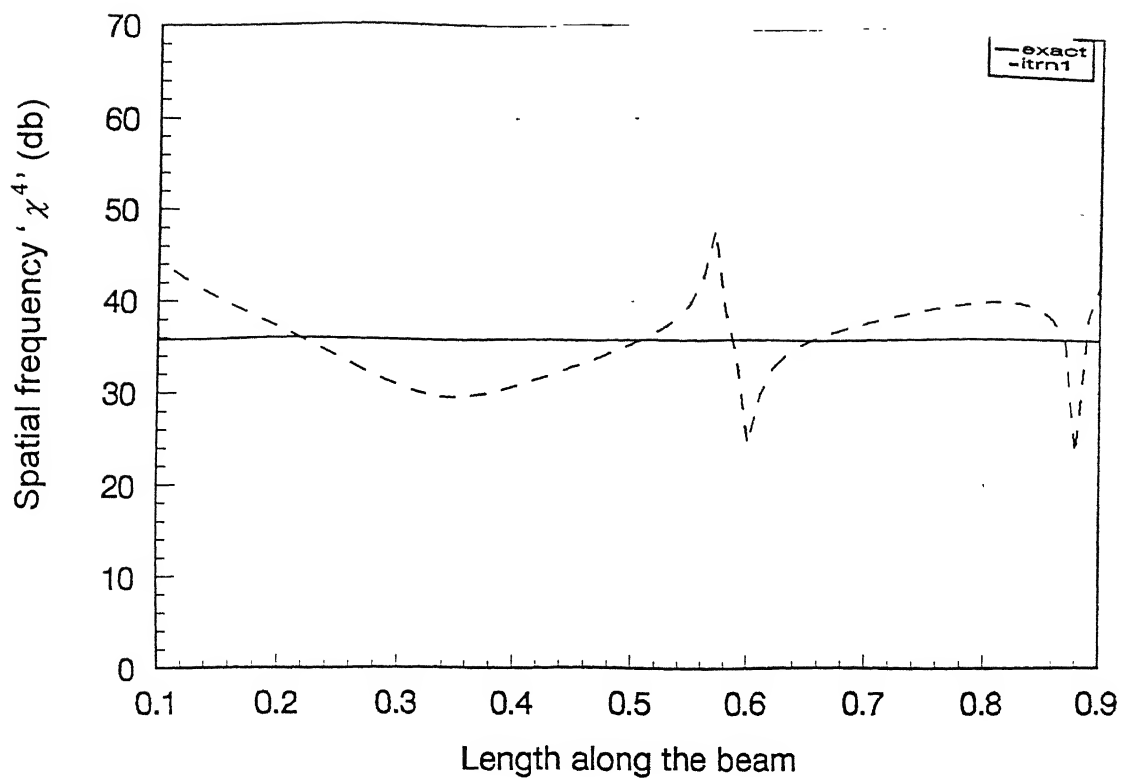


Fig. 3.23(a) First approximation of Spatial frequency: mode 2: fixed-fixed beam

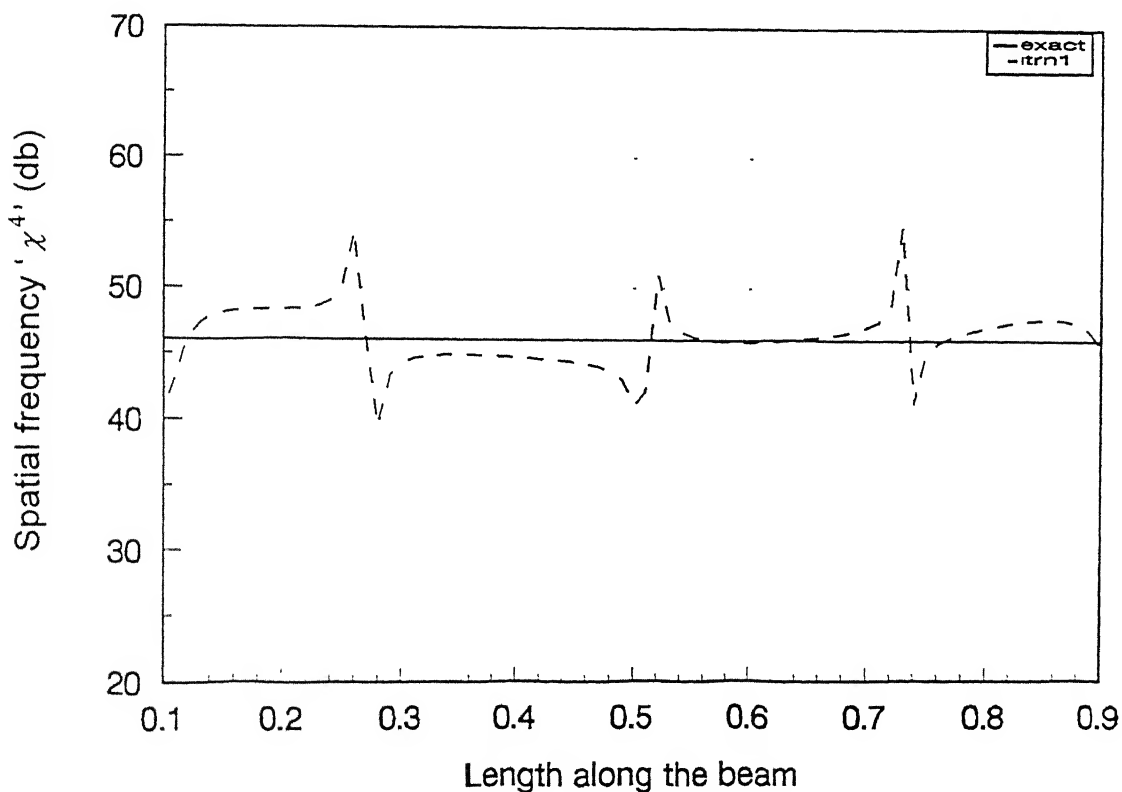


Fig. 3.23(b) First approximation of Spatial frequency: mode 4: fixed-fixed beam

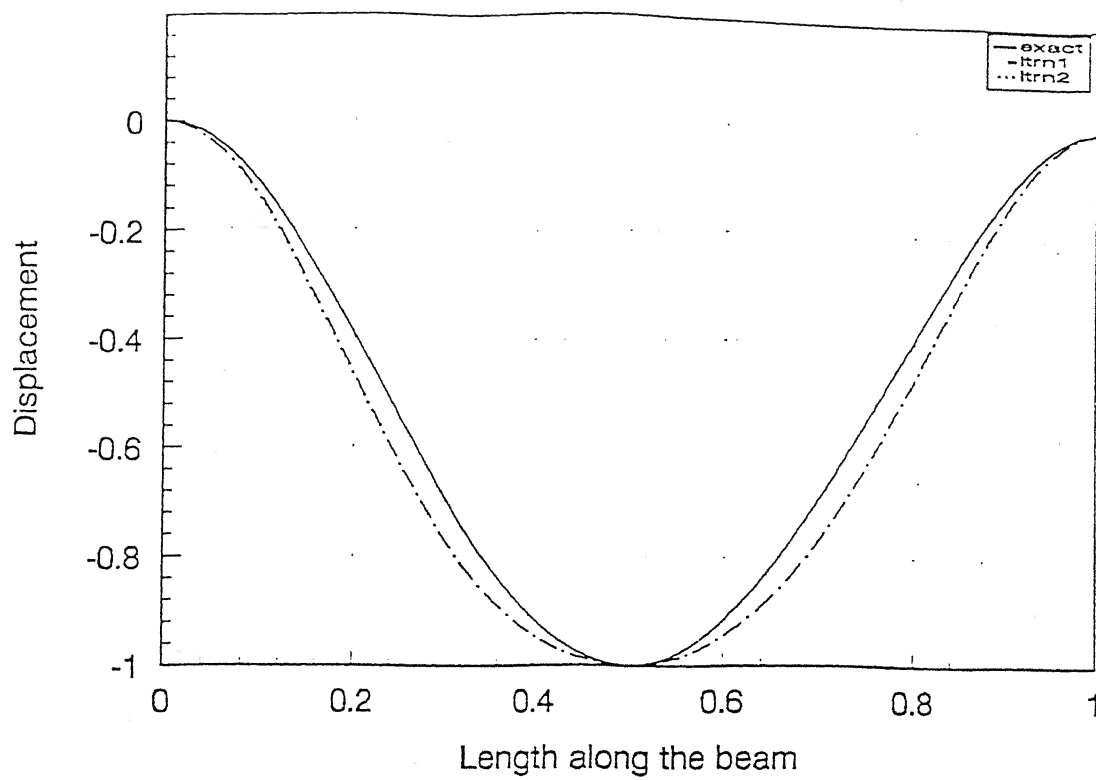


Fig. 3.24(a) Refinement in mode shapes: mode 1: fixed-fixed beam

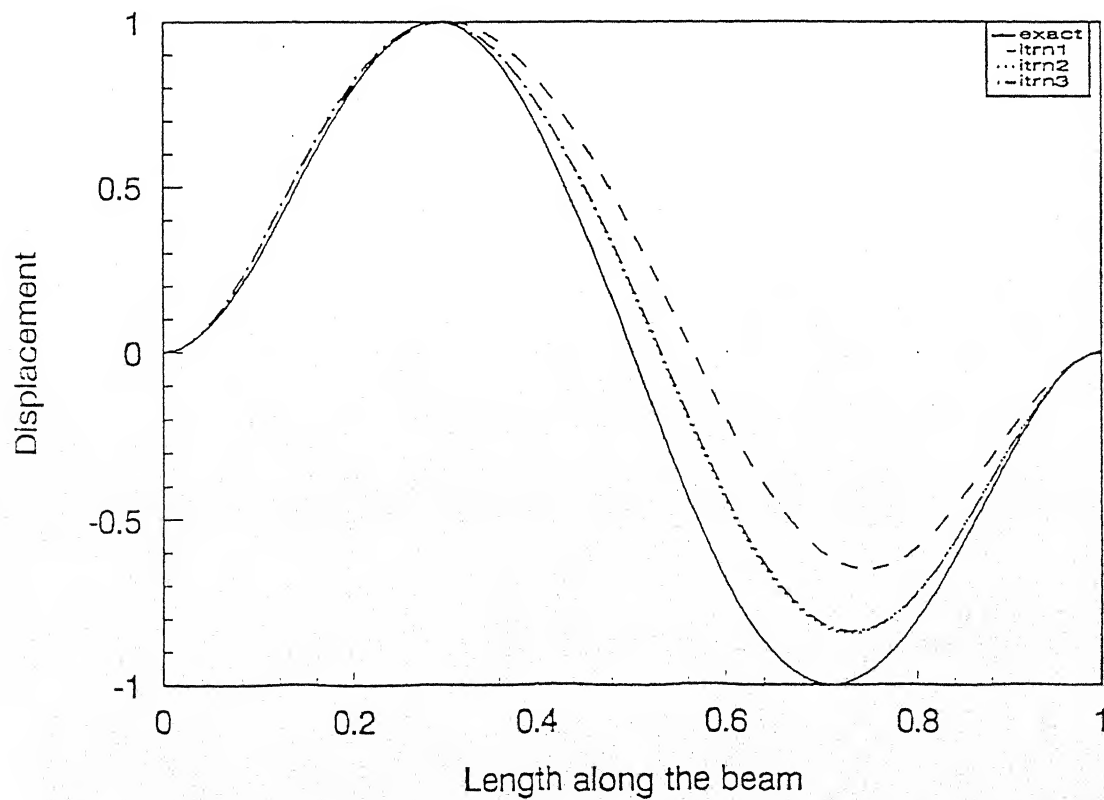


Fig. 3.24(b) Refinement in mode shapes: mode 2: fixed-fixed beam

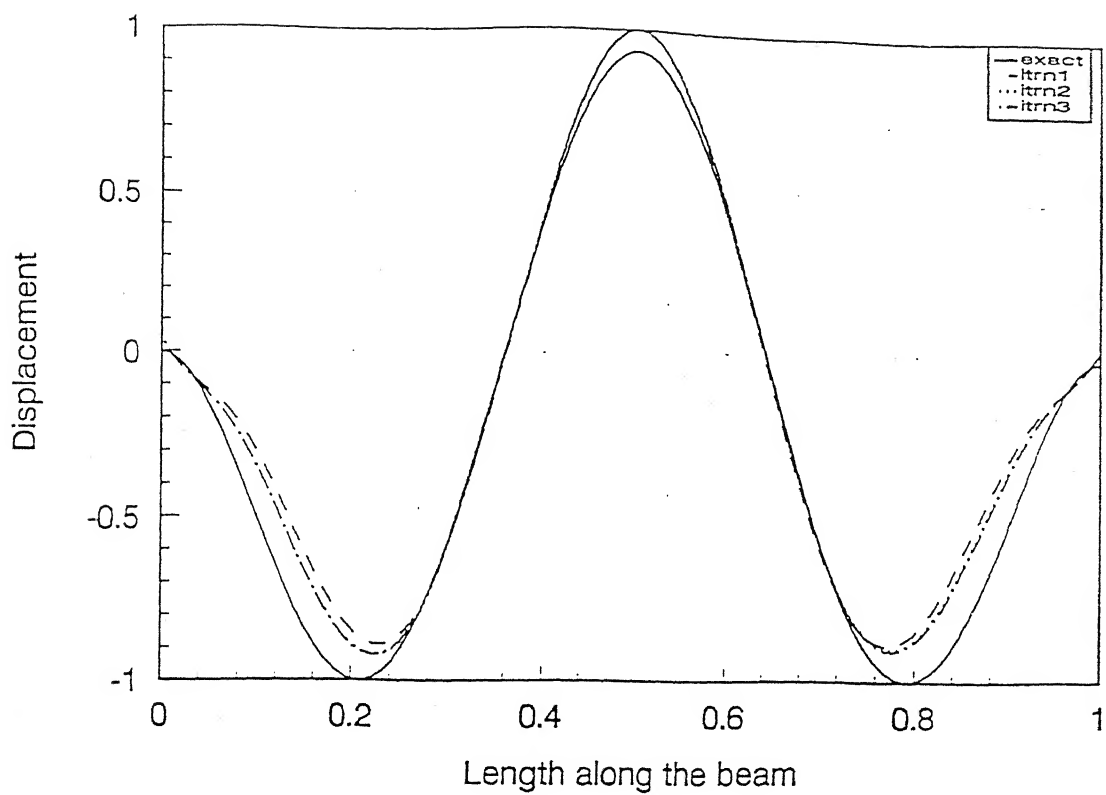


Fig. 3.24(c) Refinement in mode shapes: mode 3: fixed-fixed beam

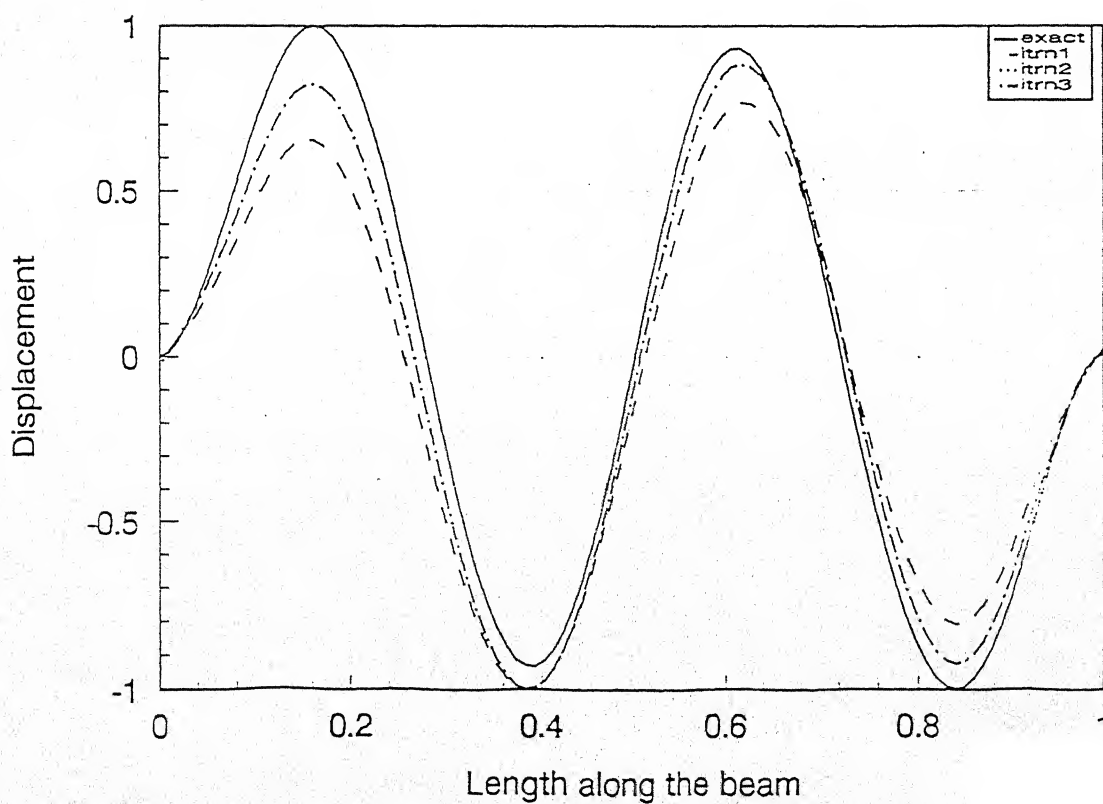


Fig. 3.24(d) Refinement in mode shapes: mode 4: fixed-fixed beam



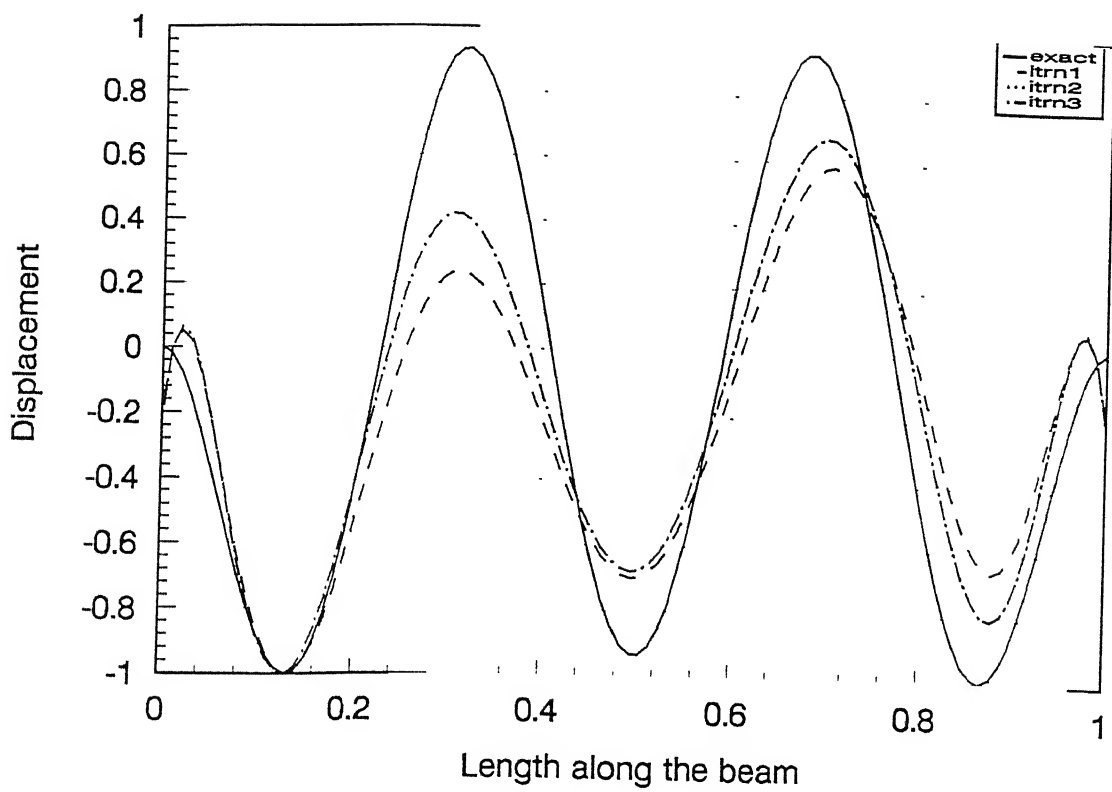


Fig. 3.24(e) Refinement in mode shapes: mode 5: fixed-fixed beam

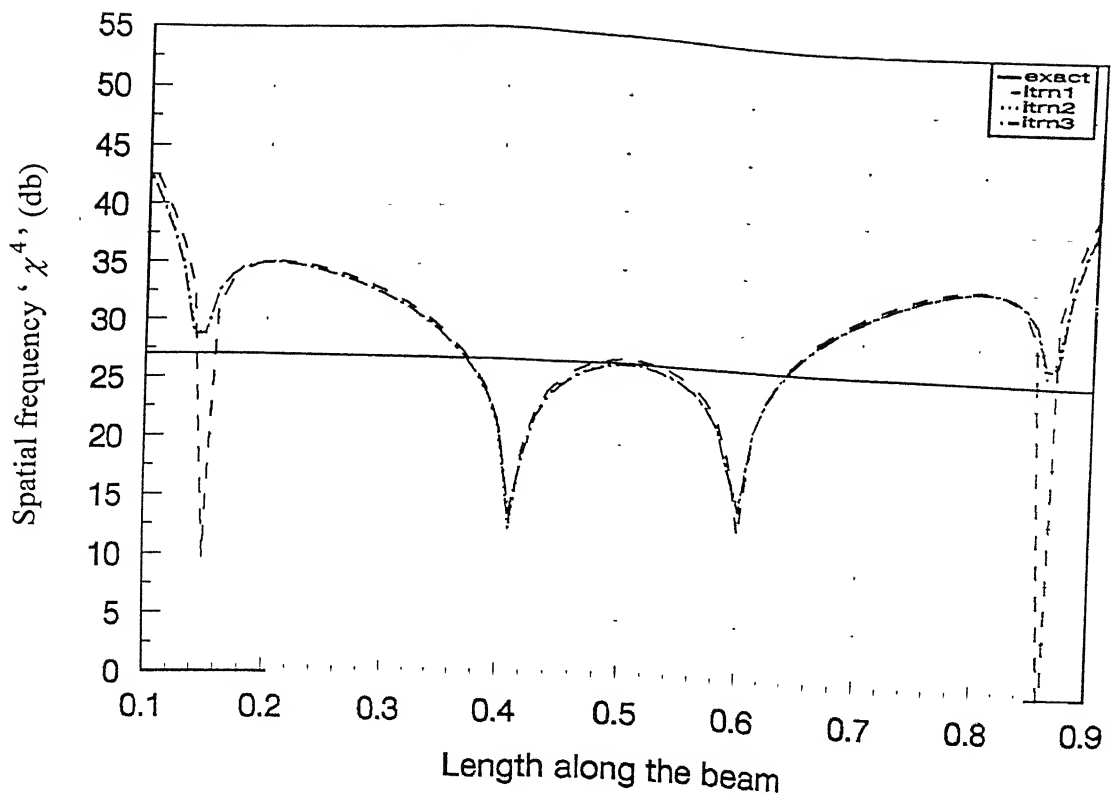


Fig. 3.25(a) Refinement in Spatial frequency: mode 1: fixed-fixed beam

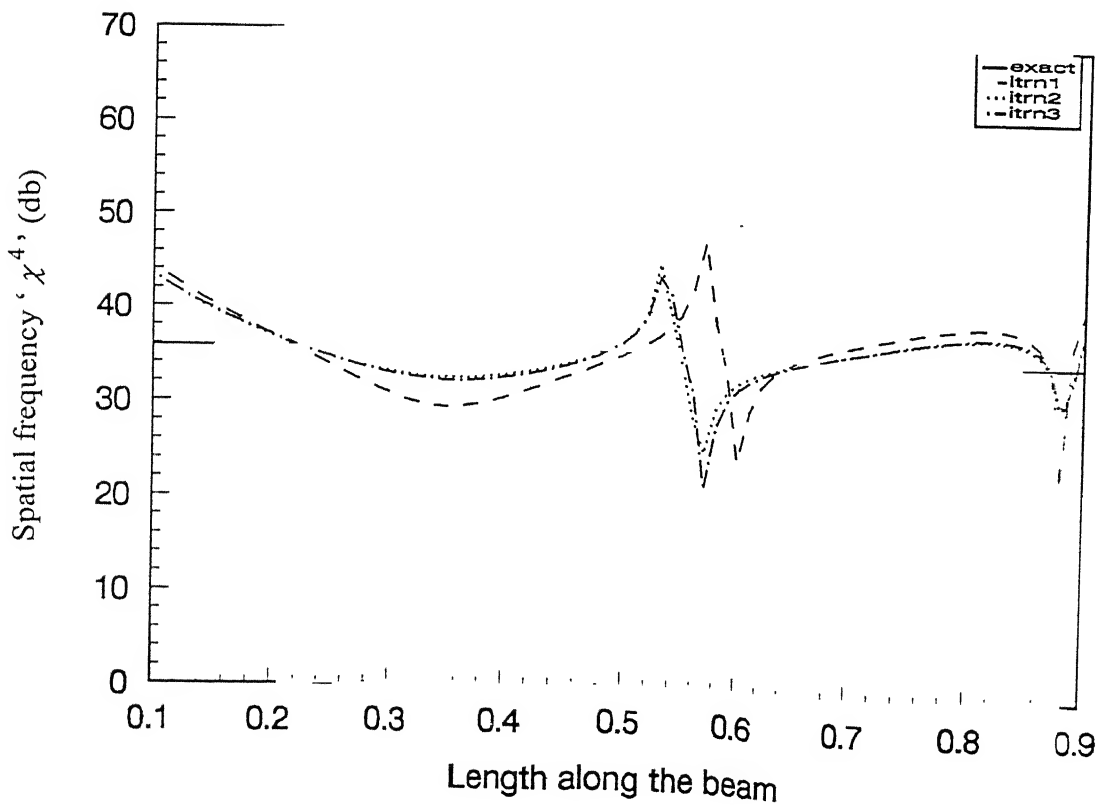


Fig. 3.25(b) Refinement in Spatial frequency: mode 2: fixed-fixed beam

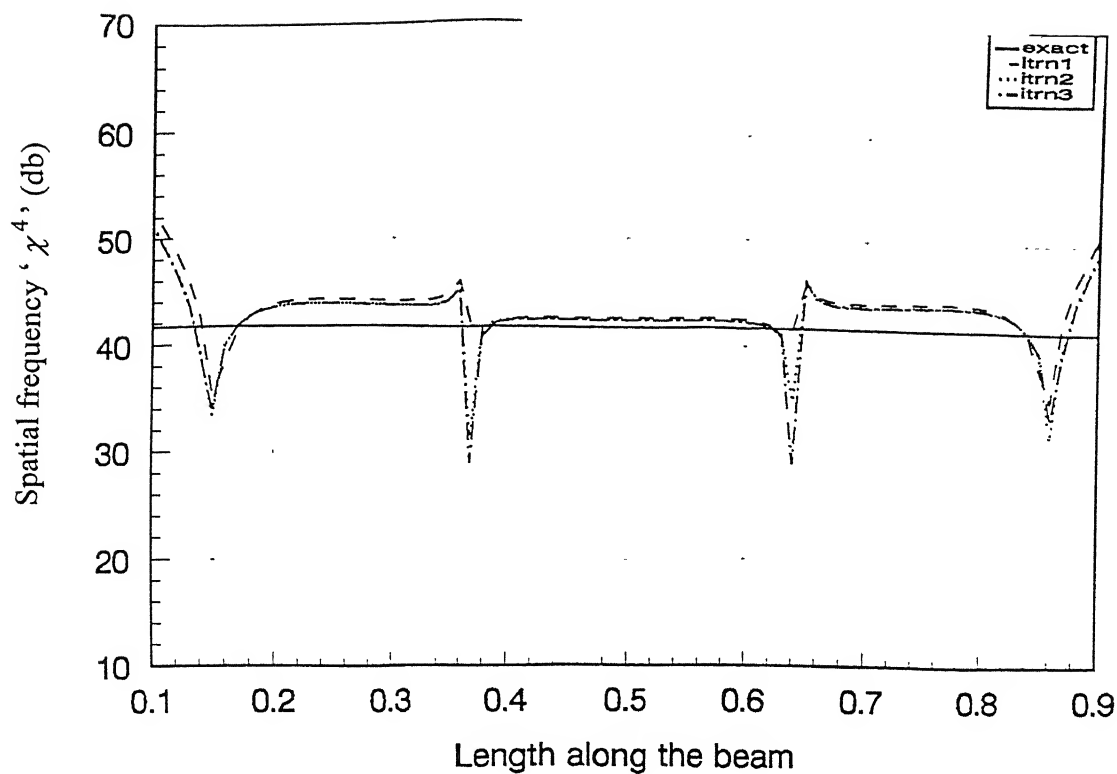


Fig. 3.25(c) Refinement in Spatial frequency: mode 3: fixed-fixed beam

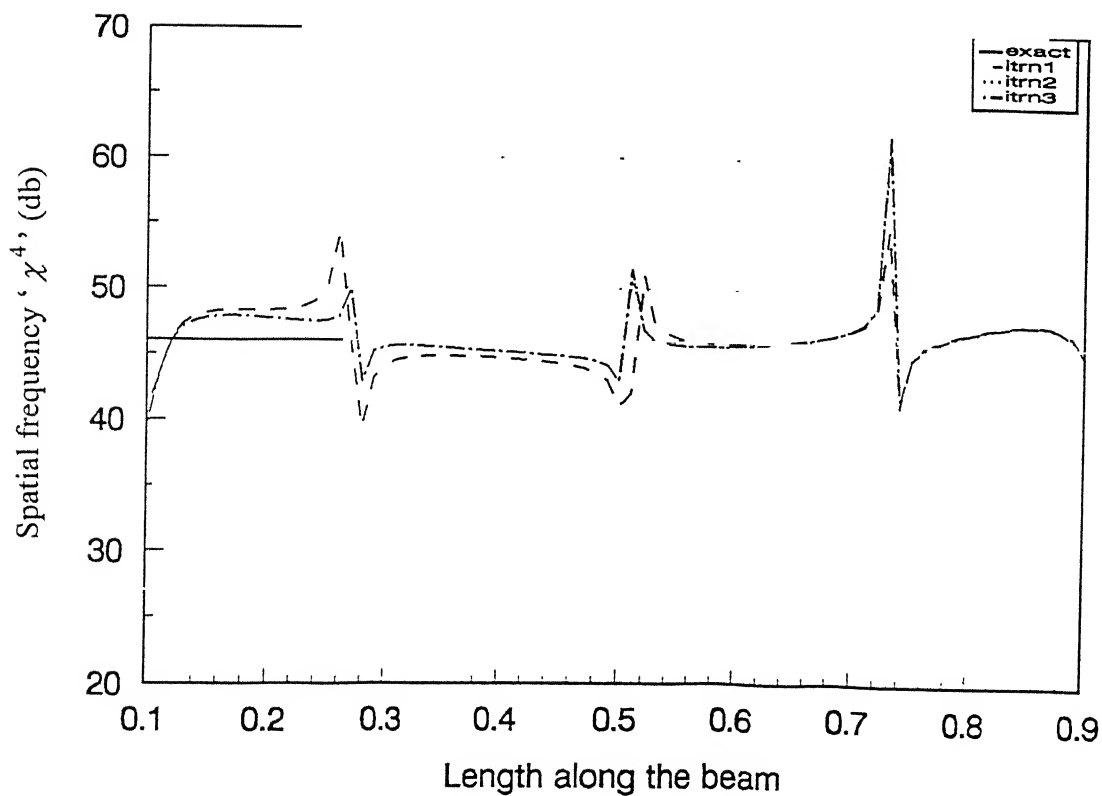


Fig. 3.25(d) Refinement in Spatial frequency: mode 4: fixed-fixed beam

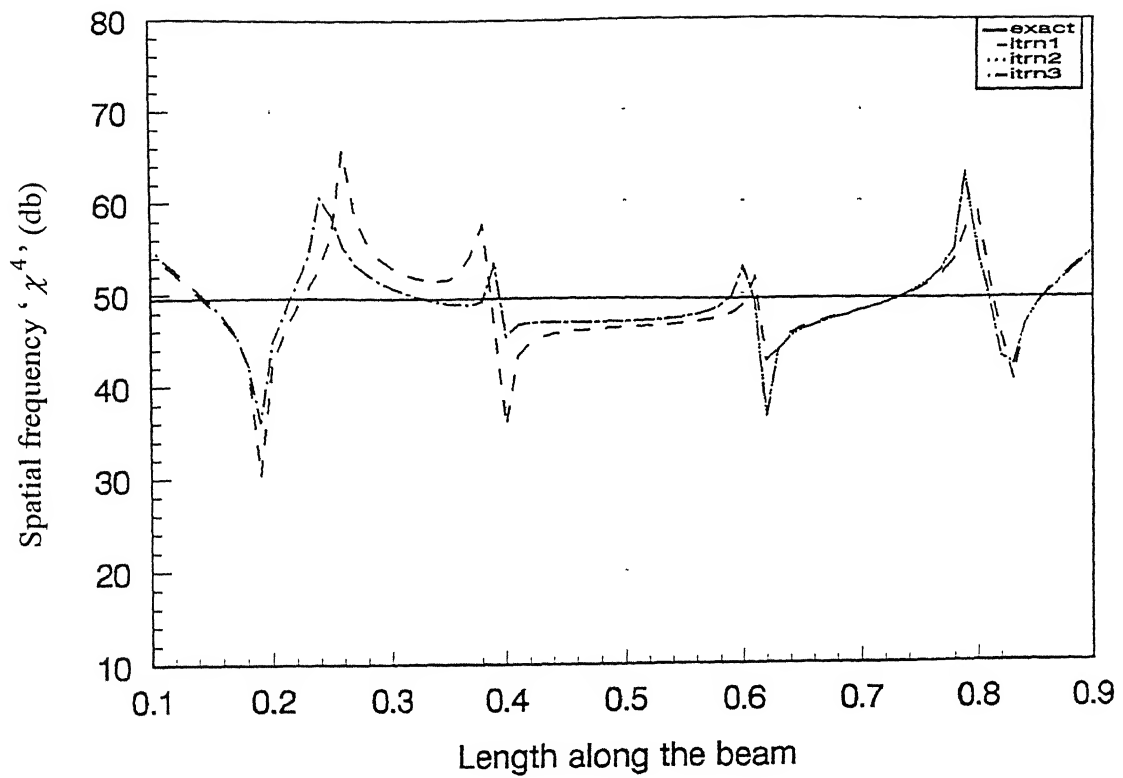


Fig. 3.25(e) Refinement in Spatial frequency: mode 5: fixed-fixed beam

### Cantilever (Clamped-free):

The fundamental frequency, for the cantilever (for  $\kappa = 0.1$ ) is found out to be 1.10 rads/s.

- (a) First the beam is harmonically at its free end at a frequency of 1.32 rads/s ( $=1.2 \times 1.1$  rads/s). The computer simulated spatial response  $H(x)$ , using equation (3.2), is given in Figs. 3.26 (a) and (b). The response in this case is constituted of contributions from all the natural modes (modes 1, 2, 3, 4.....) of the beam. For the first iteration, making an assumption that the modes (1 and 2) lying closest to the excitation frequency, are the major contributors to the overall response, the algorithm is implemented to obtain approximations for the mode shapes (Figs. 3.27 (a)-(b)) and spatial frequencies (Figs. 3.28 (a)-(b)) of modes 1 and 2. The corresponding natural frequencies obtained from the means of the  $\chi$  curves, are 0.973 rads/s. for mode 1 and 6.221 rads/s. for mode 2.
- (b) Approximations are obtained next for the set constituted of mode numbers 2 and 3, by choosing the excitation frequency above the second natural frequency estimated above 7.465 rads/s. ( $=1.2 \times 6.221$  rads/s). The contribution of the first mode, estimated in step (a), is subtracted from the response and fed as input to the algorithm. The estimated mode shapes and spatial frequencies are shown in Figs. 3.29(a)-(b), 3.30(a)-(b), respectively. The natural frequencies obtained are 5.785 rads/s. for mode 2 and 21.365 rads/s. for mode 3.
- (c) The process is continued in a similar manner to obtain approximations for successive sets of modes. The excitation is always given at the free end at a frequency higher than the highest estimated in a previous run. Approximations have been obtained up to mode 5.

The 'first estimates' are refined, by iterating through the above procedure. Since the 'first estimates' of all the modes of interest are available, the possible participation of all modes not lying adjacent to the selected excitation frequency can be computed and subtracted from the overall response. The resultant thereby forms the refined input constituted of the participation of only those modes, which are being estimated by the

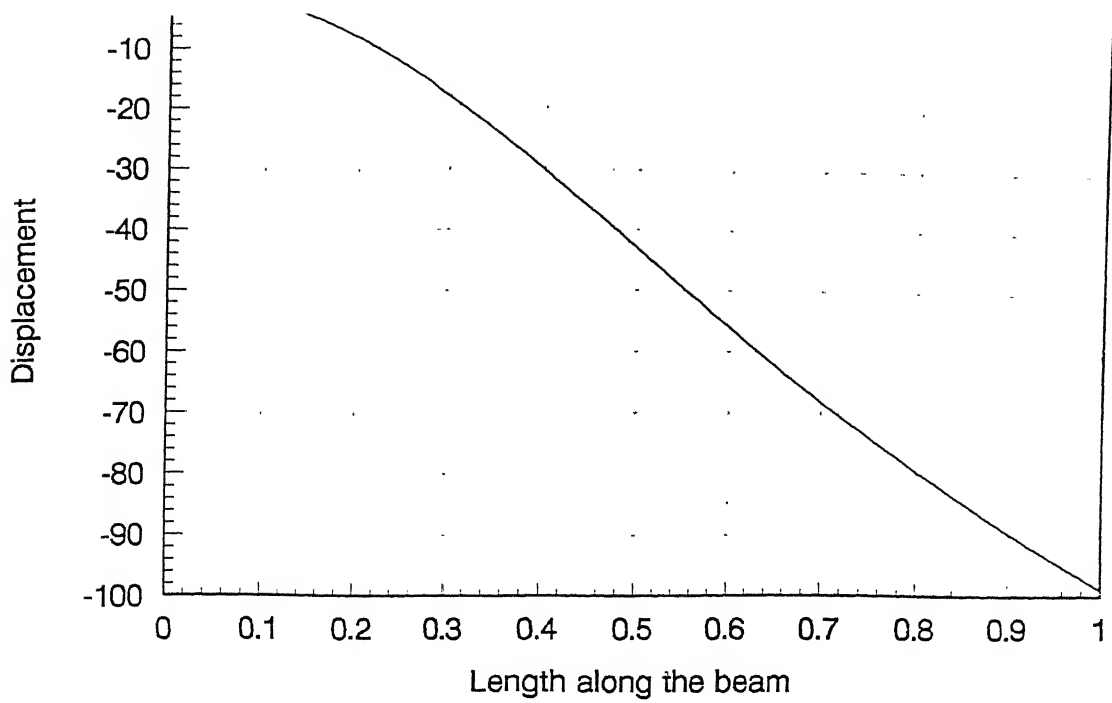


Fig. 3.26(a) In-phase response of the cantilever beam  
 (Location of excitation force,  $x/l = 1.0$   
 Frequency of excitation = 1.32 rad/s)

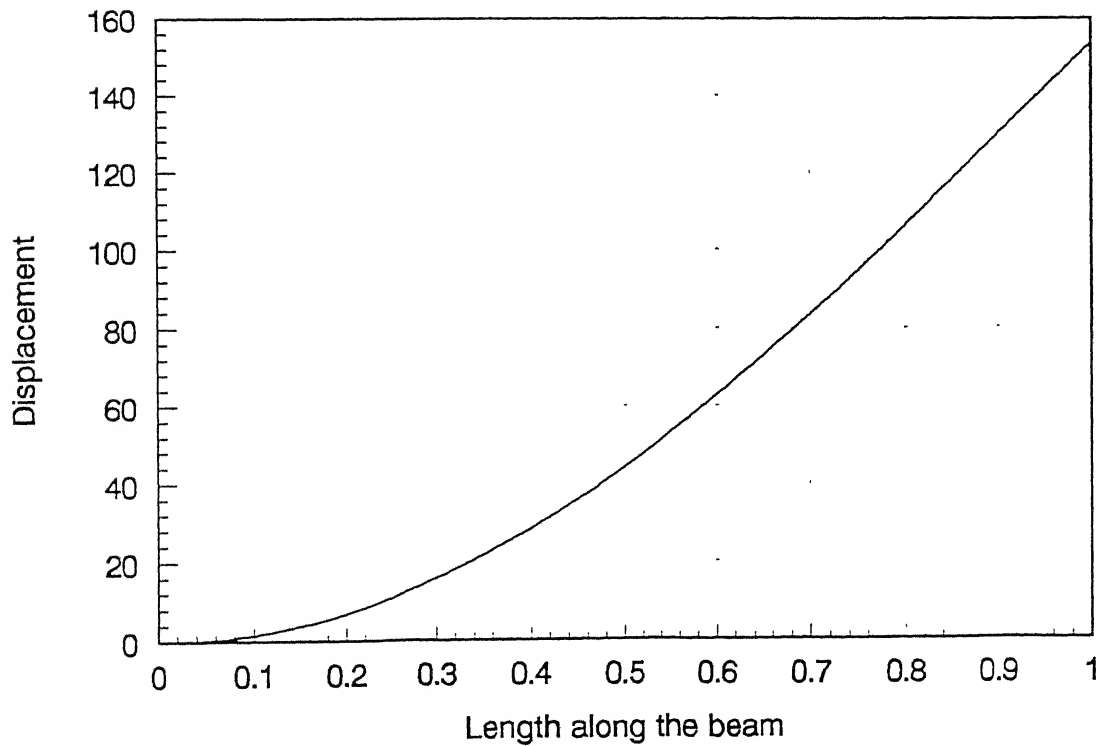


Fig. 3.26(b) Out of phase response of the cantilever beam  
 (Location of excitation force,  $x/l = 1.0$   
 Frequency of excitation = 1.32 rad/s)

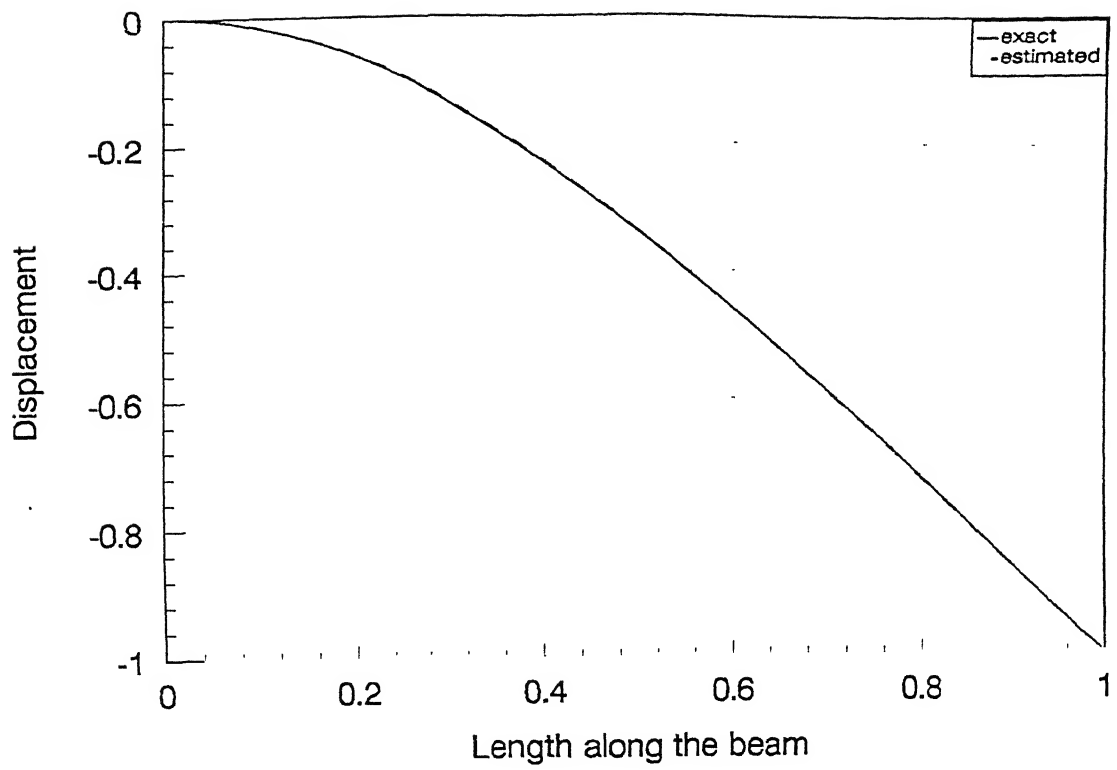


Fig. 3.27(a) First approximation of mode 1; cantilever beam

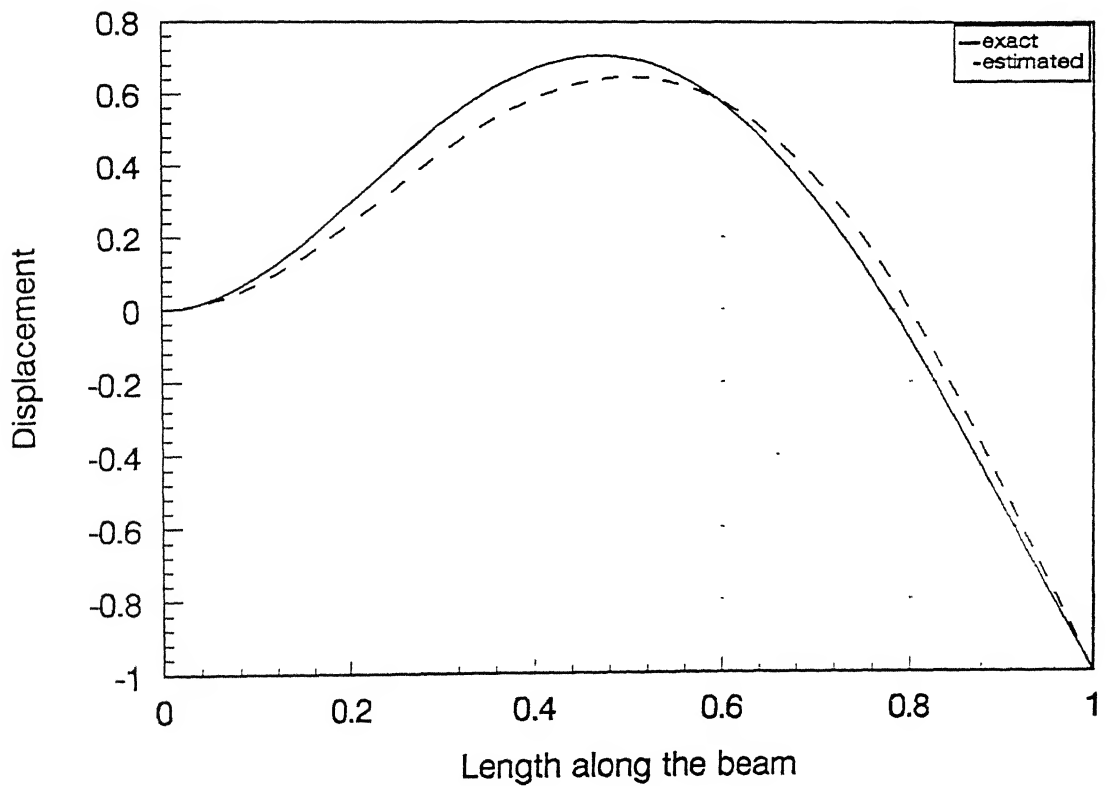


Fig. 3.27(b) First approximation of mode 2; cantilever beam

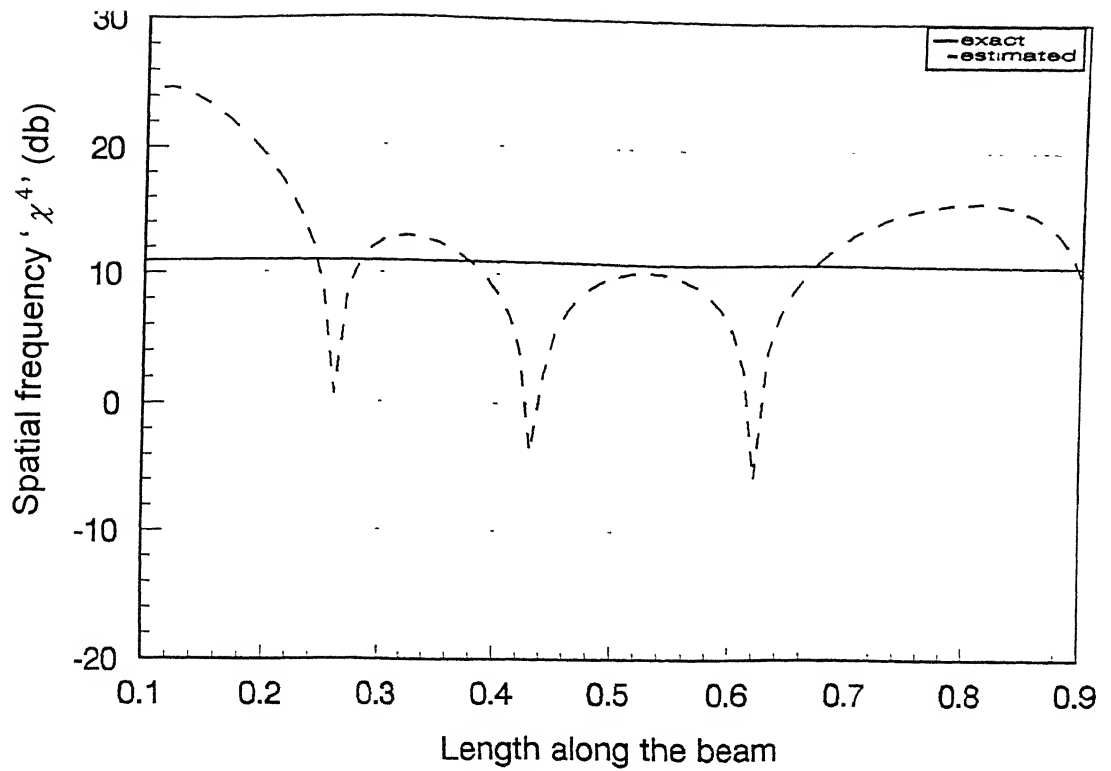


Fig. 3.28(a) First approximation of Spatial frequency: mode 1: cantilever beam

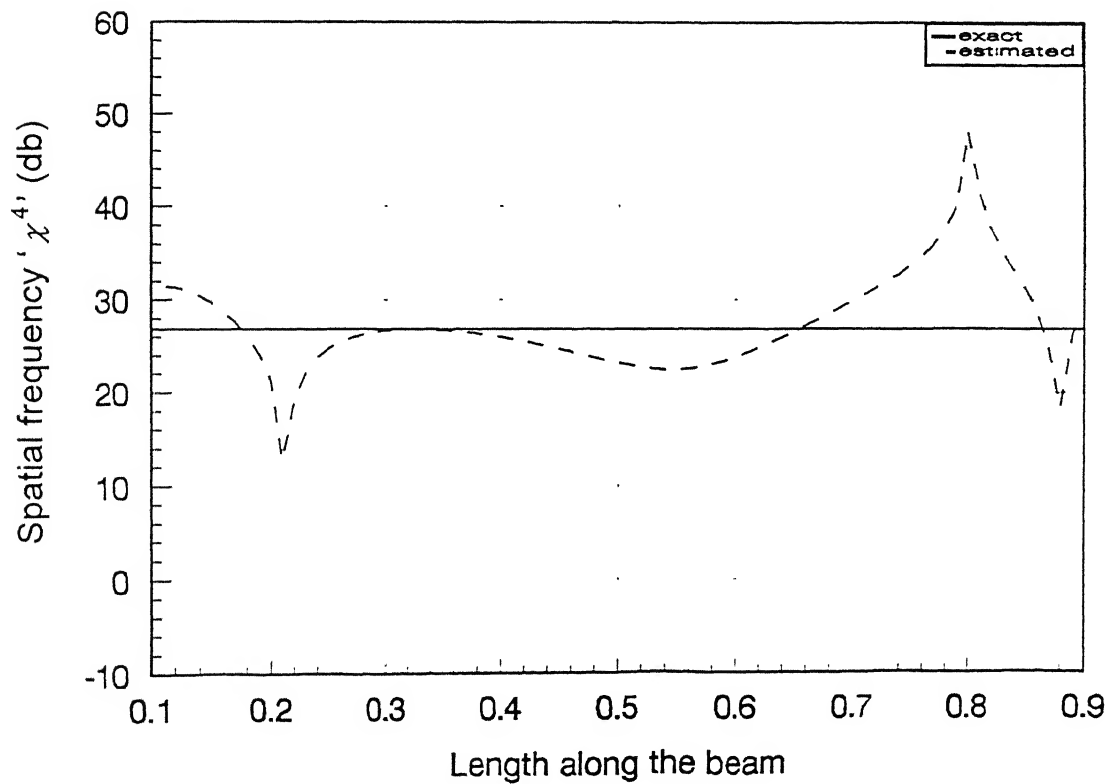


Fig. 3.28(b) First approximation of Spatial frequency: mode 2: cantilever beam



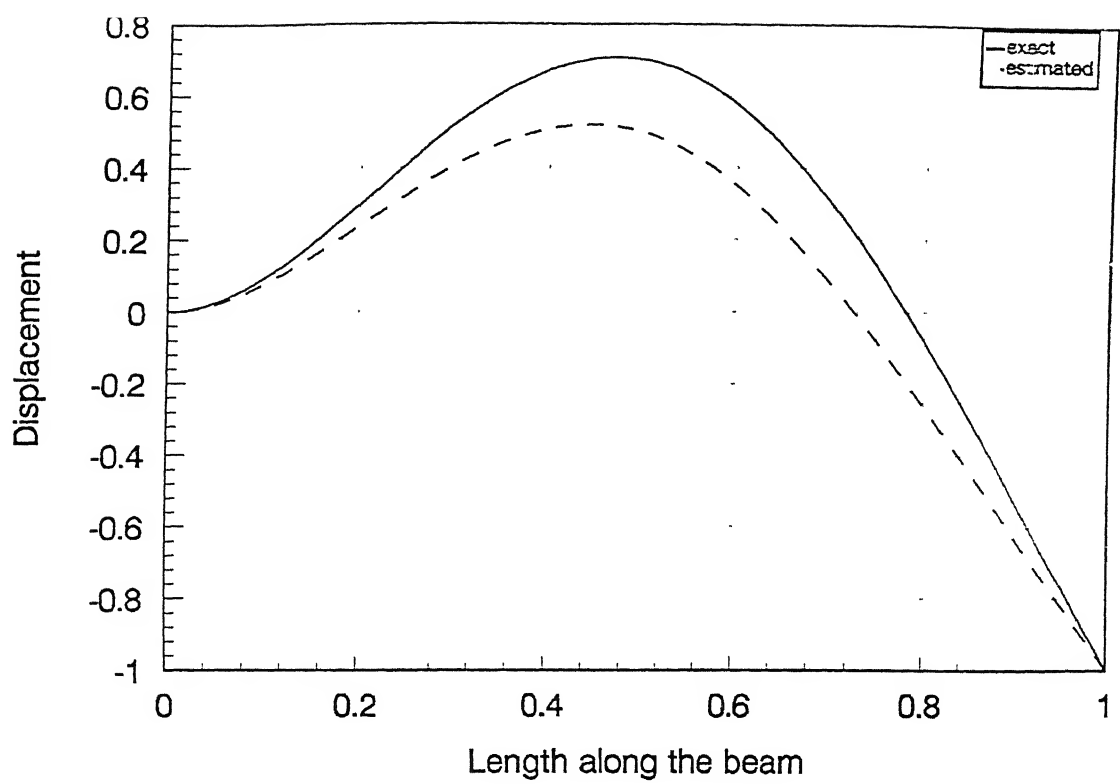


Fig. 3.29(a) First approximation of mode 2; cantilever beam

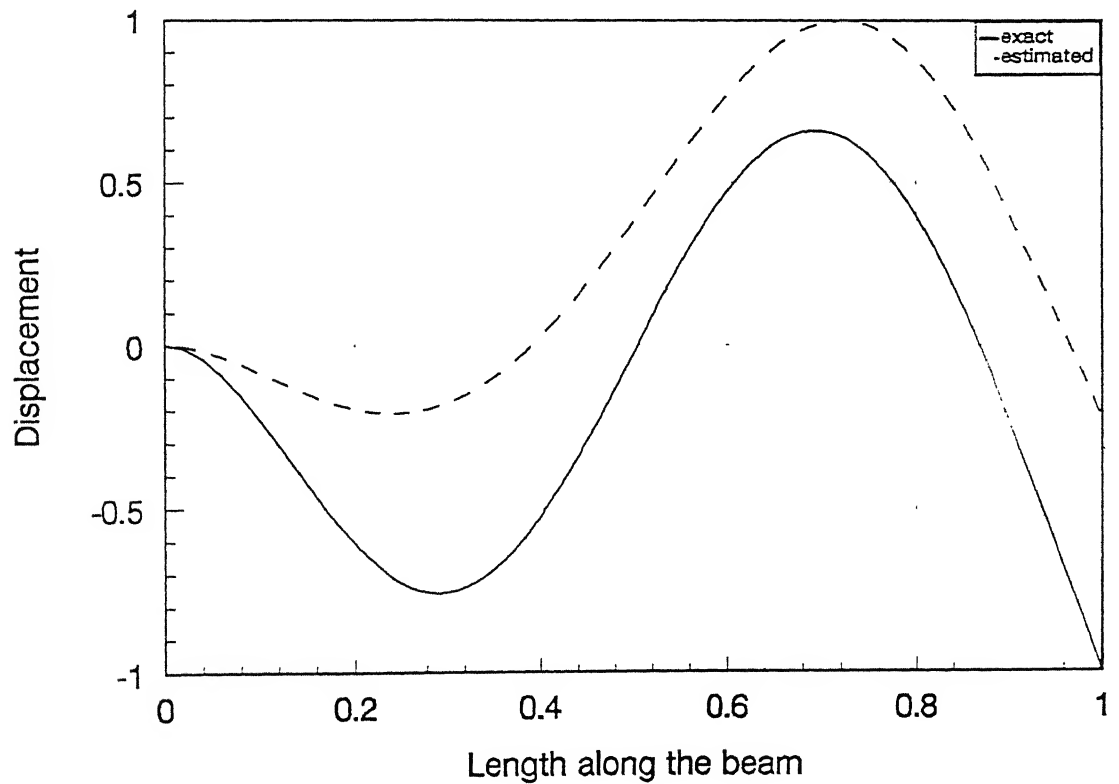


Fig. 3.29(b) First approximation of mode 3; cantilever beam

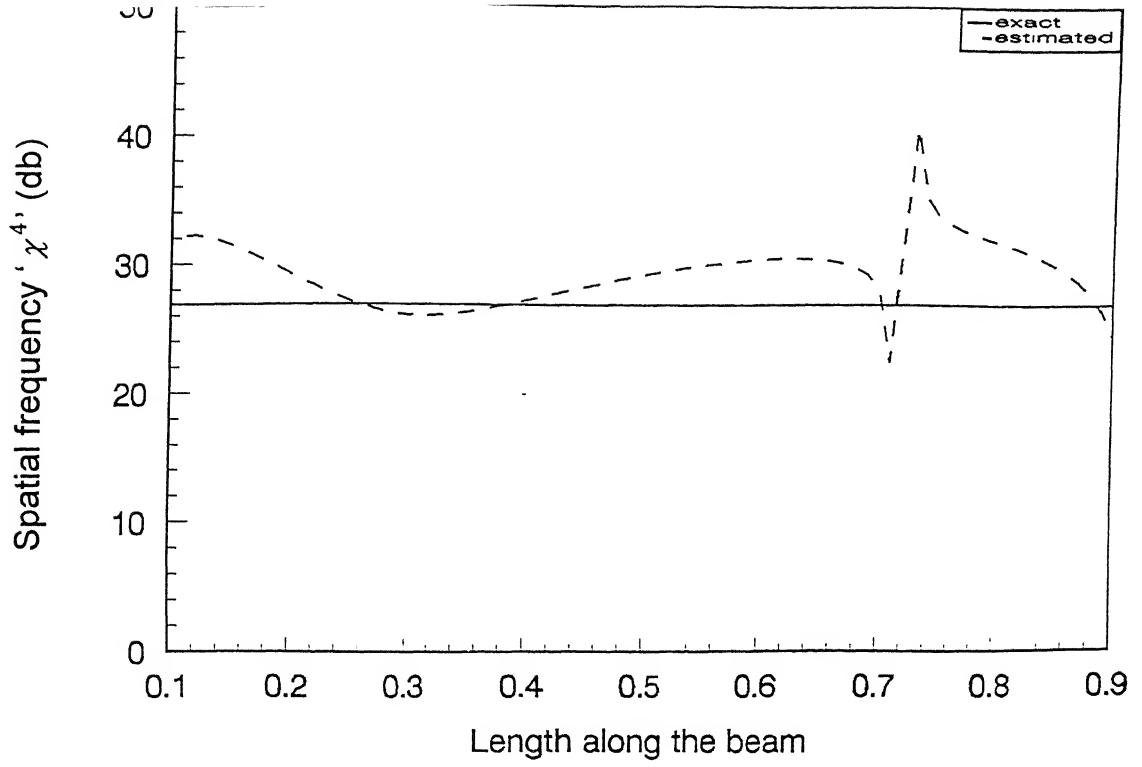


Fig. 3.30(a) First approximations of Spatial frequency: mode 2: cantilever beam

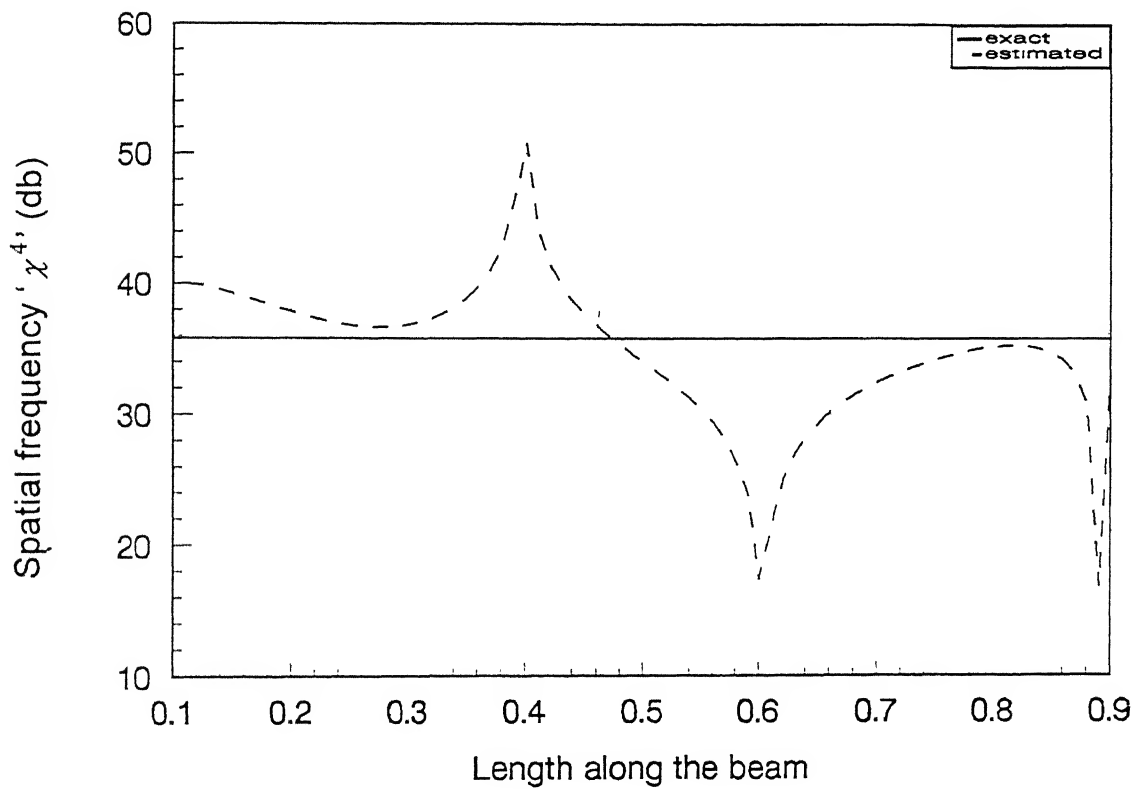


Fig. 3.30(b) First approximations of Spatial frequency: mode 3: cantilever beam

algorithm. The input to be fed to the algorithm is refined by computed by subtracting the contributions of the modes not of interest from the overall beam response. The refinement obtained in the first five mode shapes is shown in Figs. 3.31(a)-(e), while the corresponding data on the spatial frequencies is depicted in Figs 3.32 (a)-(e). The natural frequencies  $\omega_m$ , obtained through the formula given in equation (2.24) are listed in Table 3.3, for each iteration, along with the corresponding exact values.

**Table 3.3 Estimated and Exact Natural Frequencies  
of cantilever beam**

	Mode 1	Mode 2	Mode 3	Mode 4	Mode 5
<b>Iteration 1</b>	0.973	6.221	21.365	42.102	55.698
<b>Iteration 2</b>	1.084	6.823	18.322	41.030	57.490
<b>Exact</b>	1.101	6.955	19.320	37.867	62.597

### 3.4 Remarks

The results obtained through the numerical illustration are self-explanatory. The procedure can be seen to obtain very accurate estimates of mode shapes. For example, the maximum error in the simply supported case ranges from about 0.015 % for mode 1 to 10 % for mode 5. A similar trend can be observed in the other beam configurations. Presently, the estimation is restricted to the fifth mode in all cases. For improvement in the fifth mode approximations, higher modes (6<sup>th</sup>, 7<sup>th</sup>,...) need to be considered in the analysis. The errors are found to be maximum in the vicinity of the nodal points. The exact displacement at these points is zero. The computer algorithm, however do not approximate these displacements as exact zeros. The same trend is observed in the approximations of the spatial frequencies. The errors at the nodal points is more pronounced in the case of spatial frequencies since a fourth order numerical derivative is involved in the computational procedure.

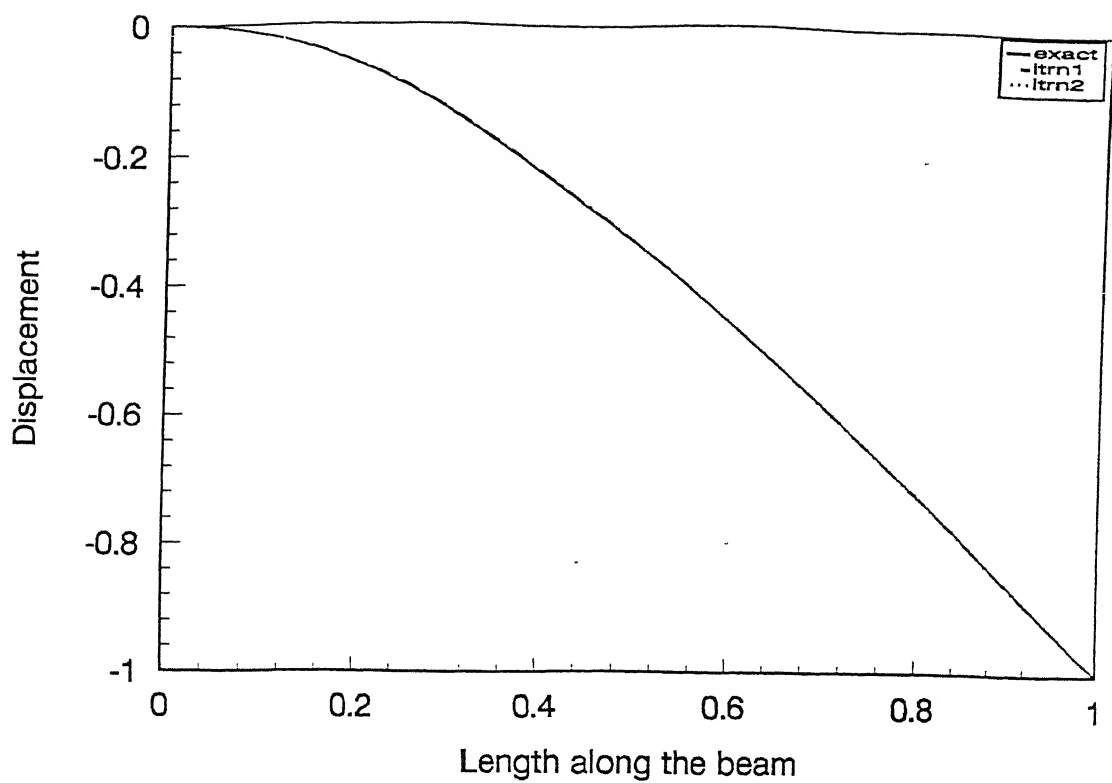


Fig. 3.31(a) Refinement in mode shapes: mode 1: cantilever beam

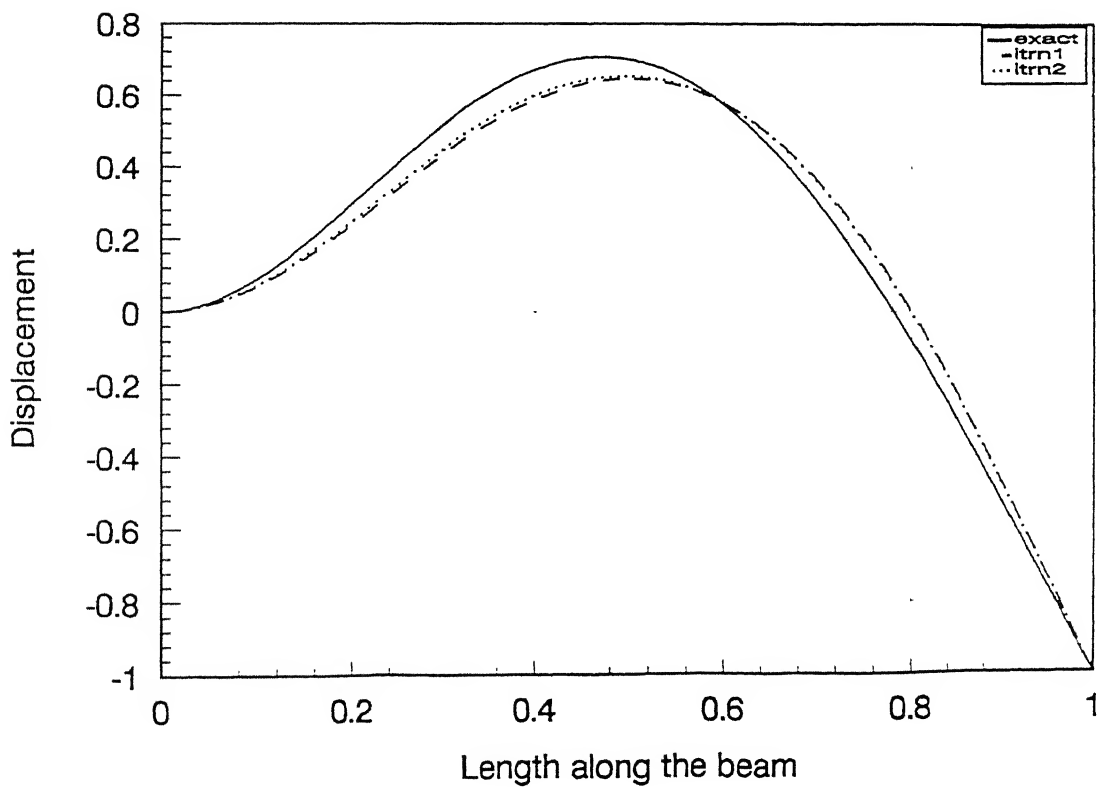


Fig. 3.31(b) Refinement in mode shapes: mode 2: cantilever beam

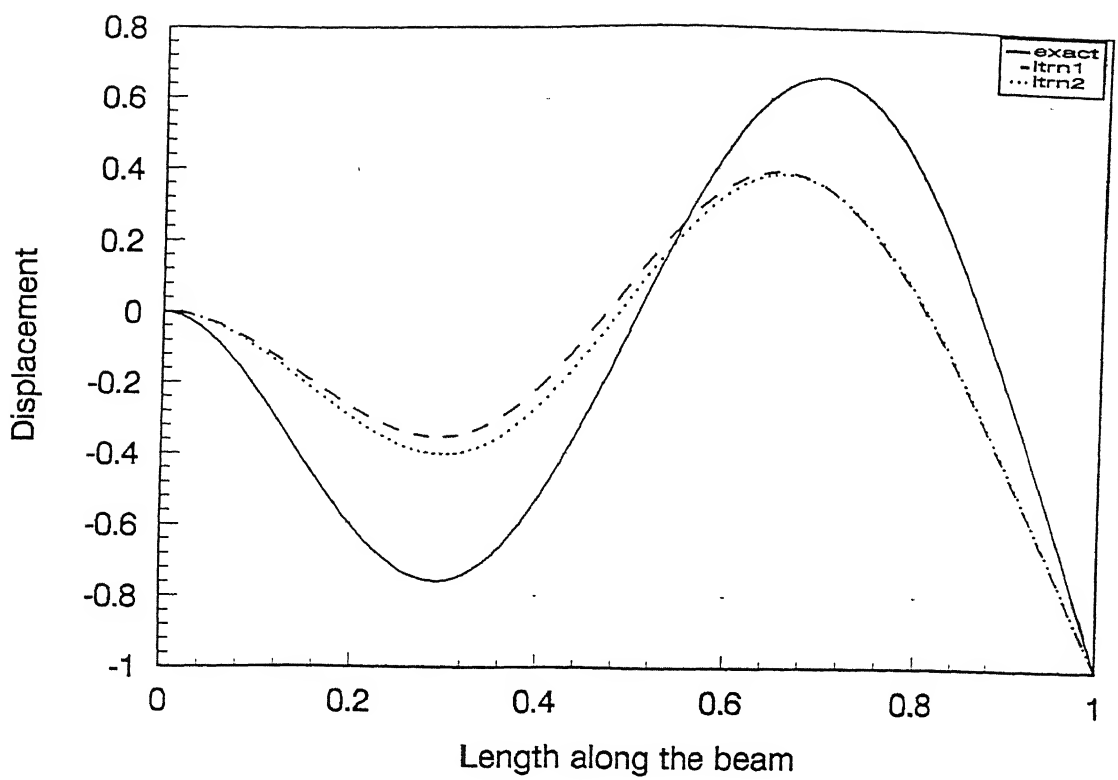


Fig. 3.31(c) Refinement in mode shapes: mode 3: cantilever beam

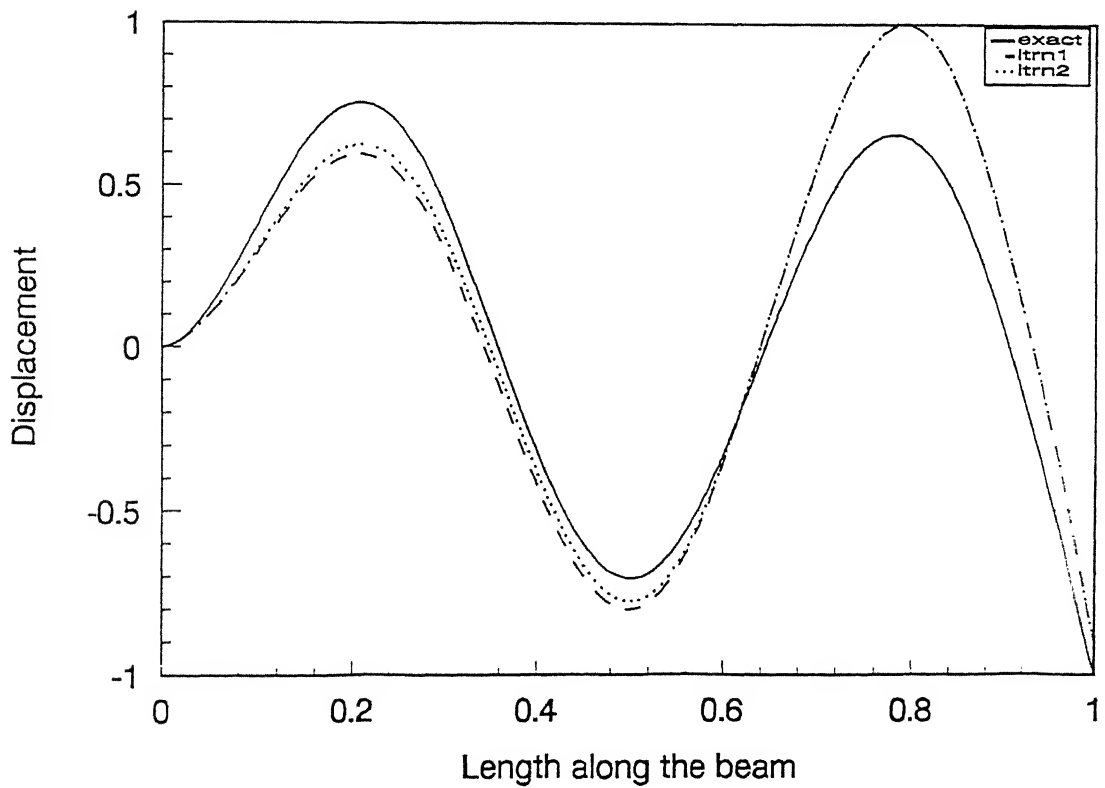


Fig. 3.31(d) Refinement in mode shapes: mode 4: cantilever beam

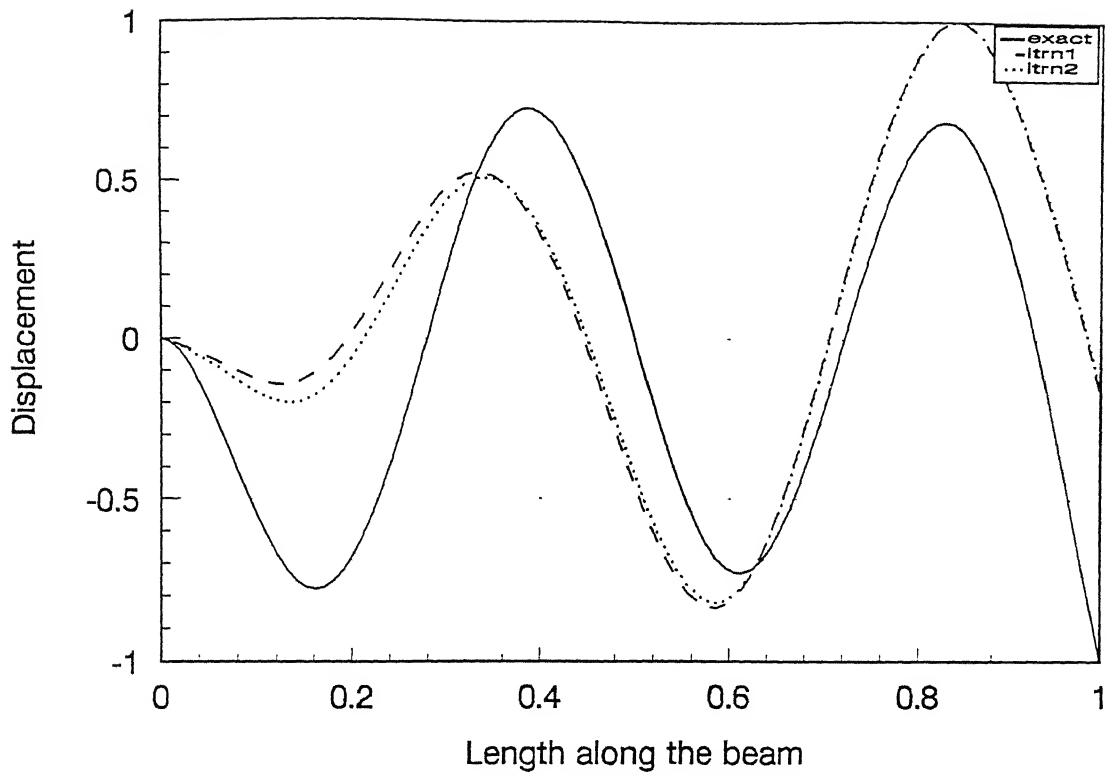


Fig. 3.31(e) Refinement in mode shapes: mode 5: cantilever beam

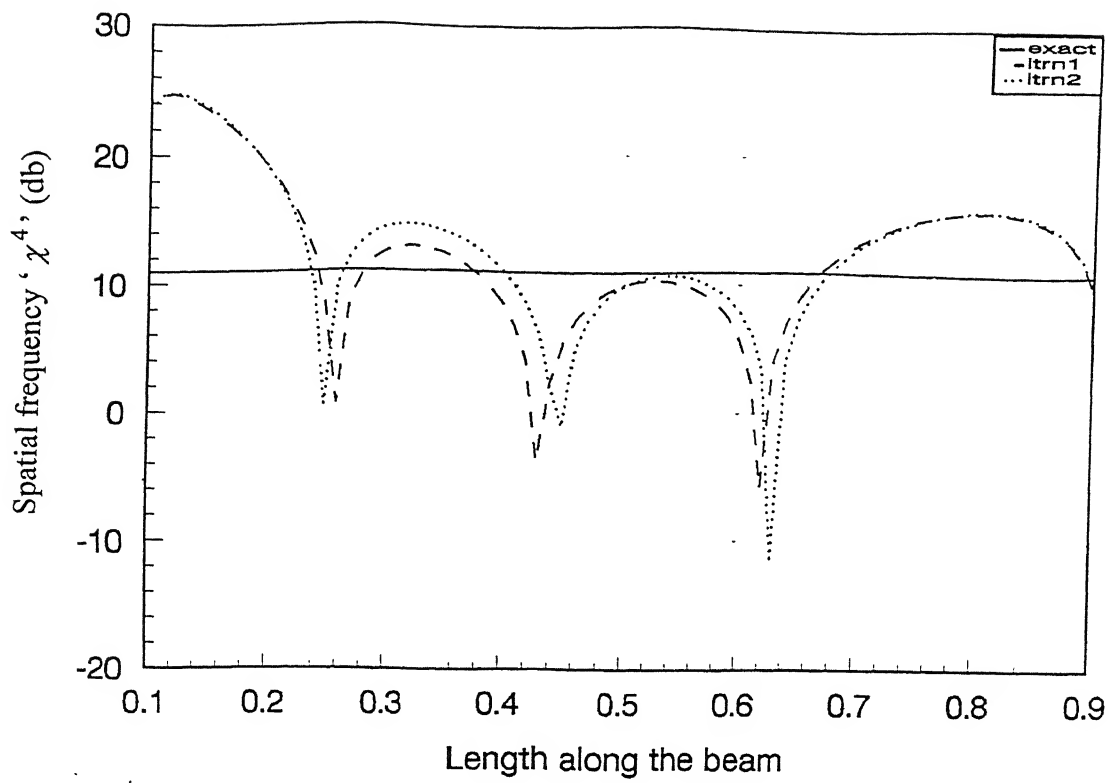


Fig. 3.32(a) Refinement in Spatial frequency: mode 1: cantilever beam

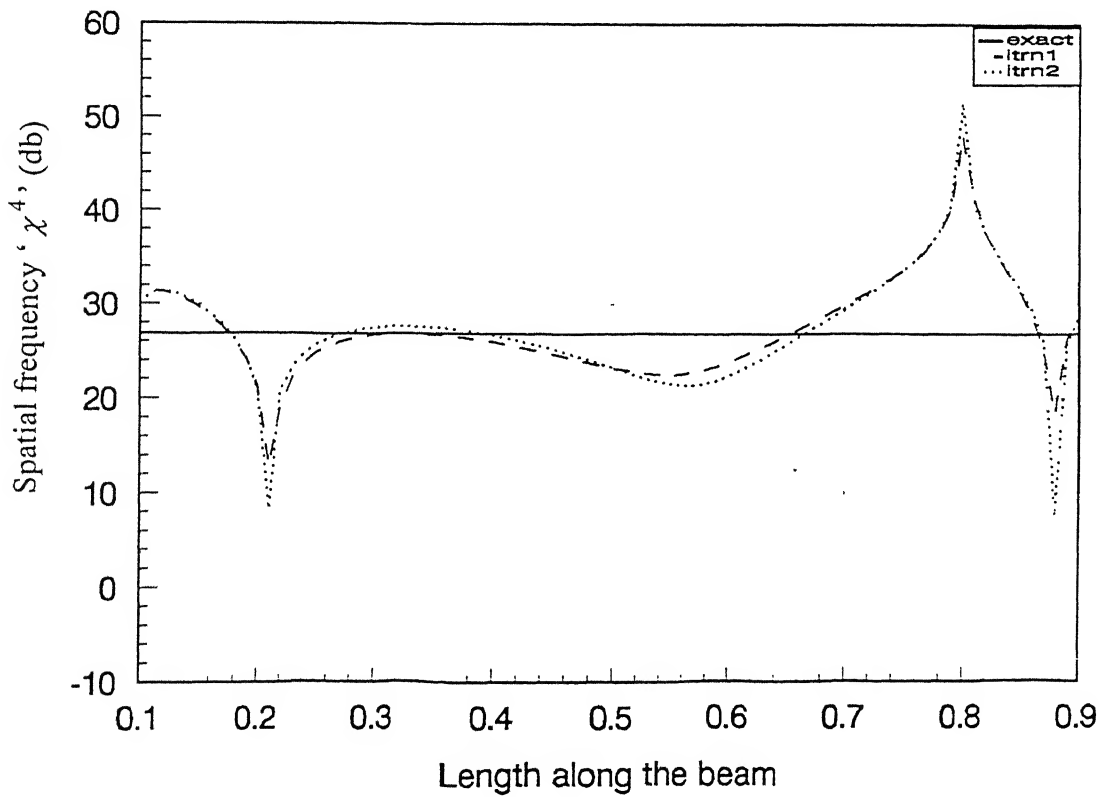


Fig. 3.32(b) Refinement in Spatial frequency: mode 2: cantilever beam

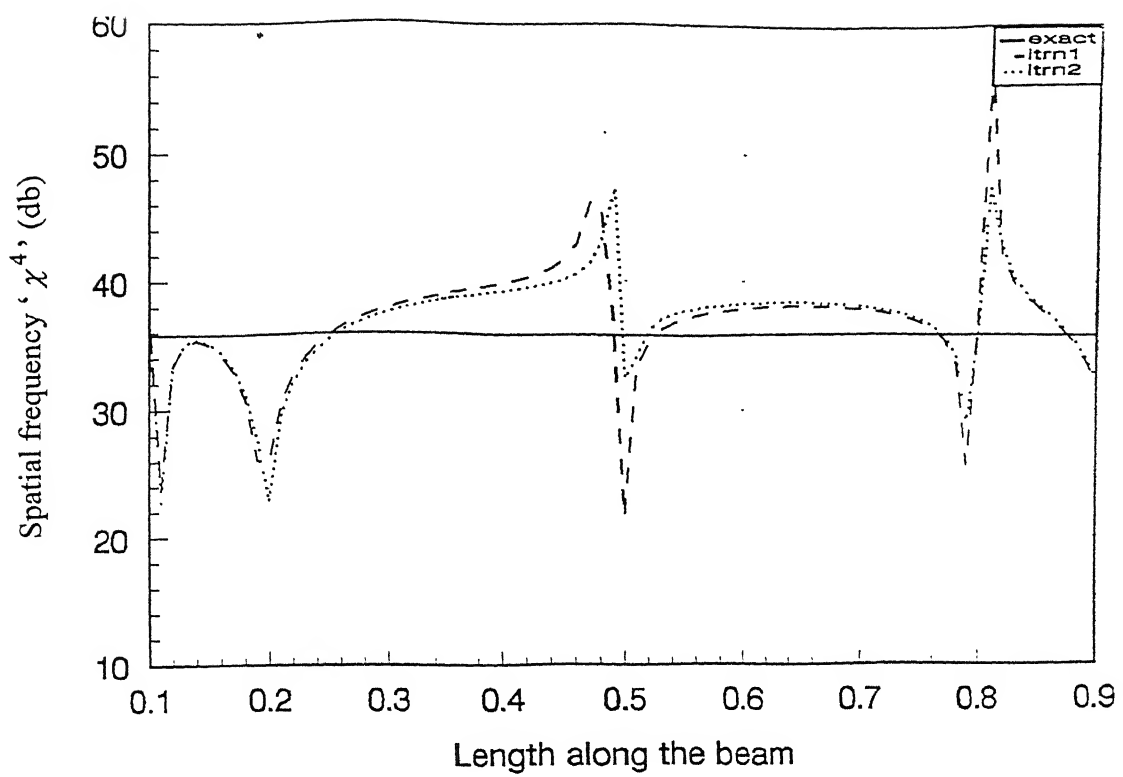


Fig. 3.32(c) Refinement in Spatial frequency: mode 3: cantilever beam

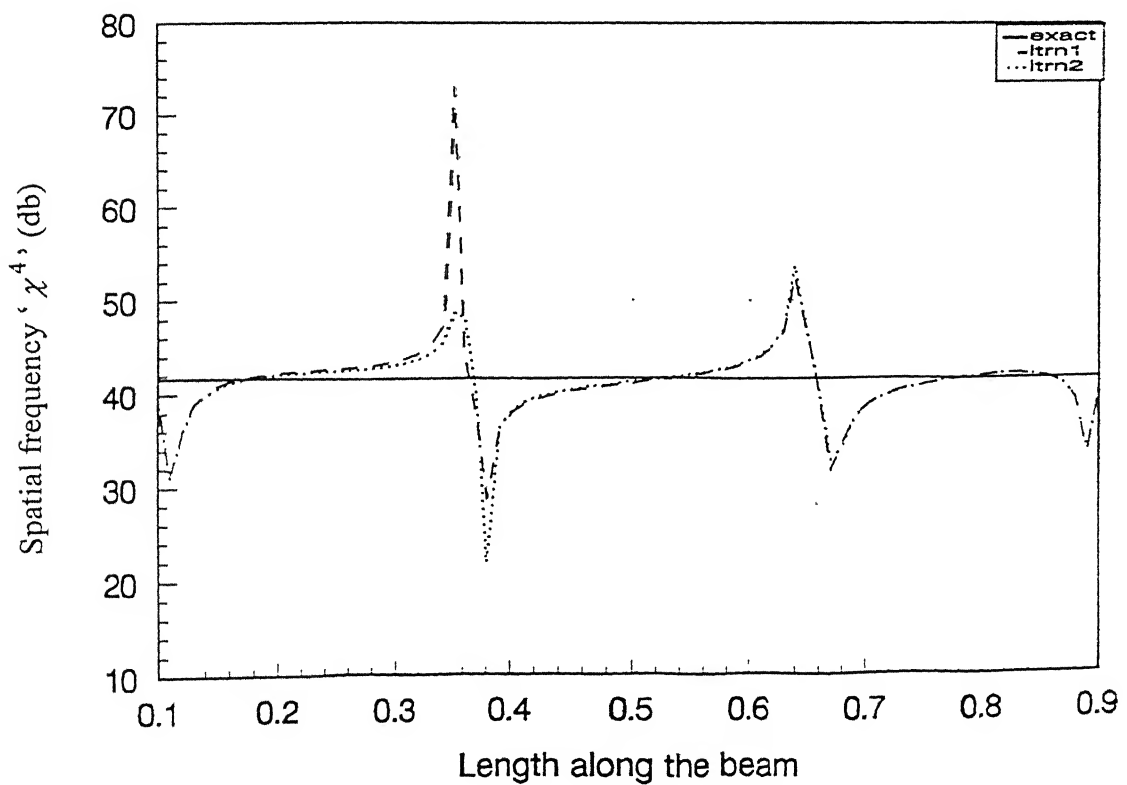


Fig. 3.32(d) Refinement in Spatial frequency: mode 4: cantilever beam



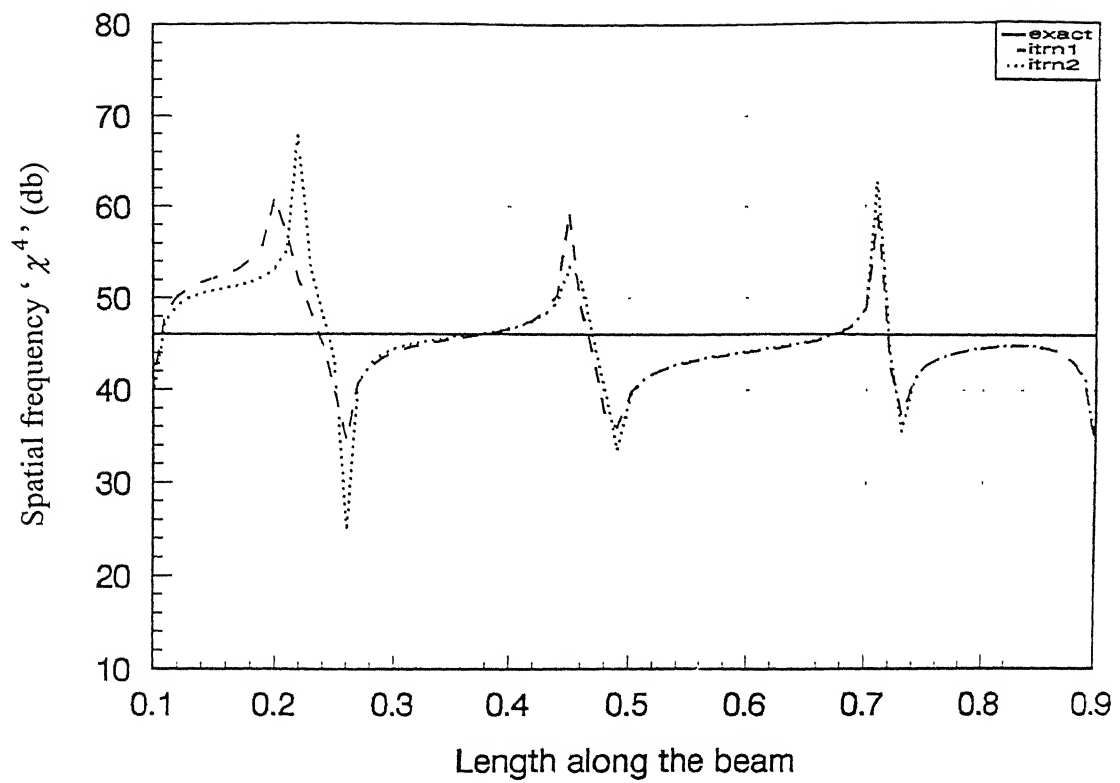


Fig. 3.32(e) Refinement in Spatial frequency: mode 5: cantilever beam

## CHAPTER 4

### CONCLUSIONS

The work presented in this thesis is an extension of the existing Spatial Modal Analysis procedures, dealing with estimation of single (or two) natural modes, of a vibrating beam, which is (are) close to the frequency of excitation. An algorithm has been developed, during the present study, for step-by-step approximation of successive beam modes. The procedure involves variation of the frequency and location of the excitation force. The general procedure constitutes of estimation of mode shapes, as well as calculation of natural frequencies, from steady state spatial data of beam excited at a specified frequency and location. The deflected beam shape is approximated by employing recursive form of Forsythe polynomials and Least Square technique is used to curve fit the measured responses and obtain the coefficients of Forsythe polynomials. Orthogonality properties of the normal mode functions are further employed to decompose the Forsythe polynomial representation into the individual mode shapes of the beam contributing to the response. The individual mode shape estimates are further processed to fit the governing fourth order spatial equation of beams to obtain the spatial modal frequency. Successive beam modes are approximated, step-by-step, by changing the frequency and location of excitation force. The procedure has been illustrated through computer simulation for beams with standard boundary configurations. The procedure is found to give accurate descriptions of the mode shapes. The estimates of the natural frequencies however, are not accurate. The natural frequencies have been computed through the estimates of the spatial natural frequencies, involving fourth order numerical differentiation. The central-difference scheme employed for numerical differentiation, carries inherent errors. It can be said that the present spatial modal analysis scheme is not ideally suited for natural frequency estimation, which is carried out more accurately through conventional modal analysis routes (free or forced vibration tests). The focus of the spatial analysis procedures, of the present study, should remain confined to obtaining accurate descriptions of mode shapes.

The procedure needs to be experimentally validated. Since spatial modal analysis procedures require intensive response data from the space coordinates, conventional contact type sensors like accelerometers, which can provide data at limited number of spatial locations, are not suitable for such applications. A non-contact type of sensor like the Laser Vibrometer is essential to get the dynamic information at sufficient number of stations on the beam. Influence of the number of Forsythe polynomials in the mode shape approximations, also needs to be investigated. An investigation is also required to explore and account for the errors incurred due to inaccuracies in the force application point. The study also opens the possibility of developing similar procedures for plate vibration applications. Possibilities of application of multiple-point excitations can also be investigated.

## REFERENCES

- Allemang, R. J., *Experimental Modal Analysis Bibliography*, Proc IMAC 2, 1984
- Archibald, C. M., *An Analysis of Sample Rate Considerations for Parametric Sinusoidal Estimation Methods*, Proceedings 10<sup>th</sup> International Modal Analysis Conference, SanDeigo, Ca, 1992
- Archibald, C. M. and Wicks, A. L., *An Alternative Time Domain System Identification Algorithm*, Proceedings 9<sup>th</sup> International Modal Analysis Conference, Florence, Italy, 1991
- Bishop, R. E. D. and Gladwell, G. M. L., *An Investigation into the Theory of Resonance Testing*, Proc. Roy. Soc. Phill Trans 255(a) 241, 1963
- Ewins, D. J., *Modal Testing Theory and Practice*, John Wiley and Sons Inc., 1986
- Ewins, D. J. and Griffin, J., *A State of the Art Assessment of Mobility Measurement Techniques*, J. Soc. Indust. Appl. Math, Vol. 5, No. 2, P. 197-222, 1981
- Forsythe, G. E., *Generation and Use of Orthogonal Polynomials for Data Fitting with a Digital Computer*, J. Soc. Indust. Appl. Math., Vol. 5, No.2, June 1957, P. 75-88
- Kennedy, C. C. and Pancu, C. D. P., *Use of Vectors in Vibration Measurement and Analysis*, J. Aero. Soc., Vol. 14, No. 11, 1947
- Mitchell, L. D., *Modal Analysis Bibliography – An Update-1980-1983*, Proc. IMAC 2, 1984
- Pisarenko, V. F., *The Retrieval of Harmonics from a Covariance Function*, Geophysics J. R. Astr. Soc., Vol. 33, P. 346-366, 1973
- Rao, S. S., *Mechanical Vibrations*, Addison-Wesley, 1986
- Vaze A. V., *Spatial Modal Analysis in Beams*, 1998
- West, R. I., Archibald, C. M., and Wicks, A. L., *Spatial Modal Analysis Using Regressive and Autoregressive Techniques*, Proceedings 11<sup>th</sup> International Modal Analysis Conference, Orlando, Florida, 1993

**A 128082**

